

Overtopping hazard reduction at Churchill Barriers, Scotland

Y ZHANG



Supervisors:

Prof. dr. ir. S.N. (Bas) Jonkman, TU Delft

Dr.ir. Hofland. B, TU Delft

Dr. ir. Bricker. J. D, TU Delft

Ir. Marcel. Westerink, Antea Group

Jan-Bert. de Hoop, Antea Group

Delft University of Technology

Department of Civil engineering and Geosciences, Hydraulic engineering

Delft, 2019

Preface

This MSc thesis project is not only a conclusion of my Master study, but also a final harvest of my years of study. At 18 years old, I graduated from the best-grade high school in my hometown, where no weekend, no summer or winter break, and no holidays are allowed, where every student is required study in classroom from 7:00 to 22:00 every day, where 60 students sit in a small busy classroom breathing the foulest air ever. This experience makes me cherish my Bachelor and Master study life as well as its freedom more than anyone else. I appreciate SCU and TU Delft for giving me opportunity to learn knowledge and explore my interest while enjoying my youth.

This thesis focuses providing technical advice on overtopping flood hazard reduction at Churchill Barriers. I am motivated to work on topic because it combines my interest in numerical model and risk analysis with passion for flood hazard reduction. To apply knowledge and theory I learned from lecture to a real case is not only interesting but also challenging. I spend plenty of effort to develop an approach that can lead to a solution of research question, which was revised ten of times while realizing it. Finally, the approach gives not only results of overtopping prediction and evaluation on current manual flood alert system, but also economical flood protection strategy that combines barrier closures and wave wall design. On top of that, I have been thinking about how to improve flood protection system, including flood protection structure and hazard alert, for overtopping prone shoreline worldwide to reduce damage cost and loss of life. The approach used in this study can be applied to not only Churchill Barriers, but also overtopping prone areas in the UK, where can be closed during extreme event.

There are many important experiences have learned from this study. I was lucky to work in a civil engineering company and get to know the working environment and see what colleagues do spend a working day. During academic research, I have approached many engineers and project managers in Australia and the UK who participated in this project in the past. Thanks for their help, I have been able to collect useful information and strength my communication skills.

The last but not the least, I would like to express my appreciation to everyone who support me throughout this study. I would not have been able to obtain mt Msc diploma without any of you. First, I want to thank my graduation committee members, prof. dr. ir. Jonkman, dr. ir. Bas Hofland, and dr. ir. Jeremy Bricker, for the helpful supervision and patient support. I would also like to thank Mr. Marcel Westerink and Mr. Jan Bert de Hoop for helping me throughout this thesis ride, Mr. Piet Akkermans for giving me the opportunity to work in Antea Group. Furthermore, I would like to thank OIC and JBA for their support in information collection. To my lovely friends, Oliver, Elmo, Xuexue, and everyone of you, thanks for being there when I need you. Finally, a big thanks to my parents who not only support my education with their selfless dedication but also provide me financial spouse.

Abstract

Churchill Barriers, a series of four causeways in Orkney Islands, Scotland were constructed during Second World War and now serve as a critical link for South Ronaldsay and Burray to the Orkney Mainland. Due to their location and design, causeways are exposed to storm waves generated in the North Sea. During coastal storms, some waves are able to overtop the barriers, damaging cars and potentially washing vehicles off the barrier. Due to overtopping risk, the barriers are closed to vehicles around five times per year, with the number of closures increasing. Closures are manually operated by policeman who are sent to barrier. Their responsibility is watching overtopping situation and close the barrier when they think it is too dangerous to drive across.

This Master Thesis aims to provide insight in the optimal strategy of reducing wave overtopping volumes and frequency of closure of Churchill Barrier No.2, by investigating overtopping volumes of plain and recurved wave walls for various closure frequencies, and exploring tolerable wave overtopping volumes in line with local condition.

Because barrier locate in relatively uninhabited area, design closure frequencies are between 0.2 to 5 times per year, which is much higher than normal design. In order to simulate wave overtopping, boundary conditions are required. Since wave conditions at barrier toe are of complete lack, extreme offshore waves are transformed to barrier toe by Numerical Model SWASH. The results of SWASH are used as input of statistic model that can generate wave condition and water level at barrier toe for each design return period. Afterwards, wave overtopping volumes are simulated as a function of no wave wall, present wave wall, plain vertical wave wall with various height, and recurved wave wall with bullnose with various height and bullnose angle. The simulation uses most up-to-date and suitable empirical equations obtained from academic research. Wave volume of present wave is used for evaluating policeman's estimation on closure. It shows that policeman did a good job in estimation. However overtopping splash is a very dynamic process, the evaluation is subjected to many limitations. Wave volumes of plain vertical wave wall and recurved wave wall are used for wave wall design. Various sensitivity analysis is carried out to find the optimal wall height and bullnose shape. It is proved that recurved wall is more effective in wave overtopping reduction than plain wave wall.

Afterwards, cost-benefit analysis (CBA) is undertaken to explore the most economical wall design and its return period. CBA concludes that optimal design is recurved wave wall of three years return period. Wave wall is 1.7m high with 70 ° bullnose angle. With this wall, barrier need to be closed only once in every three years.

In the end, some recommendations are given to general approach and method to collect raw data and accumulate engineering experience of local overtopping situation, which will contribute to an automatic road gate system in the further.

Contents

Preface	i
Abstract	iii
Contents	v
List of Figures	vii
List of Tables	ix
List of Symbols	xi
1 Introduction	1
1.1 Project background	1
1.2 Research question	1
1.3 Approach	2
2 Physical Context and Literature Study	3
2.1 Physical context	3
2.2 Previous study on Churchill barrier No.2	5
2.2.1 Project history	5
2.2.2 Input information collection	5
2.2.3 Overtopping hazard at Churchill Barriers	6
2.3 Wave transformation	8
2.4 Run-up and overtopping at sloping structure	8
2.5 Wave overtopping discharge	10
2.5.1 Basic formula - simple armour slope	11
2.5.2 Very steep slopes	11
2.5.3 Composite steep slope with vertical wall on crest	12
2.5.4 Vertical walls	13
2.6 Individual wave overtopping volumes	14
2.6.1 Recurved wave wall with bullnose - reduction factor	15
3 Wave Transformation and Overtopping Modelling	19
3.1 Approach	19
3.2 Boundary condition	21
3.2.1 Datum	21
3.2.2 Life time and return period	21
3.2.3 Climate changes	22
3.2.4 Bathymetry, foreshore and barrier cross-section	22
3.2.5 Water level	24
3.2.6 Wave Condition	26
3.2.7 Joint probability analysis	26

3.3	Wave transformation	27
3.3.1	Model requirement and description	27
3.3.2	Model set-up	27
3.3.3	Wave transformation result	28
3.4	Individual wave overtopping volume	28
3.4.1	Individual wave overtopping volume of barrier without wave wall	29
3.4.2	Individual wave overtopping volume of present barrier and wave wall	33
4	Barrier Closure Analysis	37
4.1	Analysis of closure record	37
4.1.1	Relation between closed times and tide	38
4.1.2	Relation between closed times and wind	40
4.2	Analysis tolerable Vmax estimated by policeman	41
4.2.1	Limitation	41
5	Wave wall design	43
5.1	Effect of plain vertical wave wall on wave overtopping	43
5.1.1	Results	45
5.2	Effect of recurved wave wall on wave overtopping	45
5.2.1	Sensitivity analysis - angle of wave return wall	46
5.2.2	Sensitivity analysis - wave wall height	47
5.2.3	Results	50
6	Cost-benefit Analysis	51
6.1	Economic optimization	51
6.1.1	Investments	52
6.1.2	Risk	53
6.2	Cost-benefit analysis for plain vertical wall	57
6.3	Cost-benefit analysis for recurved wall	58
6.4	Conclusion	59
7	Conclusions and Recommendations	61
7.1	Conclusions	61
7.2	Limitations	62
7.3	Recommendations	62
	Appendix	65
A	Water level and wave condition	65
A.1	Method of computing hydraulic boundary conditions of design return periods	65
A.2	Water height	66
A.3	Wave period	69
A.4	Water level	72
B	Numerical modelling of wave transformation	76
B.1	SWASH script of wave transformation simulation for 1 and 5 years return periods	76
B.1.1	Limitation of wave transformation model	77
C	Cost-benefit analysis	81
	Bibliography	83

List of Figures

1.1	General approach	2
2.1	Map of Churchill Barrier No.2.	3
2.2	The Churchill Barriers from the air.	4
2.3	Birdview of Churchill barrier No.2 on a sunny day.	4
2.4	Five sections along barrier No. 2, divided by overtopping rate	5
2.5	A wild day at Churchill Barrier No.2	7
2.6	Type of breaking wave on a slope	9
2.7	Relative run-up on straight rock slopes with permeable and impermeable core, compared to smooth impermeable slope given by	9
2.8	Wave run-up for (very) steep slopes compared to gentle slopes and situations with (very) shallow foreshores – mean value approach. Based on Victor (2010).	10
2.9	Data of Victor, (2012) with very steep slopes from $\cot\alpha = 0.36$ to 2.75 and fairly low relative freeboards (non-breaking data only).	12
2.10	Definition sketch for assessment of overtopping at composite vertical walls Meer et al. [2016].	14
2.11	Wave wall with significant bullnose at Cascais, Portugal. Courtesy L. Franco.	16
2.12	Parameter definitions for structures with bullnose / wave return walls.	17
2.13	Decision chart summarising methodology for tentative guidance for seaward overhanging bullnose/wave return wall. It is important to note, that the symbols R^*0 and m^* shown in the chart are only used at intermediate stages of the procedure and are defined in the boxes in row 2 of the figure.	18
3.1	Existing barrier, foreshore and bathymetry profile	23
3.2	Cross section sketch of barrier, with present wave wall on crest.	24
3.3	Offshore and barrier toe position	26
3.4	Limits for overtopping for people and vehicles (Meer et al. [2016])	29
3.5	V_{max} as a function of return period	32
3.6	Exceedance probability distribution of V_{max} as a function of return period	32
3.7	Cross section sketch of barrier, with present wave wall on crest.	33
3.8	Definition sketch for assessment of overtopping at composite vertical walls Meer et al. [2016].	34
3.9	Present V_{max}	35
4.1	Number and duration of closure between 2002 and 2016	38
4.2	Tidal environment recorded during campaign.	39
4.3	Probability of a closure happens in each month from 2003 to 2016.	39
4.4	Probability of difference between the time closure happens and high tide from 2013 to 2016.	40

5.1	Effect of plain vertical wave wall on wave overtopping volumes of one-year return period. (Upper horizontal red line is V_{\max_limit} for vehicles, lower red line is V_{\max_limit} for walking people.)	44
5.2	Parameter definitions for structures with bullnose / wave return walls (Meer et al. [2016]).	46
5.3	Wave overtopping volumes as function of bullnose angle range, for various of wave wall heights and return periods.	47
5.4	Variations of wave overtopping volumes on different recurved wall heights with certain bullnose angle.	49
6.1	Tree diagram of circumstances and consequences that would happen to barrier. Unit of V_{\max} is m^3/m	54
6.2	Total cost, investments, and risk cost of plain vertical wave wall, as a function of return period.	58
6.3	Total cost, investments, and risk cost of recurved wave wall with bullnose, as a function of return period.	59
A.1	Visualized results of trials of logarithm and polynomial curve fitting to available offshore extreme wave height, as a function of return period between 1 to 200 years.	67
A.2	Visualized results of trials of logarithm and polynomial curve fitting to available offshore extreme wave height, as a function of return period between 1 to 50 years.	68
A.3	Visualized results of trials of logarithm and polynomial curve fitting to available offshore extreme wave height, as a function of return period between 1 to 5 years.	69
A.4	Visualized results of trials of logarithm and polynomial curve fitting to available offshore extreme mean wave period, as a function of return period between 1 to 200 years.	70
A.5	Visualized results of trials of logarithm and polynomial curve fitting to available offshore extreme mean wave period, as a function of return period between 1 to 50 years.	71
A.6	Visualized results of trials of logarithm and polynomial curve fitting to available offshore extreme mean wave period, as a function of return period between 1 to 5 years.	72
A.7	Visualized results of trials of logarithm and polynomial curve fitting to available offshore extreme water levels, as a function of return period between 1 to 200 years.	73
A.8	Visualized results of trials of logarithm and polynomial curve fitting to available offshore extreme water levels, as a function of return period between 1 to 50 years.	74
A.9	Visualized results of trials of logarithm and polynomial curve fitting to available offshore extreme water levels, as a function of return period between 1 to 5 years.	75
B.1	Wave transformation simulation of one year return period: wave set-up, H_{m0} , $T_{m-1,0}$	78
B.2	Wave transformation simulation of five years return period: wave set-up, H_{m0} , $T_{m-1,0}$	79
B.3	Wave transformation simulation one year return period: wave spectrum	80
B.4	Wave transformation simulation of five years return period: wave spectrum	80

List of Tables

3.1	General approach of wave overtopping simulation and wave wall design.	20
3.2	Designed return period and closure frequency	22
3.3	Existing dimensions of barrier	24
3.4	Astronomical tide levels for Burray Ness	25
3.5	Extreme water levels at the Churchill Barriers No. 2	25
3.6	Joint probability offshore extreme conditions (Bassett et al. [2015]).	26
3.7	Extreme offshore boundary conditions of design return periods.	27
3.8	Extreme wave conditions and water levels at barrier toe, as modelled by SWASH. .	28
3.9	Vmax for all return periods for barrier without wave wall	31
3.10	Present Vmax for design return period	35
5.1	Heights of plain vertical wall of each return periods for each overtopping volume limits.	45
5.2	Recurved wave wall design of each return period for vehicles.	50
6.1	Whole life cost estimate checklist for wave wall	52
6.2	Example costs from the Environment Agency Unit Cost Database associated with coastal walls.	53
6.3	Damages caused by overtopping at Churchill Barrier No.2	53
6.4	Total cost, investments, and risk cost of plain vertical wave wall, as a function of return period.	57
6.5	Total cost, investments, and risk cost of recurved wave wall with bullnose, as a function of return period.	58
7.1	Parameters of optimal wall design.	62
A.1	Joint probability offshore extreme conditions (Bassett et al. [2015]).	65
A.2	Extreme offshore wave height of design return period	69
A.3	Extreme offshore mean wave period of design return period	72
A.4	Extreme offshore water level of design return period	75

List of Symbols

Symbol	Definition	Unit
A_c	armour crest freeboard of the structure	m
b	shape parameter in the Weibull distribution	-
B	width of berm, measured horizontally	m
C	Chart Datum	
g	acceleration due to gravity (= 9,81)	m/s ²
h	water depth in front of toe of structure	m
h_n	height of bullnose	m
h_r	height of recurve / parapet / wave returnwall section at top of vertical wall	m
h_{wall}	height of storm wall on top of barrier crest	m
H_{m0}	spectral significant wave height	m
H_s	significant wave height defined as highest one-third of wave heights	m
L	wave length measured in direction of wave propagation	m
N_{ow}	number of overtopping waves	-
N_w	number of incident waves	-
p_{ow}	probability of overtopping per wave = N_{ow}/N_w	-
P_V	$P(V \geq V)$ = probability of the overtopping volume V being larger or equal to V	-
$P_{V*100\%}$	$P_V \Delta 100\%$	%
q	mean overtopping discharge per meter structure width	m ³ /s per m
R_c	crest freeboard of structure	m
R_u	run-up level, vertical measured with respect to the S.W.L.	m
R_{u2}		
s	wave steepness	-
SWL	still water level	m
T	wave period	s
$T_{m0,1}$	average wave period defined by m_0/m_1	s
$T_{m-1,0}$	spectral wave period defined by $m_1 - 1/m_0$	s
T_p	spectral peak wave period	s
V	volume of overtopping wave per unit crest width	m ³ /m
V_{max}	maximum individual overtopping wave volume per unit crest width	m ³ /m
$T_{m-1,0}$	spectral wave period obtained from spectral analysis	s
h	water depth in front of the structure	m
R_c	crest freeboard of the structure	m
W	crest width of the structure	m
α	angle between overall structure slope and horizontal	°
α	angle of parapet / wave return wall above seaward horizontal, Section 0	°

β	wave direction to the normal of barrier	◦
γ_b	influence factor for a berm	-
γ_{bn}	influence factor for a bullnose at a storm wall on slope or prom- enade	-
γ_f	influence factor for the permeability and roughness of or on the slope	-
γ_v	influence factor for a vertical wall on the slope	-
γ_β	influence factor for oblique wave attack	-
θ	direction of wave propagation	◦
$\xi_{m-1,0}$	breaker parameter based on $s_{m-1,0}$	-
Γ	mathematical gamma function	-
ε	angle of bullnose	◦

Chapter 1

Introduction

1.1 Project background

Churchill Barriers, in Orkney Island, Scotland, were constructed in 1940 primarily as naval defences to protect the anchorage at Scapa Flow, and now serve as causeways. Due to the location and design, barriers are exposed to large storm generated in North Sea, which lead to traffic disruption, and damage to properties. Previous study provided by Bassett et al. [2015] points out that most severe wave overtopping hazard happens to northern end of Barrier No.2. Based on requirement of client, this thesis focus on Barrier No.2 only.

Continuous effort has been made over past tens of years to reduce overtopping risk. In 1990, a short section of one-meter high plain vertical wave wall was constructed at northern end of barrier No.2. Besides, local administration Orkney Island Council (OIC) undertaken annual maintenance, replacement and repositioning of concrete armour blocks on the eastern side of the Barrier No.2 to replace those that have been lost during storm events. However, those measurements are not sufficient enough to provide safe traffic environment. Barriers are closed to vehicles around five times per year, with number of closure increasing. This trend is expected to continue due to the effects of sea level rise.

Due to the ongoing expectation that the roadway should remain accessible during extreme storm conditions, OIC consider the current frequency of barrier closure to be unacceptable and an improved barrier arrangement is therefore required Bassett et al. [2015]. This arrangement must reduce the volume of wave overtopping, and hence the frequency of closure, to an acceptable level Bassett et al. [2015].

In 2012, British company JBA Consulting did preliminary study on Churchill barrier. JBA's report look into a tidal energy extraction scheme at Churchill Barrier 1 and/or 2 and a wave overtopping solution at Churchill Barrier 2 only. The overtopping related part is main input information for this thesis. JBA investigated Besides the work done by JBA, OIC has been recording inspections and closures made by policeman during storms since 2003.

Besides the studies mentioned above, an interesting and valuable video was found during thesis project. An overtopping event on 26th January, 2014 was filmed by a passer-by then uploaded on YouTube ¹. This video shows splash water flying over the crest then heavily hit on passing cars. Although splash looks scary, it did not warn a closure of barrier according to closure.

1.2 Research question

This MSc thesis aims to provide insight in the optimal strategy of reducing wave overtopping volumes and frequency of closure of Churchill Barrier No.2, by investigating overtopping volumes

¹<https://www.youtube.com/watch?v=xW0CohdxJzo&t=2s&list=PLpzEiCcoABrkBysBDsIjX1U8-MvODc8EK&index=2>

of plain and recurved wave walls for various closure frequencies, and exploring tolerable wave overtopping volumes in line with local condition.

1.3 Approach

The main purpose of this study is to find economical and optimal overtopping hazard protection strategy. First step is to analysis problem and give solution based on literature study and boundary condition obtained surging this study.

Closure at barrier is operated by policeman standing at the end of barrier, in this way, closure is decided by policeman based on what he saw, which is purely empirical. Sometimes splash overtopping is safe for cars driving across, but seems danger to policeman, a unnecessary closure will be made. Threshold of closure will help reducing frequency of closure, therefore decrease cost of protection structure. To find this threshold from experience, comparison should be performed between closure and corresponding overtopping index, for example, runup height, discharge, volume, and velocity and trajectories of overtopping jets. During this study, a closure record between is obtained from OIC, but corresponding hydraulic boundary condition with time series is only available for three months. By comparing these two data resource, no closure happened during this three months. However, a relationship be severity and overtopping index will be build up.

Afterwards, protection strategy is discussed to meet requirements of desired closure frequency, followed by cost-benefit analysis.

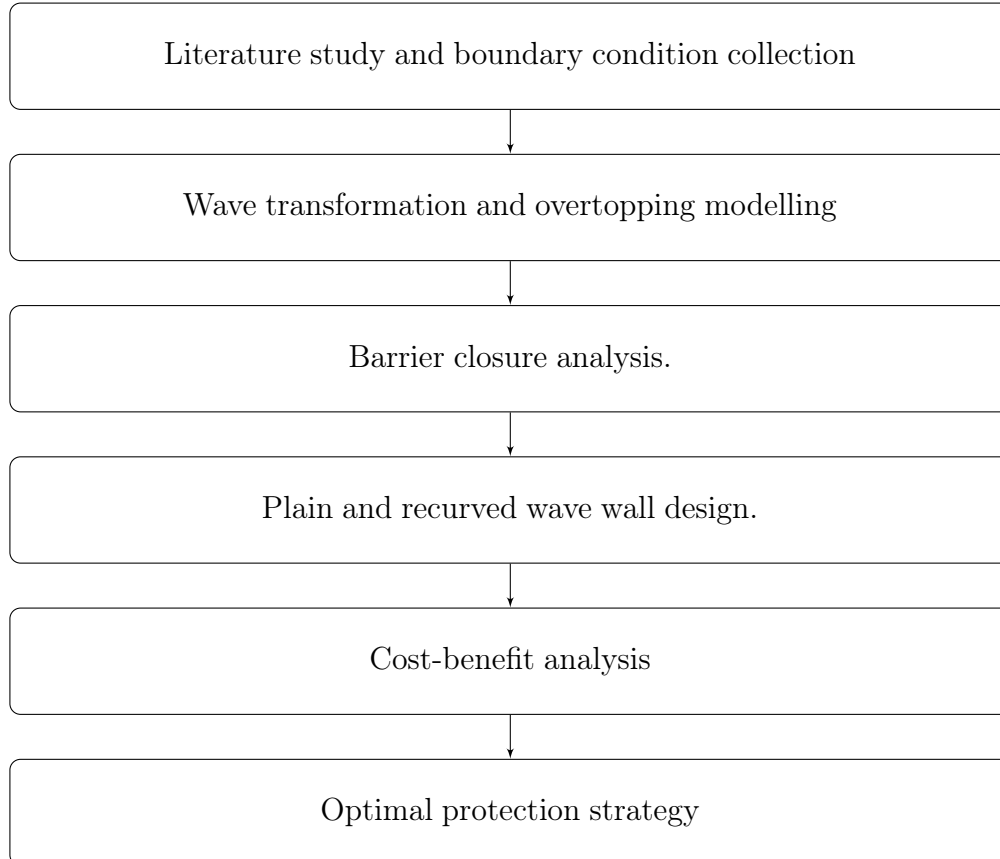


Figure 1.1: General approach

Chapter 2

Physical Context and Literature Study

2.1 Physical context

Churchill Barriers are a series of four causeways in the Orkney Islands, United Kingdom, with a total length of 2.4 km, see Figure 2.1 and Figure 2.2. Overtopping events are observed at all barriers with different frequency¹. However, the Churchill Barriers No.2 is facing most severe overtopping event and is therefore the focus of this thesis.



Figure 2.1: Map of Churchill Barrier No.2.

Churchill barrier No.2 (referred to as barrier in this study) is a 600m long causeway with open sea on east side and harbor on west side, see Figure 2.3. The Churchill Barriers were constructed between 1940 and 1945 to protect the British Naval Fleet, based in Scapa Flow. The construction

¹<https://www.visitorkney.com/news/churchill-barriers>



Figure 2.2: Bird's-eye view of Churchill Barriers (Sara Bailey [2015]).

phase used bolsters-wire cages or baskets filled with broken rock and dropped into the water of the channels. Most of this lies under the surface, with the topping and road surface built from dumped aggregate and concrete blocks.



Figure 2.3: Birdview of Churchill barrier No.2 on a sunny day.

Barrier slope is covered by a single layer of bog concrete blocks with impermeable core underneath. Slope gradient is 1:1.

2.2 Previous study on Churchill barrier No.2

2.2.1 Project history

The Orkney Islands Council (OIC) is the local authority for Orkney, Scotland. In 1990's, a short section of concrete wave return wall was installed at the northern end of barrier (section 5 in Figure 2.4) with the aim of reducing wave overtopping Bassett et al. [2015]. OIC currently manages overtopping risk associated with the barriers. In 2002, OIC started recording every closure and spray on all barriers. In 2013, JBA Consulting was commissioned by Orkney Islands Council to develop technically viable solutions to address wave overtopping experienced at Churchill Barrier Number 2 in Orkney Bassett et al. [2015]. Till now, OIC has responsibility for keeping safety of Churchill Barriers.



Figure 2.4: Five sections along barrier No. 2, divided by overtopping rate

Four overtopping hazard protection are investigated by JBA in 2015, they are offshore breakwater, refacing or rebuilding the existing barrier using rock armour or tetrapod, replacing part of the barrier with a bridge structure and an allowance for tidal energy, beach recharge or widening. The investigation on these four options will not be repeated in this thesis. In this study, a model to assess overtopping hazard is developed, and protection strategy will be proposed. JBA's report 'Churchill Barrier No. 2 Wave Overtopping and Tidal Energy Assessment' is used as basic information for this study, therefore it is briefly introduced in this section. Besides, a wave condition monitoring campaign undertaken during JBA's study will also be used in this thesis.

2.2.2 Input information collection

Input information, including physical context, boundary condition for wave transformation, barrier closure record, and video of overtopping situation are presented in this section. For convenience

of anyone who continue this study, this data and resource will be detailed.

To have a impression of how overtopping at barrier look like, a research was undertaken to collect video and picture of overtopping event. Available recourse is very limited, only a YouTube Video is found ².

A barrier closure recorded is obtained from OIC during this study. OIC has been recording observed spray and closure at Churchill Barriers since 2003. Record is made by policeman who stand on the end of barrier checking spray situation when a storm is warned. This record in in Excel form, details major activity of policeman, description of observed overtopping situation, closure with corresponding time.

Hydraulic and structural boundary condition is obtained from JBA and OIC. In 2013, OIC hired a British company JBA, to perform primary investigation on overtopping protection design and potential tidal energy development. JBA's report provides structural conditions and extreme hydraulic boundary condition. During the investigation, OIC hired Partrac Ltd to undertaken an one and a half month monitoring campaign in 2013, including wave, condition, wind condition and water level with time series. Unfortunately, OIC's closure record shows that no closure happened during this period, only three light sprays and one moderate spray were observed.

2.2.3 Overtopping hazard at Churchill Barriers

Every year, people drown being swept from UK coastal paths. Flood prone coasts are often protected by structures against erosion or flooding. Hazards from wave overtopping arise under three categories :

- Direct hazard of disruption, injury or death to people living, working or travelling in the area defended;
- Damage to property and / or infrastructure, including loss of economic resource, or disruption to a process;
- Damage to defence structure(s), short- or long-term.

The main societal response to these hazards is commonly to construct new defences, but responses should now always consider three Bruce et al. [2002]:

- The main societal response to these hazards is commonly to construct new defences, but responses should now always consider three options;
- Move or modify human activities in the area subject to flooding hazard, modifying land use category;
- Accept occasional hazard at acceptable risk by providing for temporary use with warning and evacuation systems, and/or use temporary or demountable flood defence systems to reduce direct hazards;
- Increase defence standard to reduce risk to acceptable levels by enhancing the defence and/or reducing loadings.

Churchill Barriers were constructed by an Italians in 1940. The causeways are built on gabions (wire cages filled with rocks), which were dropped into the channel and then topped with large concrete blocks. Some 40,000 cubic metres of rock were deposited in the water, which could be anything up to 70 feet in depth, using overhead cableways known as blondins. This was then topped by 300,000 tonnes of concrete blocks, which forms the routes visible today. Rock was quarried locally on Orkney, while the concrete blocks were cast on the islands. The project was huge, and involved the construction of a railway to transport the stone and concrete to the construction area, the overhead cableways, piers on the islands, and power stations to provide electricity.

²<https://www.youtube.com/watch?v=xW0CohdxJzo&list=PLpzEiCcoABrkBysBDsIjX1U8-MvODc8EK>

Wave overtopping of the barriers occurs during storm events that originate in the North Sea, with waves propagating into Holm Sound and breaking against the eastern side of the barriers. During large storm events there have been incidents where members of the public have driven across the barriers and experienced damage to their vehicles, such as broken windscreens and car body damage. Anecdotal evidence (including recent reported incidents in December 2014) suggests that the largest rate of wave overtopping at Barrier No. 2 is experienced at the northern end of the barrier. A review of road closure information (described in Chapter 4) indicates the frequency of wave overtopping events resulting in barrier closure have increased over recent years, especially in winter season.

Orkney Island Council (OIC) currently manages the overtopping risk associated with the barriers. A short section of concrete wave return wall was installed at the northern end of the barrier in the 1990's with the aim of reducing wave overtopping. OIC also undertakes annual maintenance, replacement and repositioning of concrete armour blocks on the eastern side of the barrier to replace those that have been lost during storm events. Following the forecast of large storm events OIC deploy members of staff to monitor the wave conditions at the barriers and determine whether it is safe for public use. If deemed unsafe, the barrier is closed until conditions are considered safe again. Due to the ongoing expectation that the roadway should remain accessible during extreme storm conditions, OIC consider the current frequency of barrier closure to be unacceptable and an improved barrier arrangement is therefore required. This arrangement must reduce the volume of wave overtopping, and hence the frequency of closure, to an acceptable level.

Wave overtopping is of principle concern for structure constructed primarily to defend against flooding, for Churchill barriers, termed sea defence to provide traffic on dike crest. Two forms of overtopping, first from is called 'green water' overtopping, in this case a continuous sheet of water passes over the crest, the second form of overtopping occurs when waves break on the seaward face of the structure and produce significant volumes of splash. These droplets may then be carried over the wall either under their own momentum or as a consequence of an onshore wind. An important exception is the effect of splash in reducing visibility. Figure 1 is taken by a witness of overtopping on Churchill barrier No.2 on 26th, Jan 2014. The water flying over dike crest in form of spray, this belongs to splash overtopping. The overtopping water break on the concrete armour slope and produce significant volumes of fine droplets. The splash can be carried over the wall or dike crest under their own momentum and/or driven by wind.



Figure 2.5: A wild day at Churchill Barrier No.2

Record of barrier closed event is extracted from OIC Roads home page on Twitter, which is This is used as an alert service when weather conditions are likely to result in disruption at the Churchill Barriers, and to announce Barrier closures, review times and the re-opening of the causeways. According to this record, all storm events happen in winter time, between October and December, as well as January and March.

Knowledge of just mean and/or wave by wave overtopping discharges are not sufficient enough for the assessment of direct hazard to people and vehicles on crest, which is immediately behind the seawall. The hazard of overtopping on Churchill barrier is mainly caused by the splash water over crest during storm event.

Hazard driven flow parameters are essentially the mean overtopping discharge and the maximum overtopping volume, as well as overtopping flow depths and velocities. The mean overtopping discharge is the most widely used to judge allowable overtopping. The mean overtopping discharge is the most widely used to judge allowable overtopping. An extensive database on mean overtopping discharge has been gathered in the scope of the CLASH project (<http://www.clash-eu.org>). However, the mean discharge does not always describe the real behaviour of wave overtopping, where only the larger incoming waves will reach the top of the structure and promote overtopping Carrasco et al. [2014]. JBA assessed overtopping hazard at barrier based by mean discharge, in the study, wave runup height, discharge, volumes and overtopping jets are assessed instead of only mean discharge. However, there remain also two difficulties in specifying safety levels with reference to maximum volumes rather than to mean discharges. Firstly, methods to predict maximum volumes are available for limited structure types, and are not well-validated. Secondly, data relating individual maximum overtopping volumes to hazard levels are still very rare Meer et al. [2016].

2.3 Wave transformation

Wave transformation from offshore to will be performed in this study, as wave condition at toe will be input for wave overtopping simulation. Multiple numerical models are available for wave transformation, such as SWASH, SWAN and Xbeach. The model used in this study is SWASH, since author has experience with SWASH from previous study.

SWASH will translate offshore wave condition obtained during the campaign, to wave condition at toe. SWASH, which stands for Simulating WAVes till SHore, is a wave-flow model for the coastal regions up to the shoreline (The SWASH team, 2015).

SWASH is a non-hydrodynamic model, intended for prediction of transformation of disperse surface waves from offshore to shoreline. The idea behind it is 'to provide an efficient and robust model that allows a wide range of time and space scales of surface waves and shallow water flows in complex environments to be applied.' (The SWASH team, 2015). SWASH uses nonlinear shallow water, including non-hydrostatic pressure term. Near barrier toe, non-hydrostatic is no longer negligible compared to hydrostatic pressure term. Wind term is negligible because fetch is relatively short.

2.4 Run-up and overtopping at sloping structure

Waves at barrier are generated in the North sea, then propagate to harbor. Breaker parameter can tell something about type of wave breaking on slope. Breaker parameter is defined as:

$$\xi_{m-1,0} = \tan\alpha / (H_{m0}/L_{m-1,0})^{1/2} \quad (2.1)$$

with $L_{m-1,0}$ being the offshore wave length.

This number gives a relation between fore shore slope and wave steepness to define the breaker type.

Wave run-up has always been less important for rock slopes and rubble mound structures and the crest height of these type of structures has mostly been based on allowable overtopping, or even on allowable transmission (low-crested structures). Still an estimation or prediction of wave run-up is valuable as it gives a prediction of the number or percentage of waves which will reach the crest of the structure and eventually give wave overtopping. This number is needed for a good prediction of individual overtopping volumes per wave Bruce et al. [2008].

Fig 2.7 gives 2% wave run-up heights for various rocks slopes with $\cot\alpha = 1.5, 2, 3$ and 4 and for an impermeable and permeable core of the rubble mound. The graph gives values for a large range of

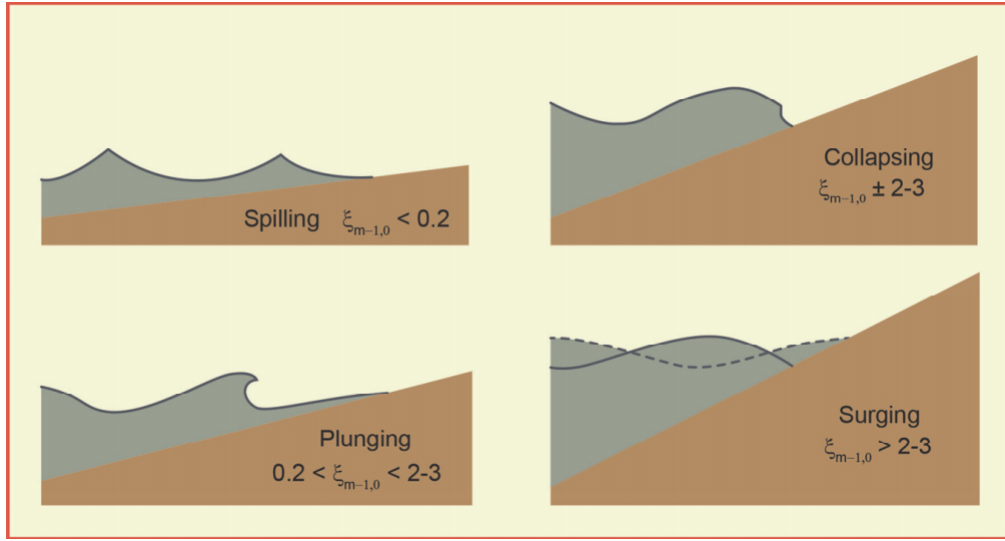


Figure 2.6: Type of breaking wave on a slope

the breaker parameter $\xi_{m-1,0}$, due to the fact that various slope angles were tested, but also with long wave periods (giving large $\xi_{m-1,0}$ values). Most breakwaters have steep slopes of 1:1.5 or 1:2 and thus the range of breaker parameters is often limited to $\xi_{m-1,0} = 2-4$.

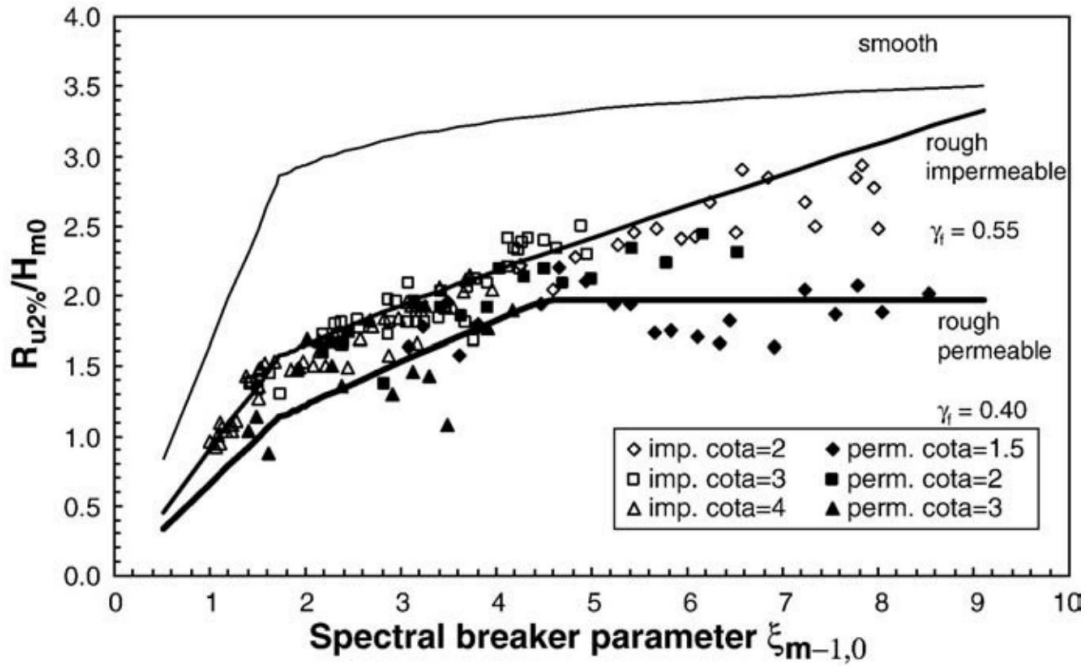


Figure 2.7: Relative run-up on straight rock slopes with permeable and impermeable core, compared to smooth impermeable slope given by

Wave run-up calculation follows equation:

$$R_{u2\%} = H_{m0} * 1.75 * \gamma_b * \gamma_f * \gamma_\beta * \xi_{m-1,0} \quad (2.2)$$

with a maximum of

$$R_{u2\%} = H_{m0} * 1.07 * \gamma_{f \text{ surging}} * \gamma_{\beta} * \left(4.0 - \frac{1.5}{\sqrt{\gamma_b * \xi_{m-1,0}}}\right) \quad (2.3)$$

With a maximum $R_{u2\%}/H_{m0}=3.21$ for structures with an impermeable core.

For steeper slope (large $\xi_{m-1,0}$ value) with a impermeable core, the surging waves only run up and down the slope and all the water spray in the armour layer, leading to fairly high run-up. The surging wave actually does not 'feel' the roughness anymore and behaves as a wave on a very steep smooth slope Bruce et al. [2008].

Victor [2012] investigated the cases of steep slopes and small freeboards for smooth sloping coastal structures. However, The study on steep rubble mound armour slope is not as sufficient as steep smooth slope. By assuming steep slopes show no influence of wave steepness on wave run-up it is possible to give a prediction formula that is only based on the slope angle $\cot\alpha$, equation given by Van der Meer et al. [2017]:

$$R_{u2\%}/H_{m0} = 0.8\cot\alpha + 1.6 \quad (2.4)$$

with a minimum of 1.8 and a maximum of 3.00.

Figure 2.8 provided by Van der Meer et al. [2017] shows relative run up for steep slopes up to a vertical wall as a function of the slope angle and excluding the influence of a foreshore.

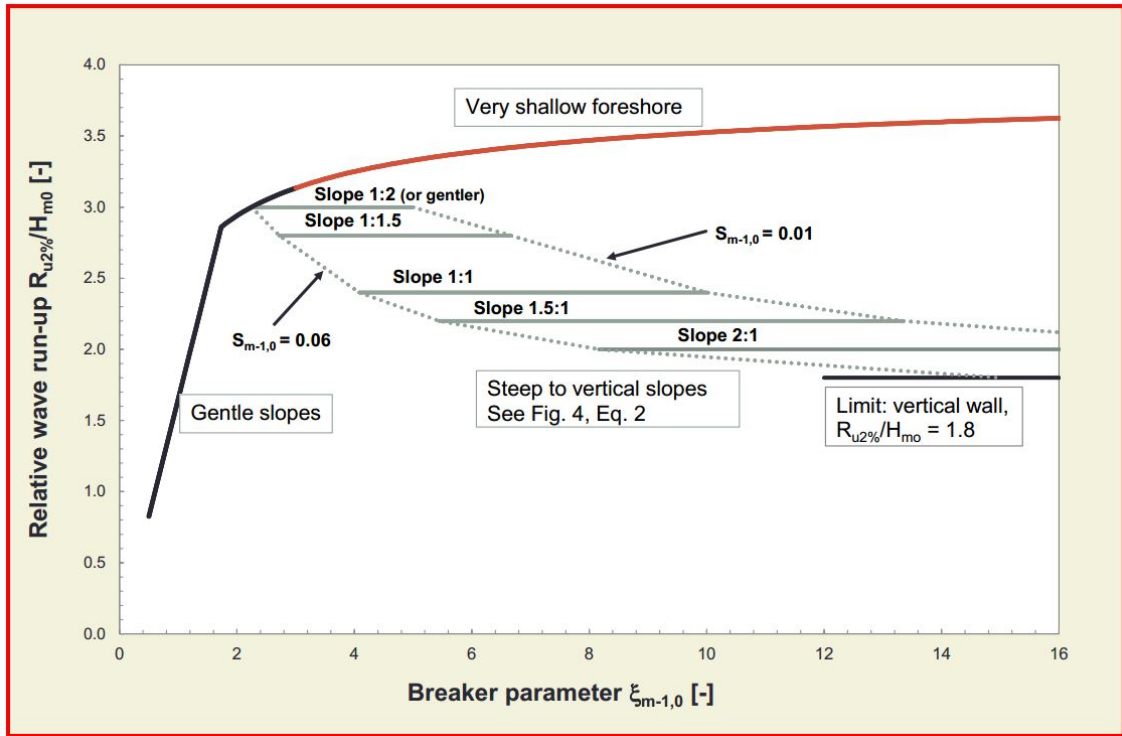


Figure 2.8: Wave run-up for (very) steep slopes compared to gentle slopes and situations with (very) shallow foreshores – mean value approach. Based on Victor (2010).

2.5 Wave overtopping discharge

The mean overtopping discharge or overtopping rate is often used to judge allowable overtopping. It is easy to measure and an extensive database on mean overtopping discharge was gathered for CLASH. This mean discharge does of course not describe the real behaviour of wave overtopping,

where only large waves will reach the top of the structure and give overtopping. Random individual wave overtopping means random in time and each wave gives a different overtopping volume. But the description of individual overtopping is based on the mean overtopping, as the duration of overtopping multiplied with this mean overtopping discharge gives the total volume of water overtopped by a certain number of overtopping waves. The mean overtopping discharge has been described in this section. The individual overtopping wave volumes is the subject in Section 2.4.3. Wave overtopping discharge can be calculated by both numerical model and empirical model. To choose the appropriate method, it is necessary to know the conditions applied to barrier. The features of barrier can be summarized as steep slope (1:1) covered by rubble mound armour, with impermeable core at relative deep foreshore.

Numerical model available are SWASH, however SWASH can not include permeability/roughness of slope in to simulation. So SWASH is not adopted in this study for overtopping rate calculation. Empirical equations are developed based on a large numbers of physical model tests and are therefore more reliable. The literature research on empirical equation will be presented in this section. Literature study is undertaken to look for a equation that works for steep slope, relative deep foreshore.

2.5.1 Basic formula - simple armour slope

Basic formulae for wave overtopping is given by Overtopping Manual 2016 Meer et al. [2016], as: with a maximum of:

$$q = \sqrt{g * H_{m0}^3} * 0.09 * \exp\left(-1.5 \frac{R_c}{H_{m0} \gamma_f \gamma_\beta \gamma_v}\right)^{1.3} \text{ for steep slopes 1:2 to 1:4/3} \quad (2.5)$$

Equation 2.5 gives the average of the measured data and can be used for predictions and comparisons with measurements (mean value approach). The reliability of Equation 6.5 is described by $\sigma(0.09) = 0.0135$ and $\sigma(1.5) = 0.15$. For a design and assessment approach it is strongly recommended to increase the average discharge by about one standard deviation, see Equation 2.6:

$$q = \sqrt{g * H_{m0}^3} * 0.1035 * \exp\left(-1.35 \frac{R_c}{H_{m0} \gamma_f \gamma_\beta \gamma_v}\right)^{1.3} \text{ for steep slopes 1:2 to 1:4/3} \quad (2.6)$$

Limitation of basic formula is that the formula is only applicable to slope gradient between 1:2 to 1:4/3. However, slope of Churchill barrier is 1:1, which is no within formula's range. More academic research is undertaken to find empirical experience regarding very steep slope.

2.5.2 Very steep slopes

What happens if slopes become steeper than say 1:1.5? The two boundaries are known: steep smooth slopes and vertical walls at relatively deep water. Recently, very interesting data by Victor [2012] became available. In total 366 tests were performed on steep and very steep smooth slopes with relatively low freeboards, see Figure 2.9. Tested slope angles were $\cot \alpha = 0.36, 0.58, 0.84, 1.0, 1.19, 1.43, 1.73, 2.14$ and 2.75 . The range of relative freeboards was $0.11 < R_c/H_{m0} < 1.7$. Some of the tests on slope angles of $\cot \alpha = 2.14$ and 2.75 belonged to the breaking wave region³, the majority was, however, non-breaking. These data have been given in Figure 2.9, together with steep smooth slopes and vertical walls at relatively deep water data.

³Equation:

$$q = \sqrt{g * H_{m0}^3} * \frac{0.023}{\sqrt{\tan \alpha}} * \gamma_b * \xi_{m-1,0} * \exp\left(-2.7 \frac{R_c}{\xi_{m-1,0} H_{m0} \gamma_b \gamma_f \gamma_\beta \gamma_v}\right)^{1.3} \text{ breaking waves} \quad (2.7)$$

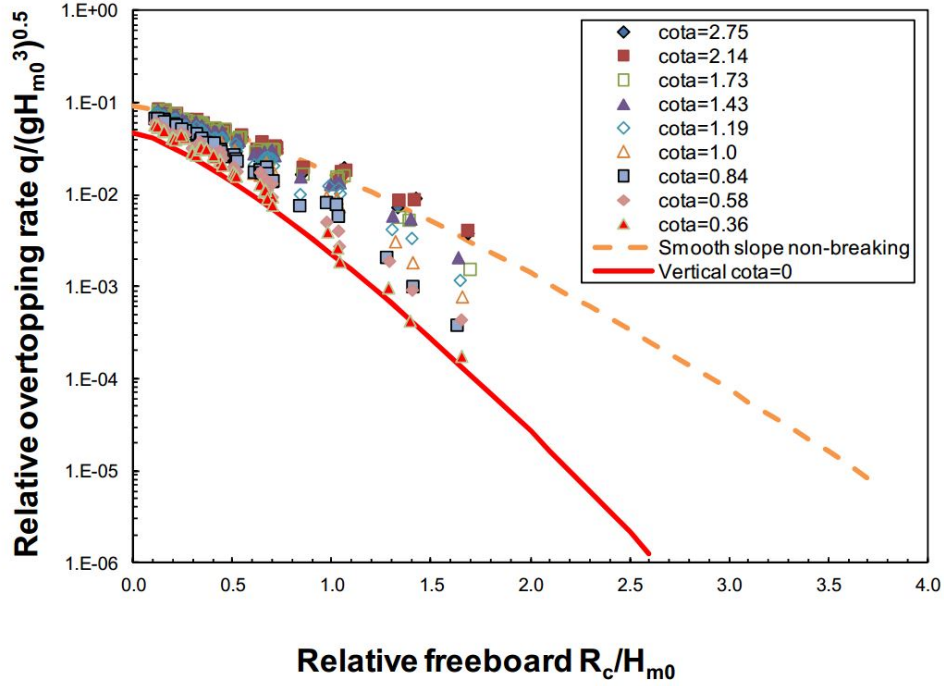


Figure 2.9: Data of Victor, (2012) with very steep slopes from $\cot\alpha = 0.36$ to 2.75 and fairly low relative freeboards (non-breaking data only).

van der Meer and Bruce [2014] discussed overtopping process at slope steeper than 1:1.5 and provides new design formulas. Equation given by van der Meer and Bruce [2014] is applicable for steep low-crested armour slope. Equation 2.8 was fitted to the data in the non-breaking region of each individual slope angle, using $c=1.3$ and fitting a and b .

$$q = \sqrt{gH_{m0}^3} * a * \exp\left(-\left(b \frac{R_c}{H_{m0}\gamma_f\gamma_\beta}\right)^c\right) \quad (2.8)$$

The following equations were found:

$$a = 0.09 - 0.01(2 - \cot\alpha)^{2.1}, \text{ for } \cot\alpha \leq 2 \text{ and } a=0.09 \text{ for } \cot\alpha > 2 \quad (2.9)$$

$$b = 1.5 + 0.42 * (2 - \cot\alpha)^{1.5}, \text{ with a maximum of } b=2.35 \text{ and } b=1.5 \text{ for } \cot\alpha \geq 2 \quad (2.10)$$

$$c = 1.3 \quad (2.11)$$

2.5.3 Composite steep slope with vertical wall on crest

Most breakwaters have a wave wall, capping wall or crest unit on the crest, simply to end the armour layer in a good way and to create access to the breakwater. For design, it is advised not to design a wave wall much higher than the armour crest, for the simple reason that wave forces on the wall will increase drastically if directly attacked by waves and not hidden behind the armour crest.

Overtopping waves that run up higher barrier crest will then hit crest wall and part of them will penetrate through the crest armour. No formulae are present to cope with such a situation, unless the use of the Neural Network prediction method, but the neural network tool actually takes the maximum of A_c and R_c to calculate the overtopping discharge. Various researchers have investigated wave walls higher than the armour crest. None of them compared their results with a graph for composite rubble mound slopes. In essence the message is: use the height of the wave

wall R_c and not the height of the armoured crest A_c . In this way composite part of slope is seen as wave wall. Its result will be slightly lower than reality, but for Churchill barrier, the difference can be neglected. This is because barrier slope is almost as steep as wave wall, wave overtopping process on composite part of slope is vertical wall as indicated in Figure ,

2.5.4 Vertical walls

Vertical wall at barrier is placed on crest, and therefore will be fronted by concrete block mounds. The present mounds can considerably, potentially modifying the overtopping behaviour of the structure Meer et al. [2016]. Three types of mound can be identified.

- Small toe mounds which have an insignificant effect on the waves approaching the wall – here the toe may be ignored and calculations proceed as for simple vertical (or battered) walls.
- Moderate mounds, which significantly affect wave breaking conditions, but are still below water level. Here a modified approach is required.
- Emergent mounds in which the crest of the armour protrudes above still water level.

Barrier falls in the category of emergent mounds. Prediction methods for these structures may be adapted from those for crown walls on a rubble mound Meer et al. [2016]. For design, it is advised not to use a wave wall much higher than the armour crest, for the simple reason that wave forces on the wall will increase drastically if directly attacked by waves and not hidden behind the armour crest.

For assessment of wave overtopping volume at barrier, many academic research was undertaken during this study. No formulae are present to cope with such a situation. In the following section, typical steps down the composite vertical walls branch of the decision chart are presented in steps 1 to 4, in which situation of barrier will be discussed.

Step 1: Is a significant foreshore present or absent?

Foreshore influence incident waves. Relative deep water should be distinguished from influencing foreshore situation. A practical definition of an influencing foreshore is a situation with shallow or intermediate depth water (i.e. not deep water) at the structure toe Meer et al. [2016]. In the case of no influencing foreshore, there is no need to proceed further steps. If an influencing foreshore is present, proceed to step 2

Step 2: Is there a significant mound present?

Analysis of van der Meer and Bruce [2014] shows that a mound, if present in front of the main steep or vertical part of the structure, begins to affect the overtopping when the water depth over the mound, d , falls below 60% of the water depth at the toe of the structure, h , i.e.

Step 3: Is there a likelihood of impulsive overtopping conditions?

Whether impulsive overtopping can occur is determined using Equation 2.12 and 2.13 with parameters defined according to Figure 2.10. Note that the wavelength parameter is calculated for deep water.

$$\frac{d}{H_{m0}} \times \frac{h}{L_{m-1,0}} > 0.65; \text{Treat as non-impulsive conditions.} \quad (2.12)$$

$$\frac{d}{H_{m0}} \times \frac{h}{L_{m-1,0}} \leq 0.65; \text{Treat as impulsive conditions.} \quad (2.13)$$

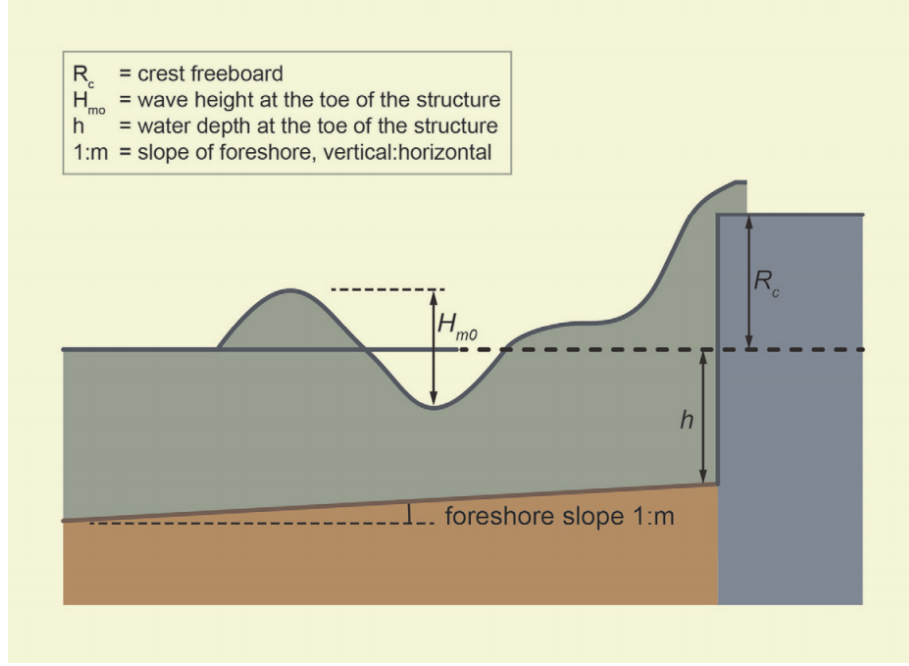


Figure 2.10: Definition sketch for assessment of overtopping at composite vertical walls Meer et al. [2016].

Step 4: Composite vertical structures; non-impulsive conditions or impulsive conditions.

Actually, there are no data available for composite vertical structures on an influencing foreshore, but with non-impulsive conditions. For prediction of the mean discharge at composite vertical walls under conditions where impulsive overtopping is expected, a modified version of the impulsive prediction method for plain vertical walls is recommended, accounting for the presence of the mound by use of the ratio of the water depth over the mound to that at the toe of the structure, d/h .

For composite vertical structures with influencing foreshore absent, equation is given by van der Meer and Bruce [2014] as:

$$\frac{q}{\sqrt{gH_{m0}^3}} = 0.047 \exp\left[-\left(2.35 \frac{R_c}{H_{m0}}\right)^{1.3}\right] \quad (2.14)$$

2.6 Individual wave overtopping volumes

In cases where hazard to pedestrians/vehicles are concerned, an admissible level of overtopping would be more appropriately based upon the volume of an individual overtopping event Bassett et al. [2015]. The finding that overtopping occurs very unevenly in time and space, only part of incident wave can overtop the crest. However, the overtopping volume of each wave may also vary significantly, only large volume can harm traffic. Wave overtopping process at different cross section geometry has different empirical equations. Barrier falls in the category of composite vertical wall, in which crest of the armour protrudes above still water level.

The probability of overtopping $P_{ov} = N_{ow}/N_w$ (the percentage is simply 100 times larger) can be calculated by:

$$P_{ov} = \frac{N_{ow}}{N_w} = \exp\left[-\left(\sqrt{-\ln 0.02} \frac{R_c}{R_{u,2\%}}\right)^2\right] \quad (2.15)$$

Overtopping wave volumes V [m^3] have been successfully approximated by a Weibull distribution,

whose shape factor appears to be larger for very large overtopping and certainly for wave overtopping combined with overflow Hughes and Nadal [2009] Victor et al. [2012]. A larger shape factor results in lower maximum overtopping wave volumes, keeping the mean overtopping volume the same. The conclusion is that the exceedence probability of each overtopping wave is a well fitted by a two-parameter Weibull distribution function:

$$P_V = P[V_i \geq V] = \exp\left[-\left(-\frac{V}{a}\right)^b\right] \quad (2.16)$$

Where P_V is the probability that an individual wave volume (V_i) exceed the specific volume V [m^3], and $P_V\%$ is the percentage of the wave volumes that will exceed the specific volume V . The coefficient b [-] determines the shape of distribution and is therefore the shape factor that helps define the extreme tail of the distribution. The shape factor b is assigned a constant value of 0.75 for sloped coastal structures by Van Der Meer et al. [1994]. This shape factor b increases with decreasing relative freeboard and only applicable to smooth and impermeable structures like a dike or levee.

The value of scale factor a [m^3/m] is equal to:

$$a = \left(\frac{1}{\Gamma(1 + 1/b)}\right) \frac{qT_m}{P_{ow}} \quad (2.17)$$

Γ is the mathematical gamma function. T_m [s] is the average wave period. P_{ow} is the probability of wave overtopping defined by 2.17. The portion of the number of overtopping waves N_{ow} and the number of waves N_w [-].

$$P_{ow} = \frac{N_{ow}}{N_w} \quad (2.18)$$

Formentin et al. [2014] describes the analysis of the Weibull b -value for conventional rubble mound breakwaters as well as for low crested structures with the crest at or just above the water level.

For smooth structure the equation is:

$$b = 0.73 + 55\left(\frac{q}{gH_{m0}T_{m-1,0}}\right)^{0.8} \quad (2.19)$$

For rubble mound armour:

$$b = 0.85 + 1500\left(\frac{q}{gH_{m0}T_{m-1,0}}\right)^{1.3} \quad (2.20)$$

His studies also shows that shape factor a has a large influence on the prediction of maximum overtopping wave volumes.

2.6.1 Recurved wave wall with bullnose - reduction factor

Crown walls or superstructures on top of permeable breakwaters are often used as a measure in existing structures to counteract insufficient design protection against overtopping, see Figure 2.11. These crest elements, generally located well above the design water level, have been found to effectively decrease the mean overtopping discharge over a dike or rubble mound structure. The current study focuses at investigating the reduction in overtopping which can be expected from crest elements on a permeable breakwater.

Coeveld et al. [2007] investigates the effects of crest elements on overtopping of permeable breakwaters. This study gain insight into the influence of crest element geometry and crest element location on wave overtopping of rubble mound breakwaters with crest elements. This study introduces a reduction factor on wave overtopping, i.e. the ratio of overtopping discharge with crest element to the overtopping discharge without crest element, Figure 2.12 gives the definitions of the various employed parameters. To gain insight of possible reductions for a fairly small bullnose, the following method also includes some aspects of geometry of bullnose wave return wall, Allsop et al. [2005] studied effectiveness in reducing overtopping is qualified by a factor K_{bn} , which is defined as:

$$K_{bn} = \frac{q_{\text{with bullnose}}}{q_{\text{without bullnose}}} \quad (2.21)$$



Figure 2.11: Wave wall with ignificant bullnose at Cascais, Portugal. Courtesy L. Franco.

The decision chart in Figure 22.13 can be then used to evaluate value k_{bn} , which can be applied by multiplication to the mean discharge predicted by the most appropriate method for the plain vertical wall. the decision chart shows three levels of decision:

- Whether the parapet is angled seaward or landward.

- If seaward ($\alpha < 90$); whether conditions are in the regime of
 - Little or no reduction (left box; relative freeboards less than the R_0^* parameter calculated in the procedure).

 - Intermediate reductions (middle box; relative freeboards lying between R_0^* and $R_0^* + m^*$, with m^* as calculated in the procedure).

 - Large reductions (right box; relative freeboards greater than $R_0^* + m^*$, i.e. lying above the intermediate reductions regime). If in this regime of largest reductions, there is a further step to determine which of three further sub-regimes (for different R_c/h) is appropriate.

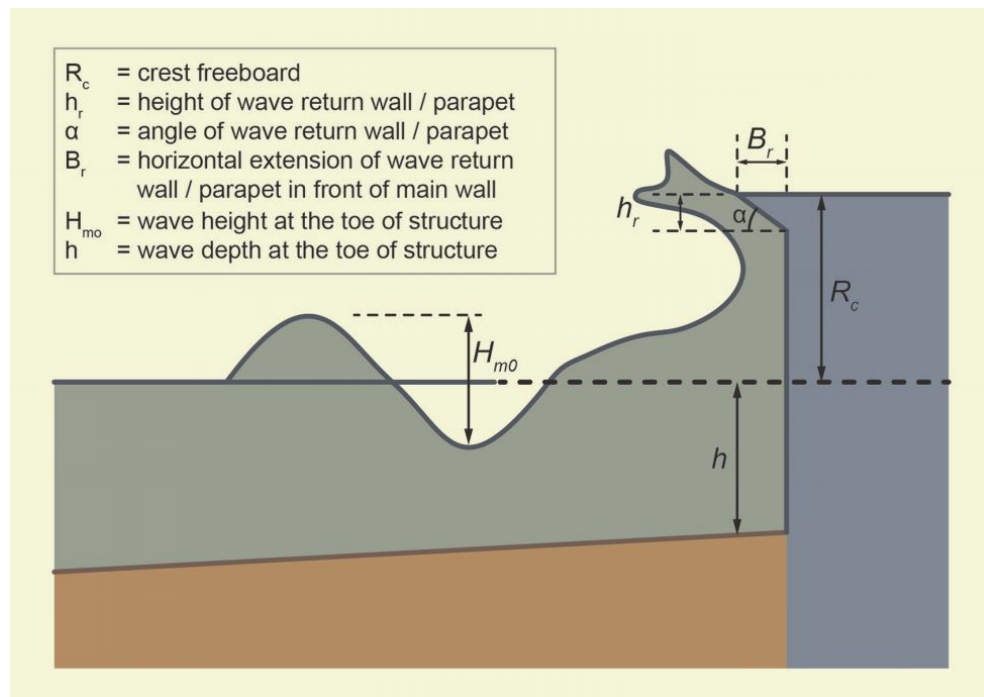


Figure 2.12: Parameter definitions for structures with bullnose / wave return walls.

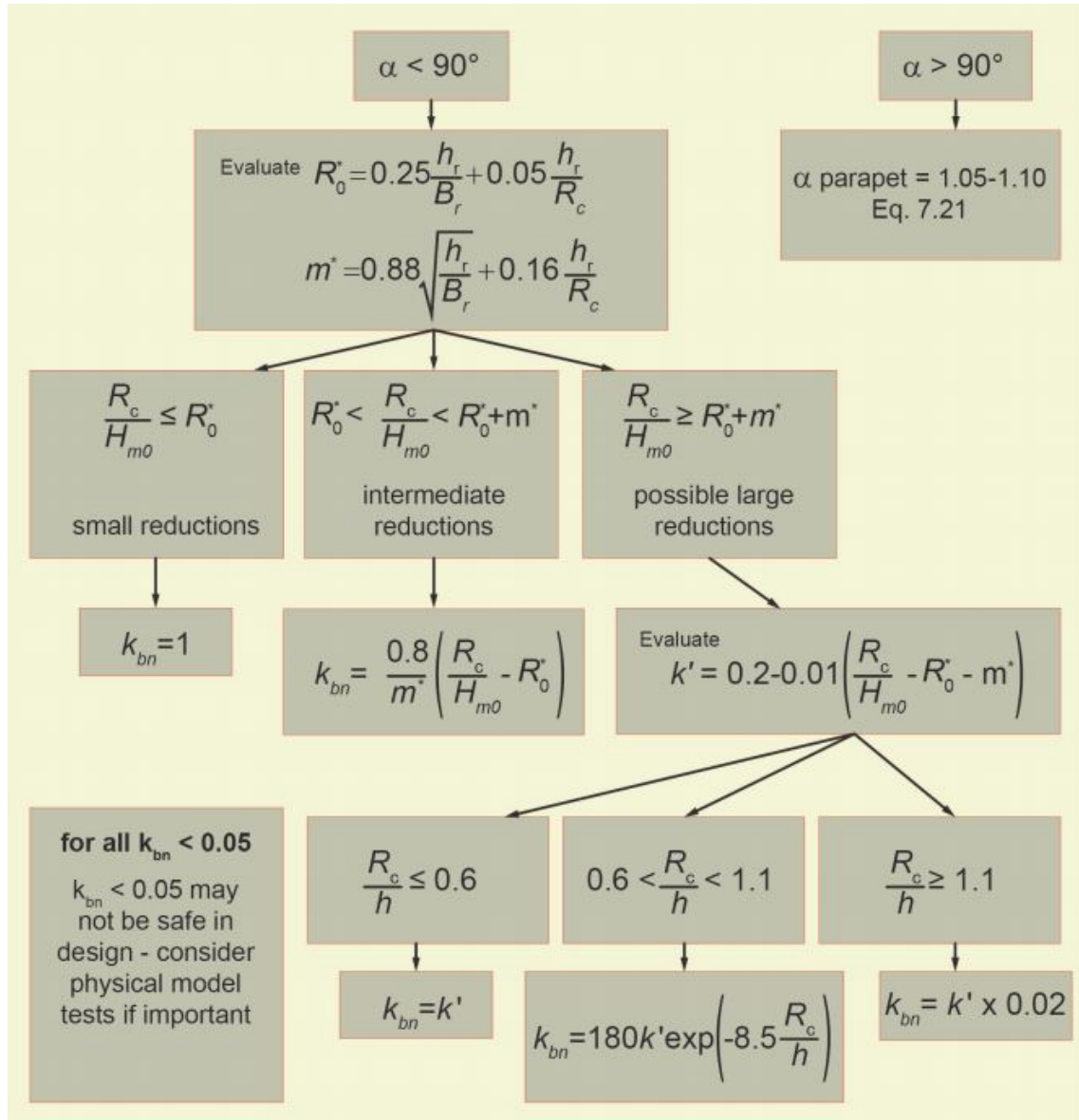


Figure 2.13: Decision chart summarising methodology for tentative guidance for seaward overhanging bullnose/wave return wall. It is important to note, that the symbols R_0^* and m^* shown in the chart are only used at intermediate stages of the procedure and are defined in the boxes in row 2 of the figure.

Chapter 3

Wave Transformation and Overtopping Modelling

This chapter aims transform waves from offshore to barrier toe, then simulate wave overtopping of each design return period. Seven extreme boundary conditions will be numerical modelled to determine wave height, wave period and water level at barrier toe, which will be used as input for wave overtopping modelling. In this chapter, a complete model is proposed, which uses limited offshore hydraulic boundary conditions as input, to compute wave overtopping volumes at barrier for seven return periods.

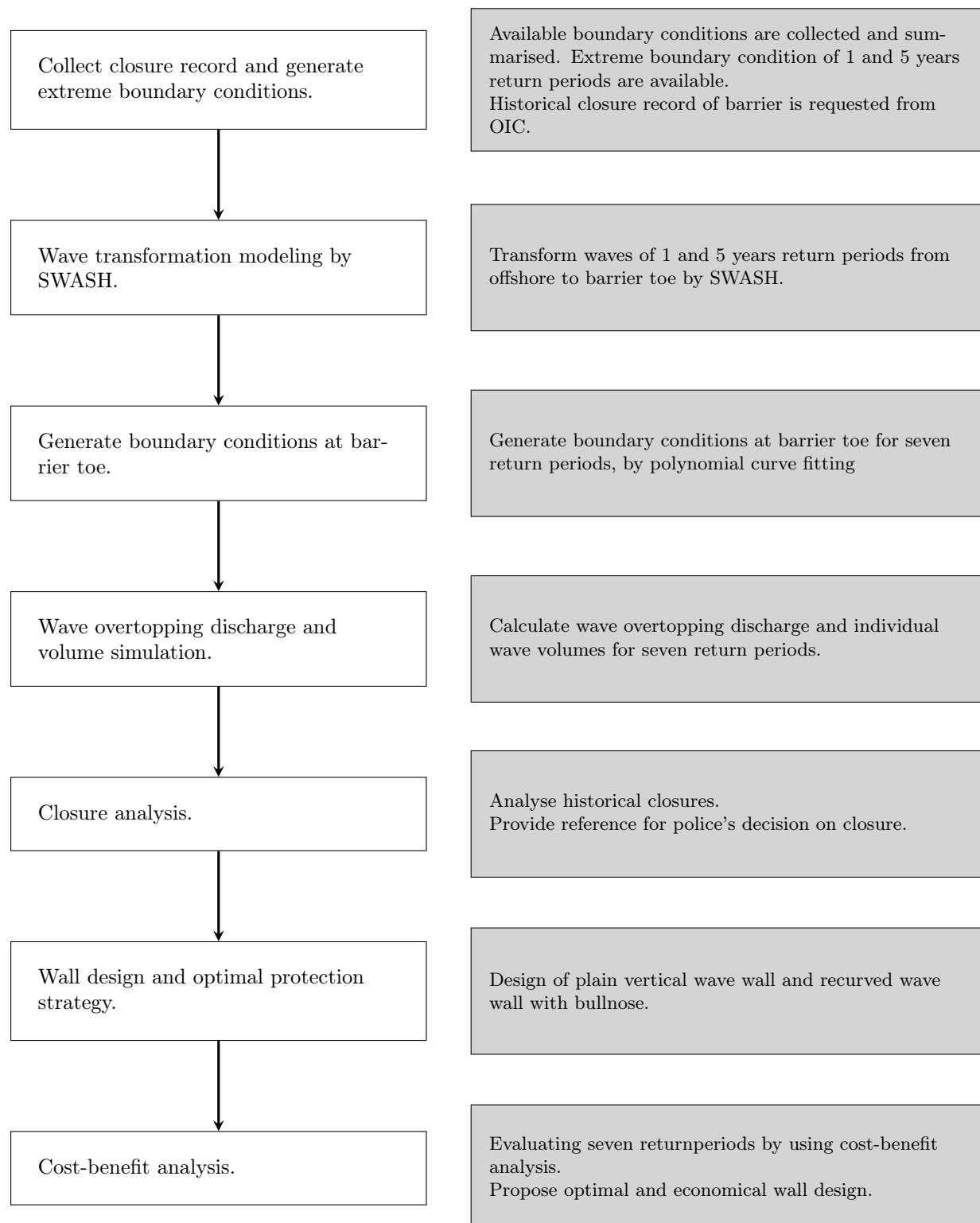
The chapter starts with introducing approach used generate boundary conditions and model wave overtopping in Section 3.1, after which boundary condition at offshore and barrier toe are presented in section 3.2. Wave transformation by SWASH is described in section 3.3. Wave overtopping modelling for barrier without wave wall, and barrier with present wave wall are presented in the last two sections.

3.1 Approach

The purpose of this chapter is to model wave overtopping volume, which will be used for barrier closure analysis and wave wall design in following chapters. Based academic research and data collection in Chapter 2, the following approach is developed, see Table 3.1. The first step towards this goal is determining input parameters of overtopping simulation. These parameters are boundary condition at barrier toe for seven return periods, including wave height, wave period and water level of seven return periods as well as barrier cross section geometry. According to boundary condition collection presented in Section 3.2, only boundary conditions of 1, 5, 10, 20, 50, 100 and 200 years at offshore are available. These are different from targeting boundary conditions that are at toe with return periods of 0.2, 0.5, 1, 2, 3, 4, and 5 years. Thus in step one, needed hydraulic boundary conditions at barrier toe of these seven return periods are generated by using statistical theory, which will be used as input for next step.

Wave transformation by SWASH is presented in section 3.3. Input is extreme offshore waves and water levels of 1 and 5 years' return period, output is extreme waves and water levels of 1 and 5 years' return period at barrier toe. Afterwards, curve fitting is used to predict extreme boundary conditions for needed return periods. Section 3.4.1, 3.4.1, and 3.4.1 present wave overtopping discharge and individual overtopping volume calculation. The present wave volumes with one meter plain vertical wave wall on crest is discussed in Section section Present overtopping volume , which will be used for analysis on historical closure record of barrier in Chapter 4. Finally, vertical and recurved wave wall design are presented in Chapter 5, afterwards these two designs will be evaluated by cost-benefit analysis in Chapter 6.

Table 3.1: General approach of wave overtopping simulation and wave wall design.



3.2 Boundary condition

In order to start wave overtopping simulation, boundary conditions at barrier toe are required. Boundary conditions included structural and hydraulic boundary conditions. Following the approach, hydraulic boundary condition should cover extreme conditions of all seven returns periods. However, plenty of academic research and data request are undertaken, valuable data is very limited. This will be explained in the following sections, to avoid wasting time for further studies. General boundary conditions are presented in Section 3.2.1 to section 3.2.3, include datum reference, designed lifetime and return periods, and climate change. Structural boundary conditions are introduced in Section 3.2.4, followed by hydraulic boundary conditions generated in Section 3.2.5 to Section 3.2.7.

3.2.1 Datum

When measuring the water level, that height must be specified relative to some other levels called the datum. In the UK, with tidal levels the two most commonly used datums are Chart Datum (CD) and Ordnance Datum, in which Chart Datum is the most commonly used for engineering purposes. Previous study on Churchill barrier project used CD as reference level, the decision was made in conjunction with OIC as majority of previously available data was presented in this format. In order to understand the relations among all water level references that could be used for further study, the definitions and conversions are given.

All elevation/depth measurements used throughout the project are quoted to Chart Datum (mCD) at station Burray Ness.

Definitions

- **Chart Datum (CD)** : CD is unique to each location and is usually set to be close to the lowest tide level that can occur under normal meteorological conditions. In case of Churchill Barriers, CD is lowest astronomical tide level in Burray Ness, UK.
- **Ordnance Datum (OD)**: Ordnance Datum is a fixed level everywhere and is common to all locations. OD is easier to relate the height of the water to levels on land.
- **Ordnance Datum Newlyn (mAOD)** : Ordnance Datum at Newlyn
- **SWL**: Still Water Level
- **MSL**: Mean sea level

Conversions

All the conversions applies to Burray Ness, which is the nearest gauge to Churchill Barrier No.2.

- CD - 1.67m = OD
- CD - 1.93m = MSL
- present CD = SWL - 3.18m
- 1 in 200 years water level including climate change: CD = SWL - 5.5m

3.2.2 Life time and return period

The target design life time for all elements is 100 years Bassett et al. [2015]. The expected closure frequency is defined as probability of failure in one year, in other words, for how times policeman need to close the barrier in a single year. The probability of failure in one year is defined as equation 3.1 :

$$P_f = 1/T_r \quad (3.1)$$

where:

- P_f is probability of failure in one year.

- T_r is return period [year/years].

In JBA report return periods are designed as 1, 5, 10, 50, 100 and 200 years Bassett et al. [2015]. More economical closure frequencies are adopted in this study. Based on literature study on physical context of Orkney Islands, barrier locates in a sparsely populated area where traffic is not intensive. Higher but acceptable closure frequency will reduce cost of wave wall. In this study closure frequency less than 0.2 time per year will not be discussed, considering barrier being closed one time in five years is good enough. So the return periods are designed as 0.2, 0.5, 1, 2, 3, 4, and 5 years, which correspond to closure frequency being 5, 2, 1, 0.5, 0.33, 0.25, and 0.2 times per year, see table 3.2.

Table 3.2: Designed return period and closure frequency

Return period (years)	0.2	0.5	1	2	3	4	5
Closure frequency (per year)	5.00	2.00	1.00	0.50	0.33	0.25	0.20

3.2.3 Climate changes

Climate change allowances for both sea level and wave height are determined based on the latest UK Climate Projections (UKCP09). Within UKCP09, estimates for sea level rise are refined by 5th, 50th and 95 percentile confidence ratings. Clients give the choice of percentile. For this study 95th percentile confidence rating is used, which gives sea level rise of 0.72 m by the year 2115 in Orkney. For changes in wave height, UKCP09 gives a prediction of the change in annual maximum wave height for the year 2115 up to 1.0 m for the UK. However, wave height increase is limited by the water depth at the barrier toe and therefore full 1.0 m is not applicable. The 1.0 is applied to offshore wave characteristics, which will be subjected to wave transformation modeling to determine the change in wave height at toe Bassett et al. [2015].

3.2.4 Bathymetry, foreshore and barrier cross-section

Wave overtopping calculation require geometric information on a number of defence characteristics. Churchill Barrier No.2 has open sea on eastern side, and harbour on western side, with normal angle of defense being 128 degrees from North. This study focuses on wave overtopping from eastern side, therefore bathymetry and foreshore to eastern side of barrier will be presented in this section.

Bathymetry and foreshore

The existing bathymetry profile that will be used in overtopping simulation is summarised from Bassett et al. [2015]. JBA report gives a representative profile based to two main resources. First one is the regional models that have incorporated offshore bathymetry based on the latest admiralty charts sourced from FindMAPS. Second one is the high resolution models of the study site have incorporated nearshore bathymetry provided by OIC. OIC also completed a topographic survey of Barrier No.2 to provide cross sections from the seabed on the eastern toe to the road crossing the barrier. It is impossible to determine a single profile that presents entire barrier, therefore a representative equilibrium bathymetry profile provided by JBA will be used in this study. For further structural design phase, a one-meter grid topographic survey is recommended. The representative bathymetry is shown in Figure 3.1.

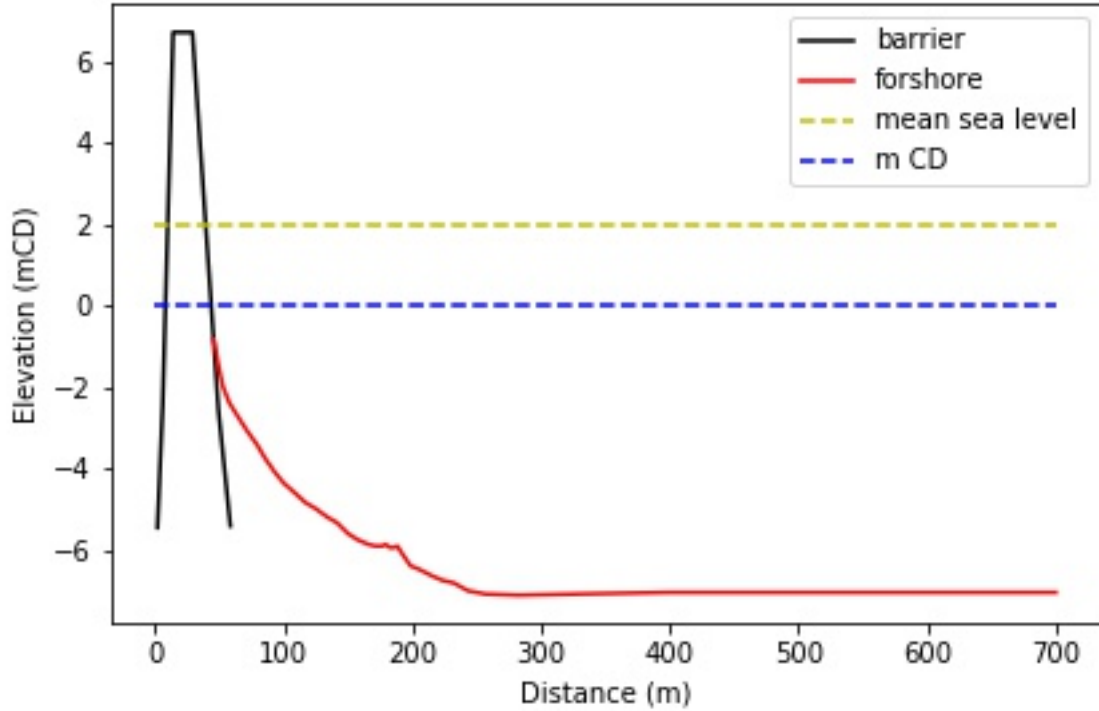


Figure 3.1: Existing barrier, foreshore and bathymetry profile

Level of offshore wave buoy position is -7.04 m CD. Near shore wave buoy is at 300 meters distance to the east of barrier. Seabed starts to go higher from 250m distance from barrier. The slope gradually increase to barrier toe, where barrier slope is 1:1.

Bathymetry is a dynamic profile which changes with sediments accretion and degradation all the time. Morphodynamic is excluded in this study, only hydrodynamic is considered. Sediment transport rate determines the variation of bathymetry in both long term and short term. The sediment transport pathways throughout Orkney are complex, with the interaction of many processes that can, individually, lead to higher or lower rates of transport. The coastline is predominantly rocky and exposed to harsh wave conditions, with sandy beaches lying in protected bays Bassett et al. [2015]. Sediment transport is generally from east to west with sand accreting at eastern barrier toe. While high flood and ebb tide currents once occurred throughout Scapa Flow, due to the constructed barriers prohibiting flow, tidal currents decrease inshore. It is therefore unlikely that tidal currents in this region have any direct effect on the movement of beach material. As a result wave processes dominate the sediment transport or non-tidal ocean circulation currents, which generally run parallel to the coast Bassett et al. [2015].

Cross section

Average barrier level on top of crest deck = 6.73 mCD (4.77m MSL). At the north end, there is a small wave return wall with its crest approximately 1.0 m above the deck level and a length of approximately 130 m; to the south of this a w-shaped vehicle crash barrier offers no additional protection from overtopping, but forms a vehicle impact protection for the public.

Barrier has very steep slope with gradient of 1:1. Slope is covered by rock armour concrete armour. The foundation depth for the causeway is unknown, but historic nautical charts show assumed bedrock levels varying between -9 and 0 mCD. Since the construction of the causeway was in 1940, the area has accumulated sand and fine sediments at a variable elevation across the causeway of between 1 and -4 mCD. Toe position is chosen to be average transition between sand sea bed and armour slope, at -2.25 mCD.

The existing barrier dimension of the causeway are shown in Table 3.3:

Table 3.3: Existing dimensions of barrier

Key Dimensions	South	North
Causeway Toe (mCD)	-9 to 0	-9 to 0
Deck Level (mCD)	6.73	6.73
Crest Height/Freeboard (mCD)	6.73	7.83
Deck Width (m)	6.50	6.50
Slope (gradient 1 in...)	~ 1.00	~ 1.00
Sand level at Causeway (mCD)	-4 to 1	-4 to 1

The face of the east side is very irregular being constructed from large concrete blocks which have moved and been added to over time. Original design of side slope is 1:1.5, however it was actually constructed to 1:1. So 1:1 is a better average figure to use for the full cross section. After years of accretion the barrier foundation was buried by sediments. On average the cross section is shown in Figure 3.2:

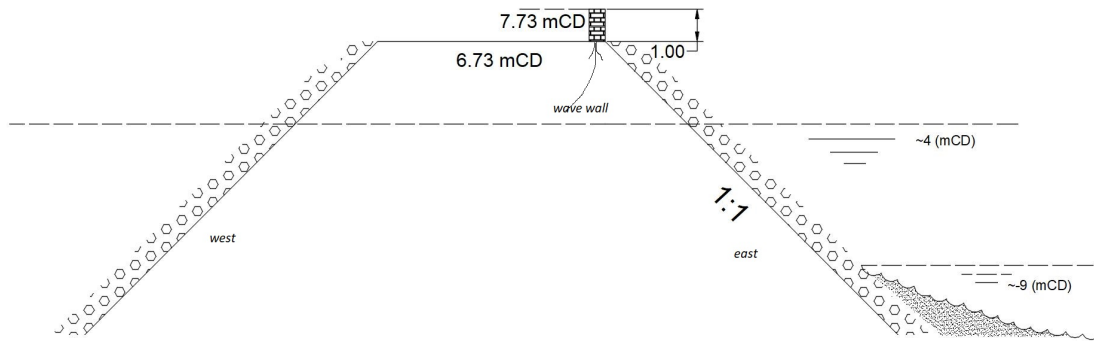


Figure 3.2: Cross section sketch of barrier, with present wave wall on crest.

3.2.5 Water level

Extreme water levels are a combination of a high tide and a storm surge. In this section, offshore extreme water levels are presented, which contains tides, storm surge and climate change. These extreme offshore water levels will be used as input for simulation of water levels at barrier toe in next Section.

Tides

The tidal water levels used in this report is based on admiralty Total Tide provided by Bassett et al. [2015]. The closest standard port to the study site is Wick, located approximately 50 km southeast of the barriers. For tide levels relevant to the study site the closest secondary non-harmonic port is at Burray Ness, which uses predictions based on the standard port at Wick. Tidal variance is included in extreme water level model. The astronomical tidal levels at Burray Ness are shown in table 3.4.

Table 3.4: Astronomical tide levels for Burray Ness

Tidal information	Burray Ness (mCD)
Ordnance datum Newlyn	-1.67
Highest Astronomical Tide (HAT)	3.80
Mean High Water Springs (MHWS)	3.30
Mean High Water Neaps (MHWN)	2.50
Mean Still Water Level (MSL)	1.93
Mean Low Water Neaps (MLWN)	1.30
Mean Low Water Springs (MLWS)	0.60
Lowest Astronomical Tide (LAT)	0.00

Storm surge

Wind blowing over surface of water generates a shear stress. Where a (shallow) water body is enclosed, for example by a coastline, this results in a slope of the water surface. The storm surge will be discussed and simulated in SWASH model in Section 3.3. Other components of storm surge caused by local low barometric pressures, are not significant influential near barrier. JBA did sensitivity testing about influence of surge on extreme offshore water levels. The final model has been forced using tidal conditions representing a typical spring-neap cycle, therefore surge values, and the associated inaccuracies are neglected.

Sea level rise

Sea level rise is dominated by effect of climate on local area. Climate changed is discussed in section 3.2.3.

Offshore extreme water levels

The extreme water levels at the Churchill Barriers have been adopted from the latest extreme sea level estimates available from SEPA, based on the "Derivation of a National Coastal Flood Hazard Dataset" project Bassett et al. [2015]. As such they are different to previous extreme estimates for Orkney; however, they are considered the most up-to-date information available. The project analysed tide level data for Class A water level gauges around the UK and undertook a statistical analysis to produce estimates of extreme water levels. The point used for this project is located approximately 5.5 km southwest of Barrier No. 2 (58.84N, -2.83E) Bassett et al. [2015]. Table 2-3 provides the estimate for extreme still water levels at the site, including sea level rise for the year 2115 ¹.

Table 3.5: Extreme water levels at the Churchill Barriers No. 2

Return period (years)	water level (mCD)	water level (mCD) + climate change in 100years
1	4.17	4.89
5	4.27	4.99
10	4.44	5.16
20	4.52	5.24
50	4.63	5.35
100	4.70	5.42
200	4.78	5.50

In order to find extreme water level of design return period needed in this study, many curve fitting trials are tested. The purpose is to make a good and simple fitting for return periods between 0.2 to 5 years. The fitting tests will be presented in Section 3.2.7.

¹Coastal Flood Boundary Conditions for UK Mainland and Islands, 2011

3.2.6 Wave Condition

3.2.6.1 Extreme wave conditions

The extreme wave conditions at the Churchill Barriers were determined based on the Environment Agency Coastal flood boundary conditions for UK mainland and islands project Bassett et al. [2015], which developed a consistent set of design swell wave conditions around Scotland, England and Wales. All wave conditions are offshore wave conditions, and not representative of the waves actually reaching the barrier. The offshore wave conditions are used for joint probability analysis before being subjected to wave transformation modeling in SWASH to calculate wave conditions at toe. Offshore and toe position are presented in Figure 3.3.

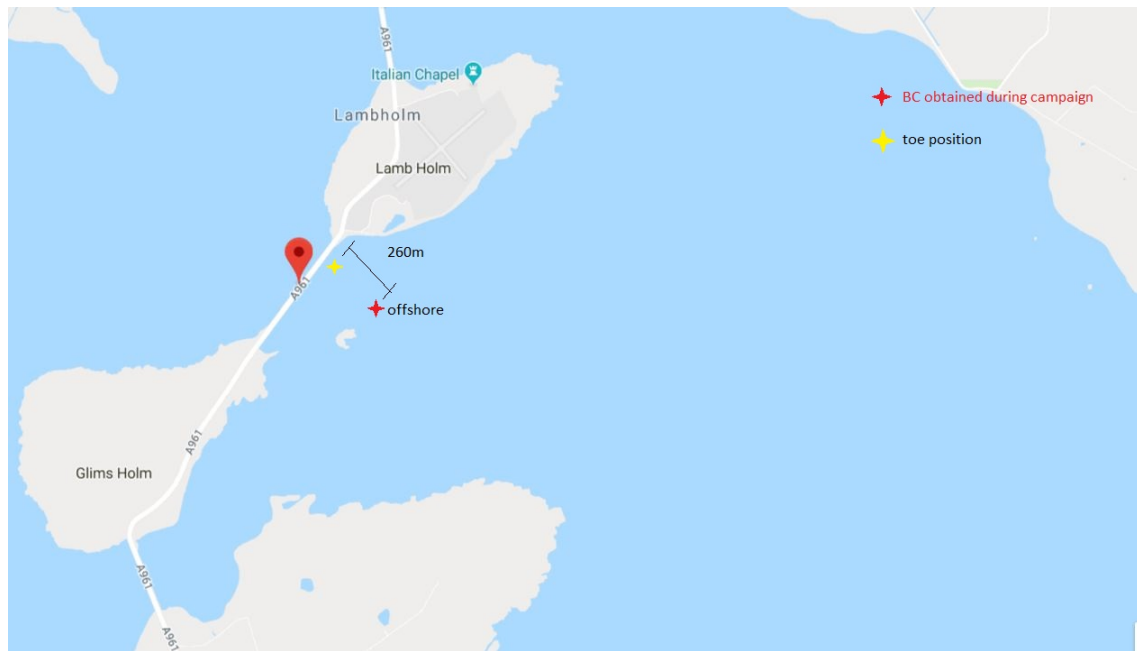


Figure 3.3: Offshore and barrier toe position

3.2.7 Joint probability analysis

In order to determine the combination of water level, wave period and wave height that constitutes the worst case scenario for a given recurrence period, a joint probability analysis must be undertaken. The analysis will be used to determine a range of possible combinations of sea level, wave height and period for each return period. Sea level rise is considered to be 0.72m for the year 2115 under a medium emissions and 95th percentile confidence Bassett et al. [2015]. The joint probability extreme boundary conditions are provided by JBA's report, see A.1:

Table 3.6: Joint probability offshore extreme conditions (Bassett et al. [2015]).

Return Period (years)	H_s (m)	T_m (s)	WL (mCD)	WL + Climate Change (m)
1	4.19	9.37	3.82	4.54
5	5.43	11.92	4.27	4.99
10	5.68	12.22	4.44	5.16
20	5.91	12.49	4.52	5.24
50	6.18	12.82	4.63	5.35
100	6.37	13.04	4.7	5.42
200	6.53	13.24	4.78	5.5

In order to generate the extreme boundary conditions for return periods of 0.2, 0.5, 2, 3, 4 years, curve fitting is carried out in this section. To fit the original data between 1 and 5 years return periods for the best, many trials are tested. Method of exploring best fitting curve and details of trials that have been tested can be found in Appendix A.

Results of extreme offshore boundary conditions of design return periods are presented in Table 3.7.

Table 3.7: Extreme offshore boundary conditions of design return periods.

RP (year/years)	Hs (m)	Tm (s)	WL+climate change (mCD)
0.2	2.95	6.82	4.09
0.5	3.66	8.27	4.34
1	4.19	9.37	4.54
2	4.72	10.46	4.73
3	5.04	11.11	4.84
4	5.26	11.56	4.92
5	5.43	11.92	4.99

3.3 Wave transformation

The section aims to compute wave height, wave period and water level at barrier toe for design return periods. Extreme offshore boundary conditions in Table 3.7 are used as input of SWASH modeling.

SWASH model requirement and description will be introduced in Section 3.3.1. Model boundary setting and key parameters are discussed in Section 3.3.2. At last, model results are presented in Section 3.3.3. SWASH model's script and limitation can be found in Appendix B.

3.3.1 Model requirement and description

The purpose of this model is to get the incident wave condition and water level at toe, which will be used as input for wave overtopping simulation. In this way the requirement of numerical modeling is clear, the model should be able to perform accurate and fast wave transformation modeling from offshore to barrier toe.

There are several numerical model available for wave transformation, SWAN, SWASH, Xbeach, MIKE21 and DELFT3D. Selection of model is made by distinguishing their characteristic. First, model should be applicable to shallow water condition, which may be the case at and before toe position. Second, model can take wind condition into calculation. For this purpose, both Xbeach and SWASH are suitable. Because author has experience with SWASH, SWASH is used in this study. SWASH, which stands for Simulating WAVes till SHore, is a wave-flow model for the coastal regions up to the shoreline (The SWASH team,2015).

The boundary condition have been defined in previous section, the distance from offshore wave climate to barrier toe is 260m. Fetch implemented in SWASH model is therefore 260m. Only hydrodynamics will be modelled.

3.3.2 Model set-up

The computational grid cell in SWASH is 0.5m. The offshore boundary location is at $x=320\text{m}$, toe location is at $x=50\text{m}$. In the vertical, depth of seabed at offshore boundary location is -9 mCD, which gives maximum water depth of computation domain. Single layer is applied throughout the whole grid.

As initial condition, velocity component are set to zero. At offshore boundary, waves are generated based on a JONSWASP spectrum with $\gamma = 3.3$. Sponge layer is set to be 15m. Offshore boundary is an open boundary and not reflective. Toe position in the model is set as open, this is because

the toe position is under water, -2.25 mCD. Since SWASH is not to consider the permeability of concrete blocks on the slope, the height of crest is reduced to complete this boundary with crest set as +3 mCD. Toe position is chosen to be transition between sand sea bed and armour slope, at -2.25 mCD.

Bottom friction is given by Bassett et al. [2015], friction factor is 0.24. Fetch of transformation is 350 meters long, which is short enough to neglect wind effect on wave transformation.

Sponge layer at toe side of computational domain. Sponge layer is effective in absorbing wave energy at open boundaries where waves are supposed to leave the computational domain freely. To make sure no wave reflection at barrier toe, the sponge layer is set to be 50m long. Values of 100m and 150 m are also tested, and result is same as 50 m.

3.3.3 Wave transformation result

Result of SWASH wave transformation is summarised in Table 3.8.

Table 3.8: Extreme wave conditions and water levels at barrier toe, as modelled by SWASH.

RP (years)	0.2	0.5	1	2	3	4	5
Hs at toe (m)	3.32	3.80	4.17	4.54	4.75	4.90	5.02
Tm at toe (s)	6.40	8.85	10.70	12.55	13.64	14.40	15.00
WL at toe (mCD)	3.60	3.95	4.22	4.49	4.64	4.75	4.84

By comparing wave conditions and water level at offshore and at barrier toe, two conclusions are made. Firstly, wave set-up is very small. This can be explained because wind effect is neglected and foreshore is not shallow enough to let wave finish shoaling. Secondly, as expected, wave period at toe is longer than wave period at offshore and wave height at toe is smaller than wave height at offshore.

3.4 Individual wave overtopping volume

By looking at the goal of this project: design wave wall that gives tolerable wave overtopping of desired barrier closure frequency, there are two main questions related: how to simulate wave overtopping and what is tolerable wave overtopping.

To answer the first question, multiple wave overtopping calculation methods are discussed, including numerical model and physical mode. Physical model is costly and time consuming, therefore it is not considered in this study. But physical model is recommended for future design. Numerical model that are commonly applied are empirical equations and neural network (NN), which are both introduced in Chapter 2. Academic research on empirical equations that can be applied to steep composite slopes with relative deep foreshore. NN can be applied to any cases. Severity of wave overtopping is usually described by mean wave overtopping discharge or individual wave overtopping volume. Mean wave overtopping discharge is calculated as volume of overtopping water divided by duration of storm. In this way mean wave overtopping discharge can not describe overtopping process of a single wave. However, waves usually overtops barrier with various severity. The largest single wave, which is the most dangerous one, must be assessed. Individual wave overtopping volume (V_{max}) can describe wave by wave overtopping and give maximum volume of one wave. Therefore, in this study, individual wave overtopping volume is used as index to assess overtopping and possible hazard.

To answer second question, tolerable wave overtopping standard provided by Meer et al. [2016] is used in this study, see Figure 3.4.

Hazard type and reason	Mean discharge q (l/s per m)	Max volume V _{max} (l per m)
People at structures with possible violent overtopping, mostly vertical structures	No access for any predicted overtopping	No access for any predicted overtopping
People at seawall / dike crest. Clear view of the sea.		
H _{m0} = 3 m	0.3	600
H _{m0} = 2 m	1	600
H _{m0} = 1 m	10-20	600
H _{m0} < 0.5 m	No limit	No limit
Cars on seawall / dike crest, or railway close behind crest		
H _{m0} = 3 m	<5	2000
H _{m0} = 2 m	10-20	2000
H _{m0} = 1 m	<75	2000
Highways and roads, fast traffic	Close before debris in spray becomes dangerous	Close before debris in spray becomes dangerous

Figure 3.4: Limits for overtopping for people and vehicles (Meer et al. [2016])

In this section, V_{max} is simulated under two situations, barrier without wave wall and barrier with present wave wall in section 3.4.1 and 3.4.2. Present wave wall is one-meter high concrete caisson, which works as a temporary flood protection structure. Results of V_{max} under these two situation will be analysed in Chapter 4.

3.4.1 Individual wave overtopping volume of barrier without wave wall

The mean overtopping discharge, q, is the main parameter in the overtopping process. It is easy to measure in laboratory wave flume or basin, by using accumulated volume divided by time. However, overtopping process is a dynamic and irregular process and the mean overtopping discharge, does not fully describe the process. Each overtopping wave give a certain volumes of water, V, so the sprays over barrier are of different severity. By knowing the storm duration, t, and the number of overtopping waves during that time, N_{ow}, it is possible to describe this irregular and dynamic overtopping, if the overtopping discharge, q, is known (Meer et al. [2016]). In order to describe the wave by wave spray flying over barrier, overtopping volumes are adopted as index in this study. In the following sections, the simulation of wave overtopping volumes will be presented.

Through civil engineering history the wave run-up and particularly the 2% run-up height was important for the design of dikes and coastal embankments. An estimation or prediction of wave run-up is valuable as it gives a prediction of the number or percentage of waves which will reach the crest of the structure and eventually give wave overtopping. This number is needed for a good prediction of individual overtopping wave volumes Bruce et al. [2008].

Before discussing wave run-up, we see breaker parameter.

Breaker parameter:

$$\xi_{m-1,0} = \frac{\text{slope}}{\sqrt{H_{m0} * L_{m-1,0}}} \quad (3.2)$$

where L_{m-1,0} being offshore wave length which is calculated with T_{m-1,0} in INPUT column in table 3.3.3. Slope of foreshore before toe at h=-2.25m CD is 0.084.

Breaker parameter indicates wave breaking type at toe. The breaker parameter results are between 0.5 and 1, indicates plunging waves breaking on foreshore.

Due to steep barrier slope, which is 1:1, wave steepness will not change but breaker parameter will change. From $\xi_{m-1,0} = 1.8$ the roughness factor $\gamma_{f \text{ surging}}$ increases linearly up to 1 for $\xi_{m-1,0}=10$: $\gamma_{f \text{ surging}} = \gamma_f + (\xi_{m-1,0} - 1.8) * (1 - \gamma_f) / 8.2$. The physical explanation for this is that if the slope becomes very steep (large $\xi_{m-1,0}$ value) and the core is impermeable, the surging waves slowly run up and down the slope and all the water stays in the armour layer, leading to fairly high run-up. The surging wave actually does not “feel” the roughness anymore and behaves as a wave on a very steep smooth slope Bruce et al. [2008].

Wave run-up calculation follows equation:

$$R_{u2\%} = H_{m0} * 1.75 * \gamma_b * \gamma_f * \gamma_\beta * \xi_{m-1,0} \quad (3.3)$$

with a maximum of

$$R_{u2\%} = H_{m0} * 1.07 * \gamma_{f \text{ surging}} * \gamma_\beta * (4.0 - \frac{1.5}{\sqrt{\gamma_b * \xi_{m-1,0}}}) \quad (3.4)$$

With a maximum $R_{u2\%}/H_{m0}=3.21$ for structures with an impermeable core. where

Roughness factor: $\gamma_f = 0.47$ (Meer et al. [2016]).

Barrier crest level = 6.73 mCD

Freeboard level of armour crest: R_c = barrier crest level - water level (mCD).

Berm width $\gamma_b = 0m$

Normal angle of barrier (degrees from Magnetic North) is 128 degrees.

Depth at barrier toe = -2.25 (mCD).

Oblique wave attack: $\gamma_\beta = 1$.

In reality the waves come from different angles, but only the main angle is given, the normal wave attack gives largest volumes. In this calculation, to predicting the largest wave volume the oblique wave attack is neglected.

Because the slope is steeper than the 1:1.5, the result is compared to figure given by Van Der Meer et al. [1994], see Figure 2.7 and result is discussed.

When breaker parameter is larger than 9, for an impermeable core a maximum is reached for $R_{u2\%}/H_{m0} = 3.21$. The physical explanation for this is that if the slope becomes very steep (large $m-1,0$ -value) and the core is impermeable, the surging waves slowly run up and down the slope and all the water stays in the armour layer, leading to fairly high run-up. For breaker parameter smaller than 9, relative wave run-up is proportional to breaker parameter and follows equation 3.4. Comparing to impermeable core of slope $\cot\alpha=2$, slope $\cot\alpha=1$ leads to lower run-up.

Now let us discuss the effect of steep slope on run-up level. As steep slopes show no influence of wave steepness on wave run-up it is possible to give a prediction formula that is only based on the slope angle $\cot\alpha$. Victor [2012] gives a equation:

$$R_{u2\%}/H_{m0} = 0.8\cot\alpha + 1.6, \text{ with a minimum of 1.8 and a maximum of 3.0} \quad (3.5)$$

With $\cot\alpha = 1$, the maximum relative wave run-up is 2.4.

The probability of overtopping:

$$P_{ov} = \exp(-(\sqrt{-\ln(0.02)} * R_c/R_u)^2) \quad (3.6)$$

Average duration of a storm is 2 hours, number of waves per storm is:

$$N_w = 2 * 3600/T_m \quad (3.7)$$

number of overtopping waves per storm is:

$$N_{ow} = N_w * P_{ov} \quad (3.8)$$

The equations give the run-up level in percentage or height on a straight(rock) slope. This is not

the same as the number of overtopping waves or overtopping percentage and Figure 6.4 shows the difference. The run-up is always a point on a straight slope, whether for a rock slope or armoured mound the overtopping is measured some distance away from the seaward slope and on the crest; often behind a crown wall. This means that Equations 6.1, 6.2 and 6.3 always give an over estimation of the number of overtopping waves.

Wave overtopping discharge: steep slope, low-crested, rubble armour slope

Victor's equation is applicable for steep low-crested armour slope, with out on top wave wall, which are the conditions for RP events. Equations given by Victor et al. [2012] are:

$$q = \sqrt{9.81 H_{m0}^3} * a * \exp\left(-\left(b \frac{R_c}{H_{m0} \gamma_f \gamma_\beta}\right)^c\right) \quad (3.9)$$

in which:

$a = 0.09 - 0.01(2 - \cot\alpha)^{2.1}$, for $\cot\alpha \leq 2$ and $a = 0.09$ for $\cot\alpha > 2$

$b = 1.5 + 0.42*(2 - \cot\alpha)^{1.5}$, with a maximum of $b = 2.35$ and $b = 1.5$ for $\cot\alpha \geq 2$

$c = 1.3$

Individual wave overtopping volume of barrier without wave wall

Distribution of individual overtopping wave volumes can be represented by the two parameter Weibull probability distribution, given by the percent exceedance distribution in Equation 3.10.

$$Pv(i) = \exp(-(V(i)/a)^b) \quad (3.10)$$

where Pv is the probability (between 0 and 1) that an individual wave volume (V_i) will be less than a specified volume (V).

The two parameters of the Weibull distribution are the non-dimensional shape factor, b , that helps define the extreme tail of the distribution and the dimensional scale factor, a , that normalizes the distribution.

Γ is the mathematical gamma function.

Maximum expected individual overtopping volume follows Equation 3.11.

$$V_{max} = a * (\log(N_{ow}))^{(1/b)}; \quad (3.11)$$

V_{max} as a function of return period is presented in Table 3.9:

Table 3.9: V_{max} for all return periods for barrier without wave wall

RP	Ru2%(m)	Pov	q(m ³ /s)	b	a	Vmax(m ³ /m)	Rc(m)
0.2	10.66	0.71	0.55	1.45	5.49	20.32	3.13
0.5	12.20	0.82	0.68	1.28	7.95	34.27	2.78
1	13.39	0.87	0.78	1.21	10.21	47.31	2.51
2	14.57	0.91	0.89	1.16	12.86	62.70	2.24
3	15.25	0.93	0.95	1.13	14.59	72.83	2.09
4	15.73	0.94	0.99	1.12	15.89	80.44	1.98
5	16.11	0.95	1.03	1.11	16.97	86.77	1.89

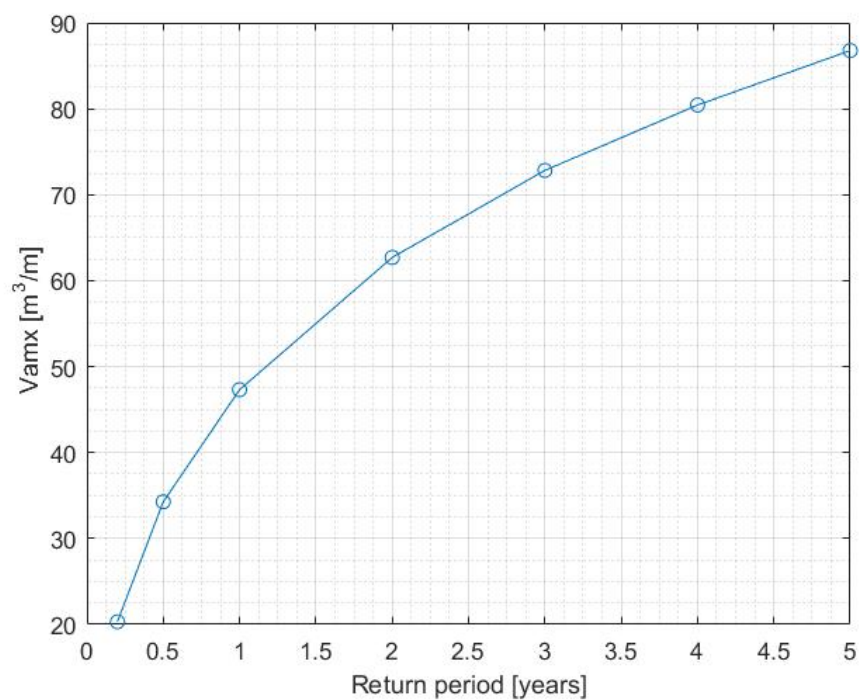


Figure 3.5: Vmax as a function of return period

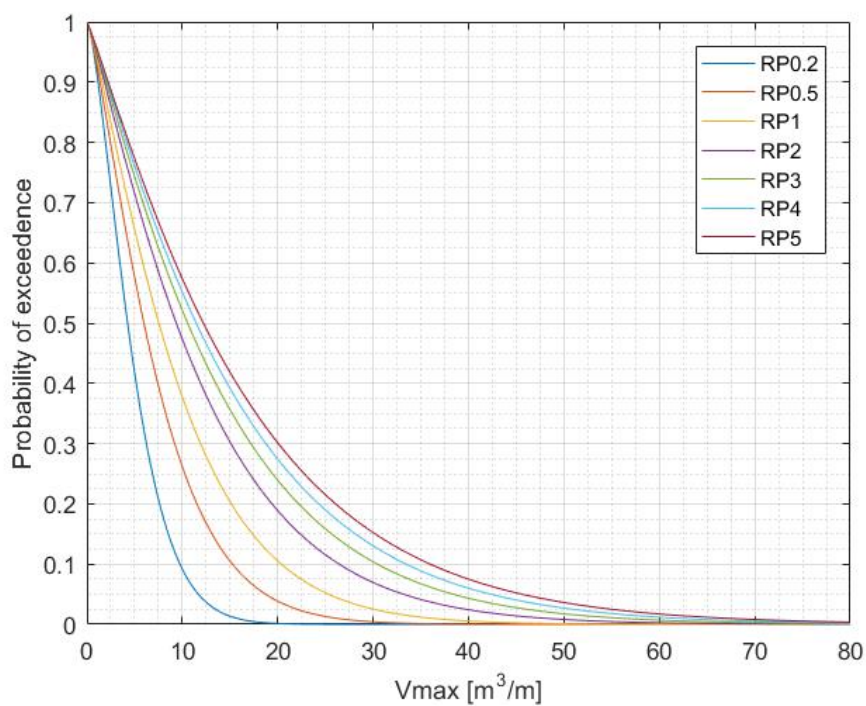


Figure 3.6: Exceedance probability distribution of Vmax as a function of return period

3.4.1.1 Limitation

Limitations of individual wave overtopping volume of barrier without wave wall will be summarised.

Limitation of input

Model input are hydraulic boundary conditions and structural boundary conditions.

Hydraulic boundary conditions including wave height, wave period and water level at barrier toe. These conditions are all predicted based on very limited offshore boundary conditions by using mathematical function. Even though optimal mathematical function that can reduce difference as much as possible has been explored, predictions are always not reality.

Structural boundary condition are barrier cross section, foreshore and bathymetry. Foreshore and bathymetry profile are equilibrium profile, however, in reality the profile varies with season and extreme weather. Variation of the profile will influence V_{max} , therefore, in reality V_{max} can be larger or smaller than predicted value.

3.4.2 Individual wave overtopping volume of present barrier and wave wall

Present wave overtopping flood at North end is protected by a one-meter high plain vertical wave wall, see Figure 3.7. This wall is made of concrete caisson as temporary structure. Present barrier with crest wall has following structural characteristics:

- Very steep slope = 1:1
- Rubble mound armour
- Composite slope: partially submerged, partially emerged
- Wave wall on crest
- Relatively deep foreshore

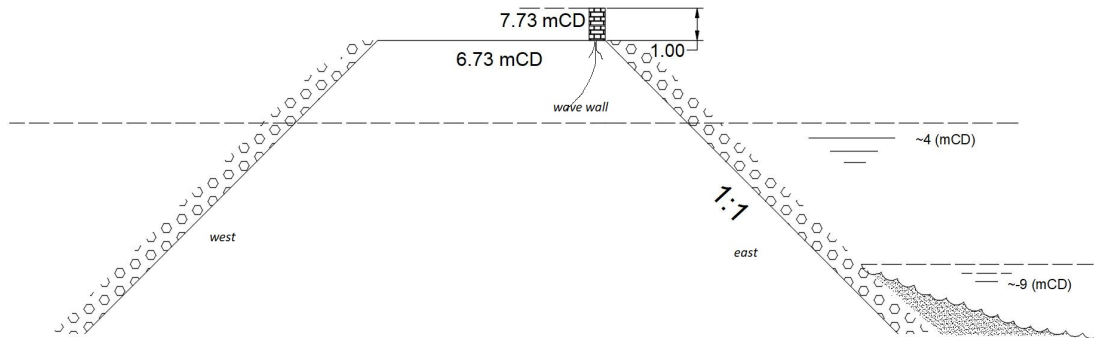


Figure 3.7: Cross section sketch of barrier, with present wave wall on crest.

No formulae are present to cope with a situation that includes all characteristics above. Details of academic research haven been discussed in Section 2.5.3. To proceed, the most similar situation that can be described by available formula is is found. The situation is vertical wall as indicated in Figure 3.8.

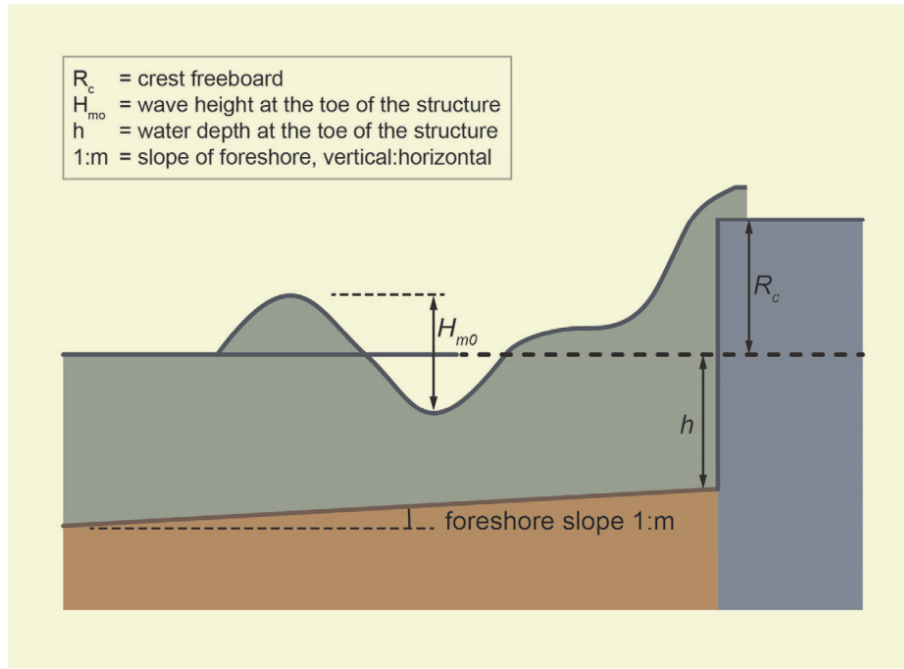


Figure 3.8: Definition sketch for assessment of overtopping at composite vertical walls Meer et al. [2016].

By applying formula of vertical wall on crest. emerged part of slope will be seen as wave wall, which gives $R_c = A_c + \text{wall height}$. Result will be slightly lower than reality, but for Churchill barrier, the difference can be neglected. This is because barrier slope is almost as steep as wave wall. Very steep slope can not dissipate wave energy as much as gentle slope. Wave overtopping process on emerged part of slope is similar to wave process on vertical wall.

Present wave volume is calculated in this section, which will be used for estimating policeman's decision on closure in 4.

For very steep slopes, overtopping discharge follows equation given by van der Meer and Bruce [2014]:

$$q = \sqrt{gH_{m0}^3} \cdot 0.047 \cdot \exp \left[- (2.35 \frac{R_c}{H_{m0}})^{1.3} \right] \quad (3.12)$$

in which $R_c = \text{free board} + \text{wall height}$.

Proportion of waves overtopping at vertical walls is described by Equation 2.20 and Equation 2.17. Maximum wave overtopping volume is

$$V_{max} = a(\ln N_{ow})^{1/b} \quad (3.13)$$

Probability distribution of V_{max} is showed in Figure 5.2

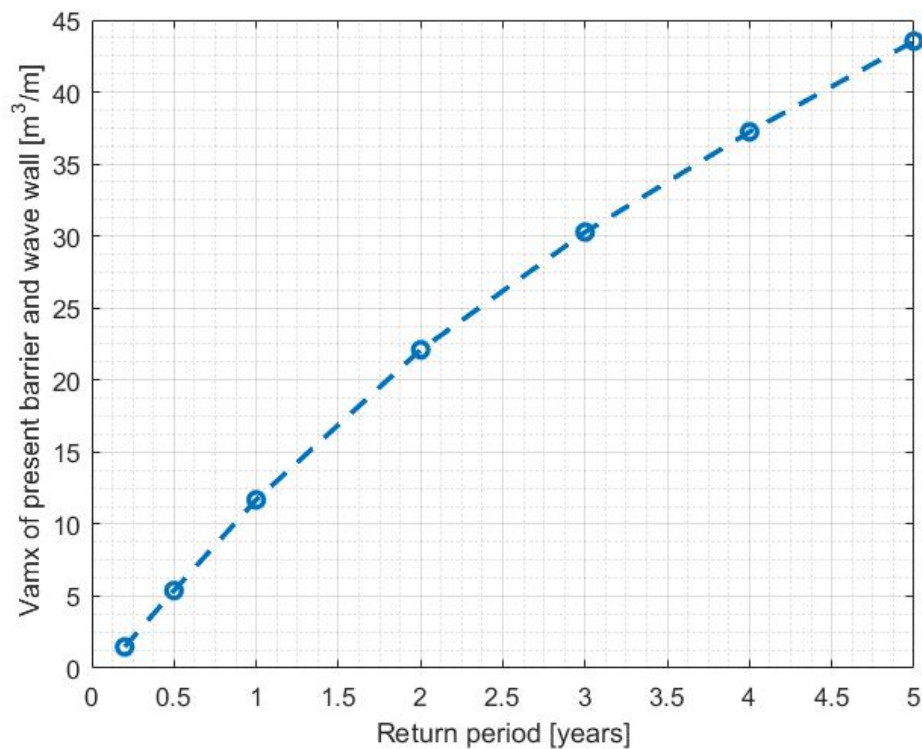


Figure 3.9: Present Vmax

Present Vmax result, see Table 3.10

Table 3.10: Present Vmax for design return period

RP (years)	0.2	0.5	1	2	3	4	5
Vmax [m ³ /m]	1.48	5.39	11.69	22.11	30.28	37.24	43.54

Present average barrier closure frequency is five times per year, correspond to return period of 0.2. Therefore present Vmax is estimated as 1.48 m³/m.

3.4.2.1 Limitation

Limitations of individual wave overtopping volume of barrier with present wave wall will be summarised.

Limitation of input

Model input are hydraulic boundary conditions and structural boundary conditions.

Hydraulic boundary conditions including wave height, wave period and water level at barrier toe. These conditions are all predicted based on very limited offshore boundary conditions by using mathematical function. Even though optimal mathematical function that can reduce difference as much as possible has been explored, predictions are always not reality.

Structural boundary condition are barrier cross section, foreshore and bathymetry. Foreshore and bathymetry profile are equilibrium profile, however, in reality the profile varies with season and extreme weather. Variation of the profile will influence Vmax, therefore, in reality Vmax can be larger or smaller than predicted value.

Limitation of empirical formula

As discussed before in this section, no formulae are present to cope with a situation that includes

all characteristics Churchill barrier has. Therefore formula of vertical wave wall on crest is used, by assuming that emerged part of vert steep rubble slope is seen as vertical wall. Limitations caused by this assumption is that predicted V_{max} will be smaller that reality. Difference between prediction and reality can not be validated duo to absence of research, but can be estimated as negligible. Because steep is very steep and impermeable, wave overtopping process and wave energy dissipated by friction factor will approximately the same as a vertical wall.

Chapter 4

Barrier Closure Analysis

OIC currently manages the overtopping risk associated with the barriers. OIC also undertakes annual maintenance, replacement and re-positioning of concrete armour blocks on the eastern side of the barrier to replace those that have been lost during storm events. Following the forecast of large storm events OIC deploy members of staff to monitor the wave conditions at the barriers and determine whether it is safe for public use. If deemed unsafe, the barrier is closed until conditions are considered safe again. Record of closures are requested from OIC for this study, which will be used analysis of closures' frequency and duration, as well as regularity of closed times. This sections aims to provide insight in closed times and give advice to staff who operate closures.

In this Chapter, barrier closure analysis start with exploring the history closures. By analysing available closure record, closure frequency and duration, relation between closure and tide, and relation is presented in Section 4.1. Afterwards, overtopping volumes of closures are compared with threshold given by overtopping manual to estimate the decisions made by stuff in section 4.2.

4.1 Analysis of closure record

Historical record of closures is requested from OIC during this study. The record is a manually entered into EXCEL file made by stuff on duty, who is responsible for not only monitoring storm and overtopping situations, but also opening and closing causeway. This record shows all closures happened from 2003 to 2016, with corresponding date and time. From 2013 to 2016, corresponding high tide time of each closure is also given.

The first question is how many closures happened in the past. An overview of all recorded closures and their duration is presented in this section. Afterwards, an investigation is carried out to find out the regulation of closed times. Main parameters that contribute to a overtopping, water level and wave height, are analysed. Wave height is dominated by wind, water level is associated with tide and storm surge, so the relations between closed times and wind, closed times and tide should be discussed. Due to limited data of wind, relations between closed times and wind are discussed theoretically in section 4.1.2. Relations between closed times and tide are presented in section 4.1.1

Closure frequency is number of closures happen per year. Due to the ongoing expectation that the roadway should remain accessible during extreme storm conditions, OIC consider the current frequency of barrier closure to be unacceptable and an improved barrier arrangement is therefore required. This arrangement must reduce the volume of wave overtopping, and hence the frequency of closure, to an acceptable level.

Closure frequency is a key criteria of design of flood defence. Smaller frequency require higher wave wall, thus increase cost. In order to explore a appropriate closure frequency, first, present closure record is analyzed, then target closure frequency is proposed in cost-benefit analysis.

Record of closure is requested from OIC during this study. Number of closures per year from 2003 to 2016, and corresponding duration are presented in table 4.1:

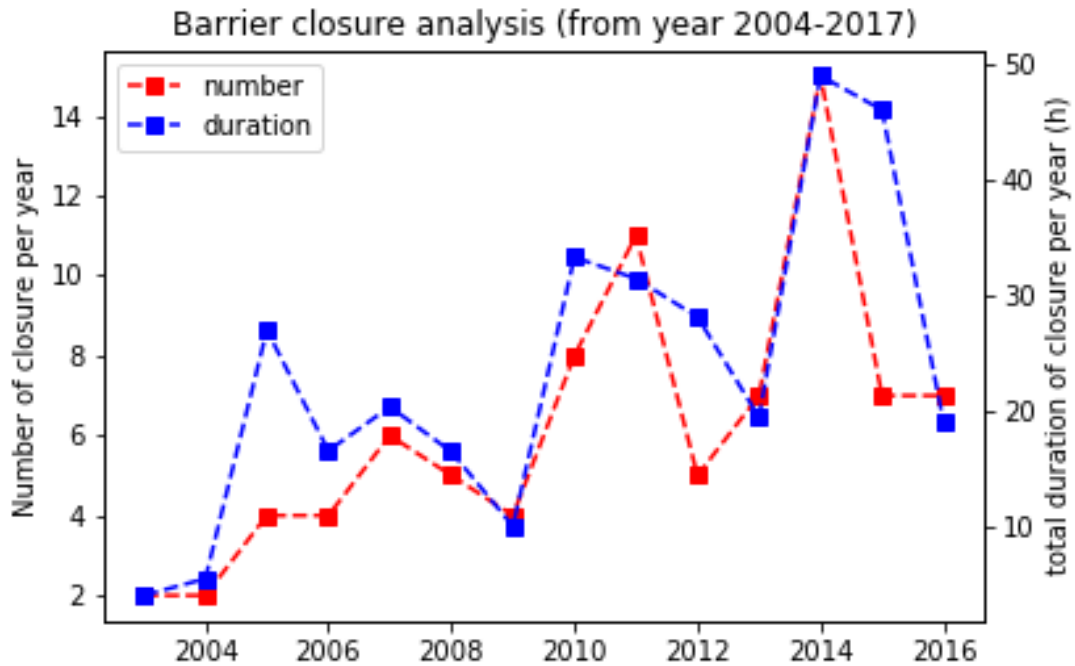


Figure 4.1: Number and duration of closure between 2002 and 2016

Closure frequency since 2003 increases gradually with great variance. The barrier is closed five times per year on average, with a closure frequency of five. This peaked with 15 closures occurring in 2014. Churchill Barrier is a relatively remote area with a small number of residents near around, also the traffic is not intensive. The higher closure frequency means a reduction in reconstruction, along with a lower cost. In order to made overtopping protection structure as economical as possible, improvement of operation management is proposed. Therefore, a series of closure frequencies are proposed, the barrier is closed every 0.5, 1, 1.5, 2, 3, 4, 5 years. In order to find out the regulation of closed times and provided reference for policeman, main parameters that contribute to a storm is analysed. The parameters are, water level, wave height, since wave height is generated by wind, water level is associated with tide, so the relations between closed times and tide are presented in this section.

4.1.1 Relation between closed times and tide

The section aims to explore relations between closed time and tide, thus provide insight in regulation of closed times. First, tidal environment is introduced, followed by discussion of effect of season, spring and neap tide and high tide on closed time.

Tidal environment at barrier

During Campaign, water level is measured and recorded. Those water levels are plotted to find out tidal environment type. The tide characters are showed in figure 4.2 Even though data is available for one and a half month, it shows a complete tidal cycle. Tidal environment at Churchill barrier is mixed type, predominantly semi-diurnal. An area has a semi-diurnal tidal cycle experiences two high and two low tides of approximately equal size every lunar day.

Closed times and season

From May to August, no overtopping event was reported. More than half of overtopping events happened in winter, from November to January. This peaked with 27% of closures occurring in January. It shows that overtopping and season have great dependence. Winter storm at barrier

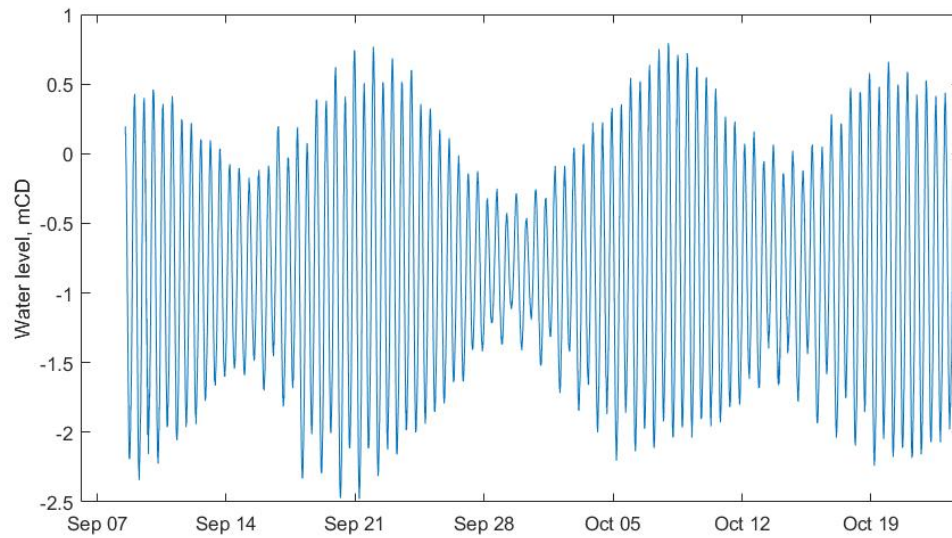


Figure 4.2: Tidal environment recorded during campaign.

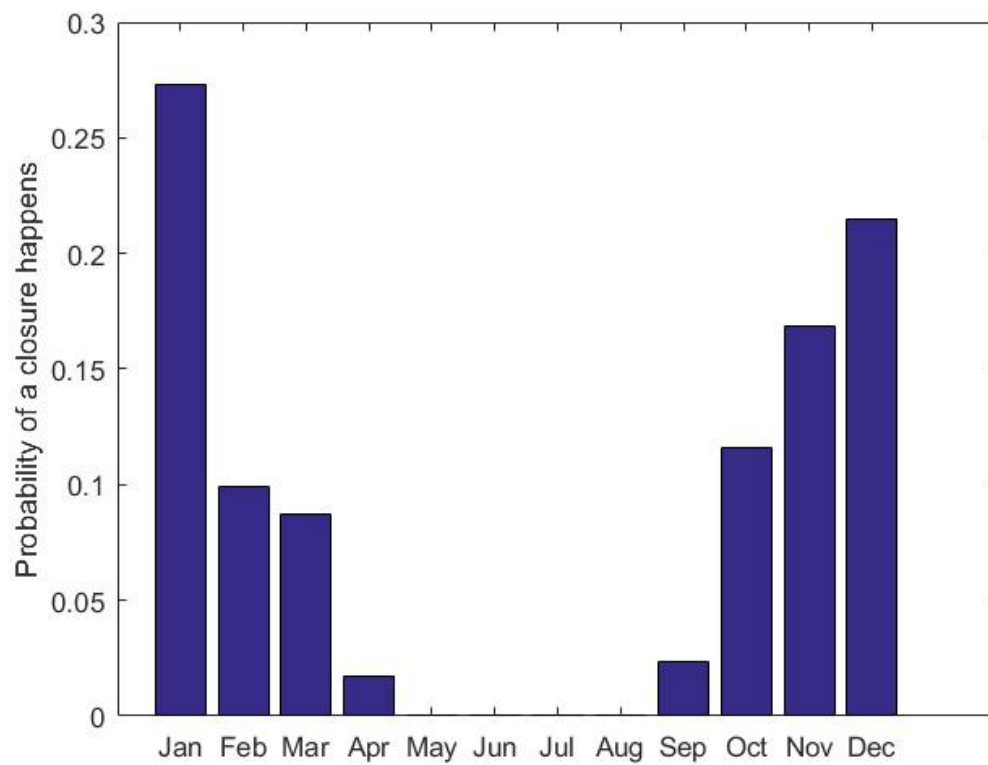


Figure 4.3: Probability of a closure happens in each month from 2003 to 2016.

is stronger than summer storm due to stronger wind in winter.

Influence of high tide

Start time of each closure is compared with start time of corresponding high tide time to analyze when do staff decide barrier should be closed. Figure 4.4 show time differences.

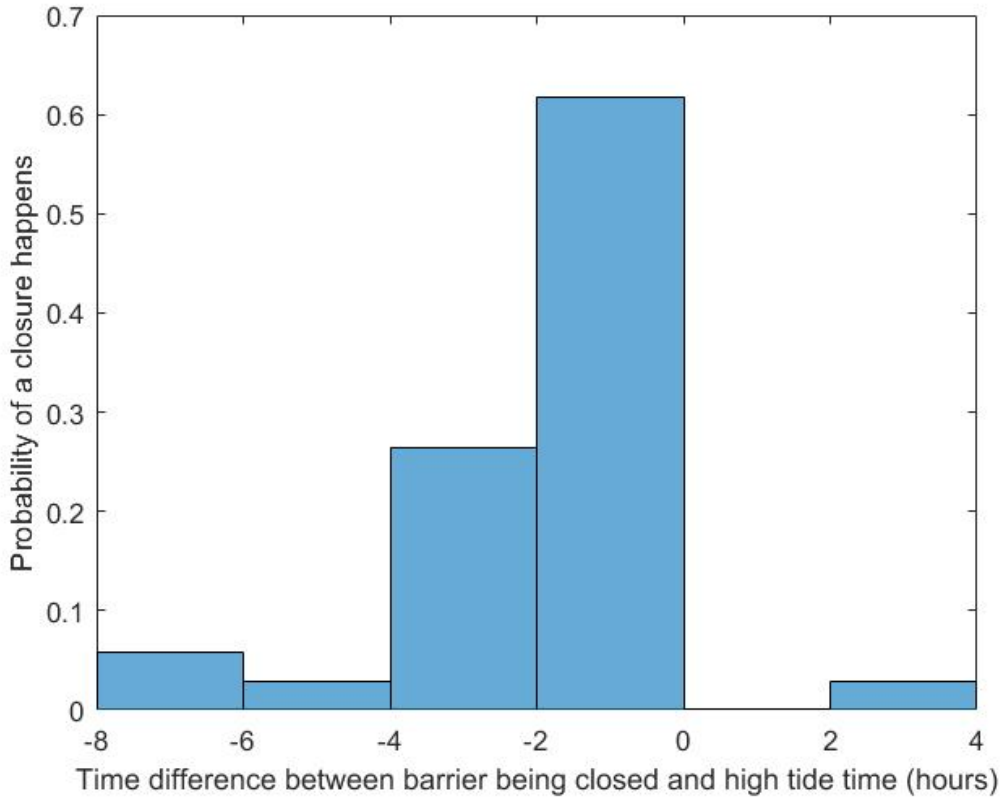


Figure 4.4: Probability of difference between the time closure happens and high tide from 2013 to 2016.

The chart shows 60% of closures started within two hours before high tide time. In other words, most of closures happened at high tide time. High water level during high tide time is a great contributor to dangerous overtopping. This indicate that, besides storm alert that sends staff to monitor the wave conditions at barrier, high tide time is also an indicator. Staff is supposed to arrive at barrier before high tide time and start monitor overtopping situation.

4.1.2 Relation between closed times and wind

Overtopping has two forms, 'green water' and wave splash. 'Green water' overtopping is case where a continuous sheet of water passes over the crest. The second form of overtopping occurs when waves break on the seaward face of the structure and produce significant volumes of splash. These droplets may then be carried over the wall either under their own momentum or as a consequence of an onshore wind Meer et al. [2016]. Barrier closure and inspection record, as well as a video filmed by passer show splash overtopping is main form.

The questions, how is splash overtopping formed at barrier. Wave conditions at toe are distinguishes by Iribarren number, because of the extremely steep slope, Iribarren number for all cases are large. Waves are considered not breaking on slope and simply run up and down the slope, and not critically influenced by the structure tow or slope. The splash overtopping can be carried over the wall under their own momentum, or may be driven by onshore wind. Effects of wind on spray overtopping is seldom modelled, largely due to inherent difficulties in scaling wind effects has not yet been established.

4.2 Analysis tolerable Vmax estimated by policeman

Currently, all closures are operated by manually. Following the forecast of large storm events OIC deploy members of staff to monitor the wave conditions at the barriers and determine whether it is safe for public use. When overtopping happens, waves overtop barrier crests one after one and give small or large splash as dynamic process. Staff observes overtopping splash water and operate closure. In this way, closures are decided based on empirical experience and visual estimation of staff. A question arises from this is, are policeman's estimation accurate? If the threshold is too strict, in other words, barrier is closed when it is safe to drive across, the cost of waiting time will increase. If the threshold is too tolerant, in other words, barrier remains open when it is dangerous to drive across, the cost of individual risk will increase. To discuss whether the decisions made by staff are accurate, tolerable overtopping estimated by staff is compared with tolerable overtopping volumes given by Overtopping Manual in this section.

Present average closure frequency is five, return period is 0.2. Wave wall is vertical plain wall with height of one meter. According to wave volume calculation given in table 3.10, present Vmax is:

$$V_{\max_present} = 1.48 \text{ m}^3/\text{m}.$$

Limits for wave overtopping for structural design given by Meer et al. [2016] shows in table 3.4. For cars on barrier crest behind sea wall, tolerable Vmax for vehicles is:

$$V_{\max_limit} = 2.00 \text{ m}^3/\text{m}.$$

Therefore: $V_{\max_present} < V_{\max_limit}$

Wave volume limit estimated by staff is smaller than tolerable Vmax, which means estimation made by staff is more than safe enough.

However, only comparison between $V_{\max_present}$ and V_{\max_limit} is not sufficient enough due to limitation of these two values. To find out whether staff's estimation are safe, academic research is carried out. Several car accidents happened at barrier in the past are found on news¹. It can be concluded that staff's limit on overtopping volume is not always accurate. Dynamic and uncertain of policeman's estimation will be discussed in 4.2.1. In following design, limit provided by Meer et al. [2016] - $V_{\max_limit} = 2.00 \text{ m}^3/\text{m}$, will be used for wave wall design.

4.2.1 Limitation

Dynamic overtopping splash

Overtopping process is a dynamic and irregular process, this wave by wave overtopping is difficult to measure (Meer et al. [2016]). The irregular process brings many uncertainties to policeman's visual estimation. Within two-hour storm, the maximum overtopping wave may happen at any time. When policeman see the very first 'dangerous wave', or when he feels wave are getting larger and larger he will close barrier to guarantee safety. However, whether these waves are real dangerous waves is unknown. Estimation on 'dangerous wave' also depend on personal experience of policeman. Each policeman has different view on threshold of 'dangerous'.

Limitation of $V_{\max_present}$ In this study, $V_{\max_present}$ is derived made on average closure frequency. Since closure frequency varies greatly with year, average value can not describe estimation that was made for each closure. Therefore, $V_{\max_present}$ can not describe estimation made by policeman for each closure.

Limitation of V_{\max_limit} V_{\max_limit} is derived from laboratory experiments considering only green overtopping. Splash overtopping could be more dangerous than green overtopping. Under green overtopping, use of vehicles may also be dangerous under wave overtopping, particularly if flood depths can 'float' the vehicle away. Under splash overtopping, part of splash will hit vehicles then fall onto causeway surface, and part of splash will directly fall onto surface. Therefore, not only flood depths can 'float' the vehicle away will happen, but also splash that hit vehicles will push vehicles away. In this way, V_{\max_limit} caused by splash water should be smaller than $V_{\max_limit} = 2 \text{ (m}^3/\text{m)}$ as given by Meer et al. [2016].

Vehicle driving speed

¹<https://www.bbc.com/news/uk-scotland-north-east-orkney-shetland-30177353>

For vehicles driven at speed on an exposed causeway, almost any overtopping will endanger the traffic (Meer et al. [2016]). No reference was found that can give guidance to driving speed. To be on the safe side, drivers should drive as slow as possible during storm.

Chapter 5

Wave wall design

Wave wall design includes two types of flood protection structure, plain vertical wave wall and recurved wave wall with a bullnose. These two structures are selected based on requirements of clients. Wave transformation result will now be used model wave overtopping volume for a range of wall height and bullnose shape. For plain vertical wall, this range covers 7 return periods, wall height from 0 to 8 meters. For recurved wall with bullnose, this range covers 7 return periods, wall height from 0 to 4 meters, bullnose angle from 0 to 90 degree.

In this following sections, plain vertical wave wall design is presented in section 5.1. Afterwards, recurved wave wall with bullnose will be designed in section 5.2, in which sensitivity analysis is carried out against dominant parameters, include wall height, bullnose angle, and bullnose height.

5.1 Effect of plain vertical wave wall on wave overtopping

Plain vertical wall is a widely used flood protection structure in the UK. At barrier, a section of one meter high concrete caisson is now placed at north end, the rest sections are not protected. In this study, wall height from 0 to 8 meters are implemented in wave overtopping equations for seven return periods. Multiple prediction methods of wave volume are introduced in Chapter 2. These methods will be discussed in this section, the optimal one will be used to compute Vmax results.

The steps introduced in section 2.5 and 2.6 is developed for barrier with submerged mounds, which has a berm at slope. However, barrier has emergent mounds slope without berm in front of wave wall. Prediction methods for no berm slope barrier is not available, bu can be adapted from those for crown walls on a rubble mound. This is because the emergent part has influence on wave overtopping process. The only difference is, part of the overtopping waves will then penetrate through the crest armour during physical models. No formulae are present to cope with such a situation. The essence the message is: use the height of the wave wall R_c and not the height of the armoured crest A_c .

For very steep slopes, overtopping discharge follows equation given by van der Meer and Bruce [2014]:

$$q = \sqrt{gH_{m0}^3} \cdot 0.047 \cdot \exp \left[- (2.35 \frac{R_c}{H_{m0}})^{1.3} \right] \quad (5.1)$$

in which R_c = free board + wall height.

Proportion of waves overtopping at vertical walls is described by Equation 2.20 and Equation 2.17. Maximum Wave overtopping volume is

$$V_{max} = a(\ln N_{ow})^{1/b} \quad (5.2)$$

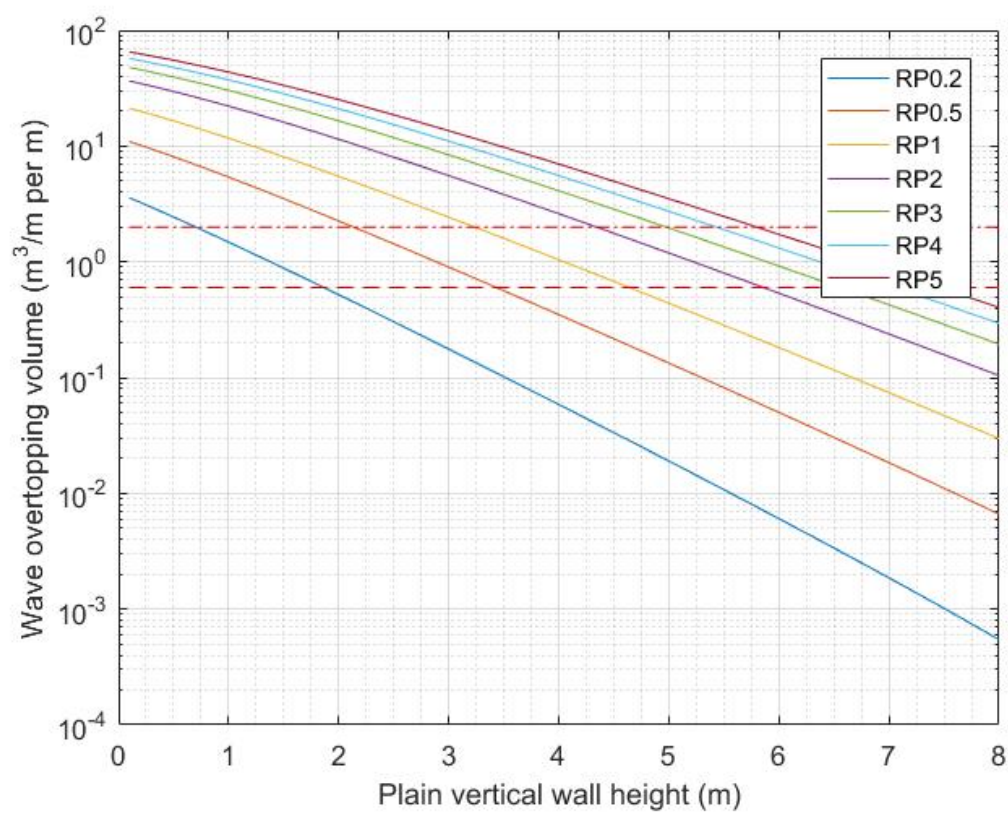


Figure 5.1: Effect of plain vertical wave wall on wave overtopping volumes of one-year return period. (Upper horizontal red line is V_{\max_limit} for vehicles, lower red line is V_{\max_limit} for walking people.)

5.1.1 Results

Results of plain vertical design for seven return periods are presented in Table 5.1

Table 5.1: Heights of plain vertical wall of each return periods for each overtopping volume limits.

RP	h _{wall} for vehicles (m)	h _{wall} for people (m)
0.2	0.80	1.95
0.5	2.05	3.50
1	3.20	4.85
2	4.25	5.90
3	5.00	6.50
4	5.45	7.10
5	5.90	7.55

The first element can be derived from the results is, some wave wall is very high, especially wave walls that meet limit for walking people. Even though detailed structure design is not included in this study, Wave wall that are higher than 4 meters are clearly too high to keep stable. All results will be included in cost-benefit design in next Chapter.

5.2 Effect of recurved wave wall on wave overtopping

Recurved wave wall is not as common as plain vertical wall, but also popular because bullnose can make up-rushing water partly fall back into the water. In this section, the aim is to find optimal wall height and bullnose shape that meet the requirements of overtopping, detailed structure design are not included.

Effectiveness of recurved wave wall on wave overtopping discharge is discussed in this section. The design of seaward overhang as part of the vertical wall is intended for reducing wave overtopping by deflecting seaward uprushing water. Parameters of bollnose for assessment of overtopping at structures with bullnose wall are:

- h_r = height of bullnose [m].
- B_r = horizontal extension of bullnose in front of main wall [m].
- α = angle of bullnose [degree]
- h = wall height [m]

The parameters are designed to meet the requirements of admissible overtopping for people and vehicles on causeway. Estimation of discharge calculation following the flowchart given by Figure 2.13. To maintain the stability of wave wall, only bullnose angle smaller than 90 is considered, this is because larger angle will more possibly cause overturning of the whole wave wall.

Sensitivity analysis on two variants, h and α , that have major influence on overtopping volumes are performed. Many trials of different combinations of freeboard and bullnose height are run in Matlab to find a one that gives tolerable overtopping. The combination is used to investigate influence bullnose angle on overtopping.

The method used for bullnose wall design is described in section 2.6.1. The limitation of this method is that, in physical models only consider situations in which connection between wall and breakwater is submerged. However, at barrier, for all return periods, this connection is no submerged. For now no research has looked into situation same as barrier, in this study, it is assumed that barrier slope is part of wall, the effect of this assumption on result is expected to be very small, because barrier slope is steep (1:1) enough to be seen as part of wall. Height if bullnose is assumed as 0.5m in sensitivity analysis, this assumption is made based on present wave wall on barrier. The present wave wall is one meter concrete caisson on north end of barrier, bullnose height is assumed as half the height of wave wall.

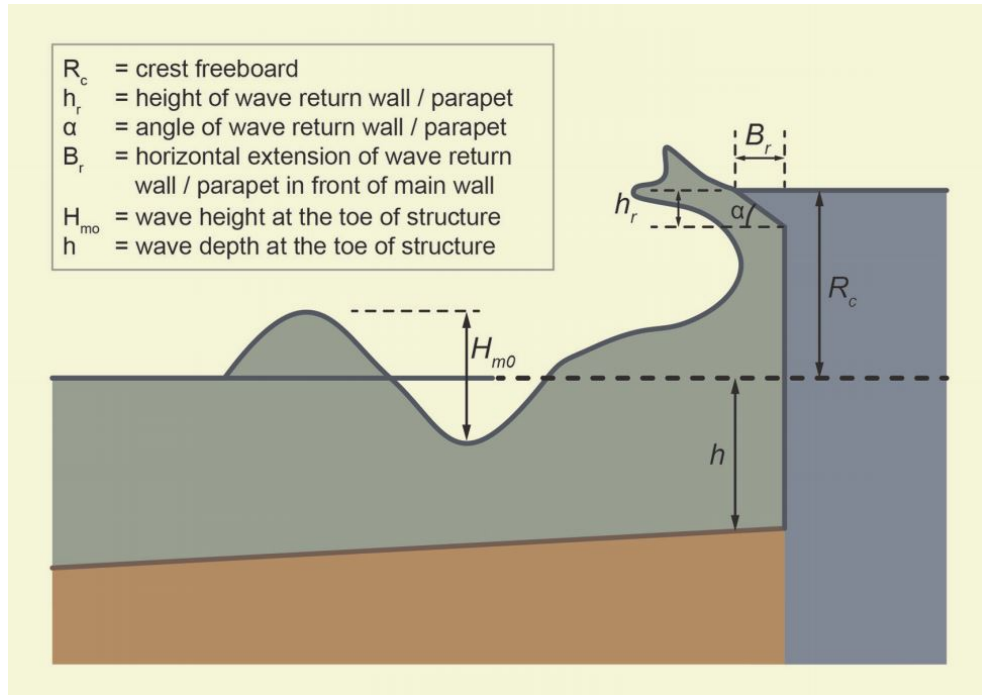


Figure 5.2: Parameter definitions for structures with bullnose / wave return walls (Meer et al. [2016]).

5.2.1 Sensitivity analysis - angle of wave return wall

To explore influence of bullnose angle on overtopping volumes, sensitivity analysis on bullnose angle is presented in this section. Effect of bullnose angle range from 0 to 90 degree. The bigger angle, the smaller bullnose will be when height of bullnose is fixed. Bullnose angle larger than 90 degree is not considered because it is chamfered backwards, which need width of wave wall at crest to be relatively big. Considering causeway crest can nor be narrowed, chamfered backwards does not have enough space to be placed.

Relation between wave volume and bullnose angle varies with height of bullnose. Tests on bullnose height between 1m to 3.5m are presented in Figure 5.3

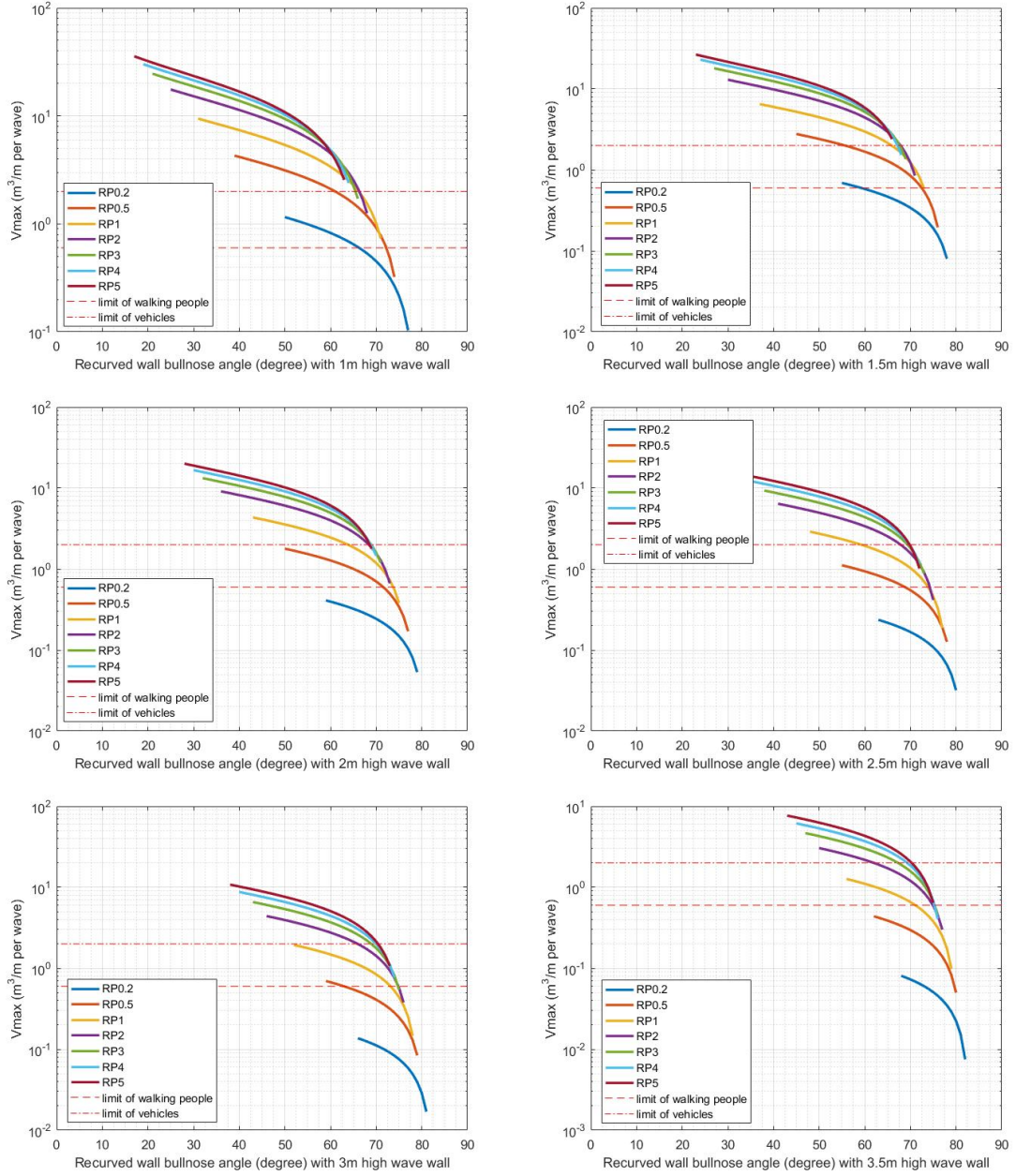


Figure 5.3: Wave overtopping volumes as function of bullnose angle range, for various of wave wall heights and return periods.

When plotting, part of line is not a smooth curve. Those parts are removed because they are outside the range of empirical model obtained from laboratory experiments. In general, V_{max} decreases as a function of bullnose angle for every wall height.

5.2.2 Sensitivity analysis - wave wall height

In order to explore influence of wave wall height on V_{max} , variable-controlling method is used. The method will generate relation between wave wall height and V_{max} under various of bullnose angle conditions. Range and grid of bullnose angle is selected based result from Section 5.2.1. The range should cover all bullnose angles that lead to tolerable V_{max} under each wave wall heights.

By checking every curve in Figure 5.3, range is set as 45° to 75° , with a grid of 5° .

The empirical equation used here is has limitation caused by physical model. This limitation causes break and straight line in Figure 5.4. The lines are supposed to be a smooth curve when equation is valid. For example, curves in upper two sub-figures have straight part following a break point. These parts should be excluded. The key parameter here is effectiveness in reducing overtopping is qualified by a factor k_{bn} . Empirical equation can predict k_{bn} larger than 0.05 as suggested. However, in this study, the figures show that k_{bn} smaller than 0.1 can lead to invalid result. Even though 0.1 is set as minimum of k_{bn} , by excluding k_{bn} that that are smaller than 0.1. Still some straight lines appears.

In general, V_{max} decreases with the increase of wave wall height, see Figure 5.4. The optimal bullnose angle is 70° , because 70° give acceptable V_{max} at the lowest wave wall.

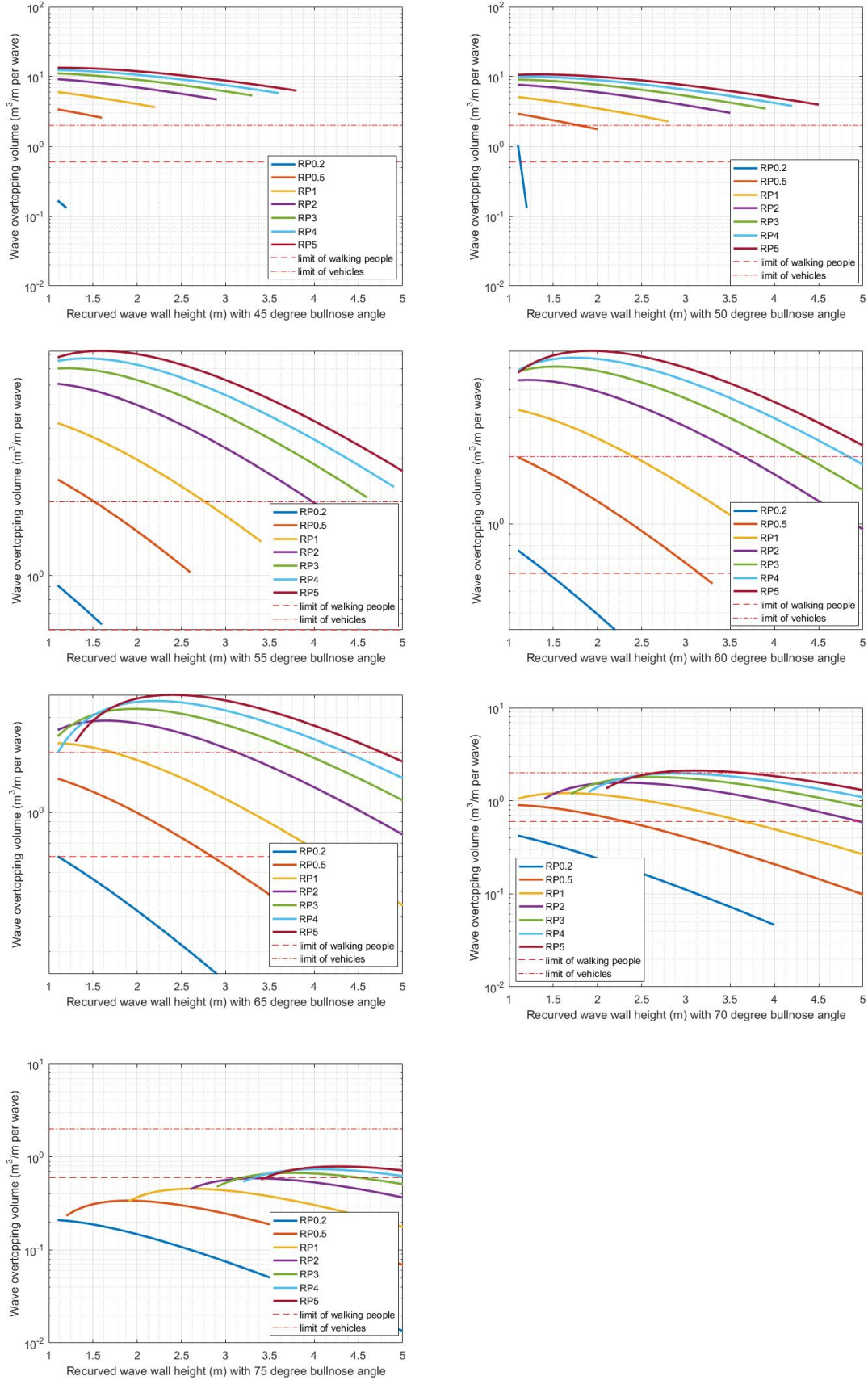


Figure 5.4: Variations of wave overtopping volumes on different recurved wall heights with certain bullnose angle.

When plotting, part of line is not a smooth curve. Those parts are removed because they are outside the range of empirical model obtained from laboratory experiments. In general, V_{max} decreases as a function of bullnose angle for every wall height. Some curves of V_{max} go up at beginning then gradually drop. It can be explained as, $V_{max} = V_{max_{no-bullnose}} * K_{bn}$, K_{bn} and $V_{max_{no-bullnose}}$ both decrease with the increase of wall height but with different decreasing gradient, so V_{max} will probably be a convex line.

5.2.3 Results

Best design is assessed as the lowest wall height that gives tolerable V_{max} . All sensitivity analysis results are manually assessed. Results of recurved wave extracted by combining the results provided by Section 5.2.2 and 5.2.1. Design of recurved wave wall with bullnose is given in Table 5.2.

Table 5.2: Recurved wave wall design of each return period for vehicles.

RP	wall height(m)	bullnose angle (degree)
0.2	1.0	70
0.5	1.0	70
1	1.0	70
2	1.4	70
3	1.7	70
4	1.9	70
5	2.1	70

Chapter 6

Cost-benefit Analysis

An important question in evaluating (engineering) projects is whether the benefits outweigh the costs. Cost benefit analysis (CBA) is generally used for appraisal of a wide range of effects of projects or interventions in order to support decision making. The cost benefit analysis starts with defining the system and existing situation. A range of effects of wall on barrier will be identified. However, closure is operated by policeman which is not a constant variant. Decision made by policeman will effect the result of economic optimization. A method to include this risk is to make a decision tree. Recording different variants, with associated risks, costs and benefits, in a matrix or decision tree, serves as an aid for making decisions. With this, the optimal selection can be made from a number of alternatives. The closure, overtopping and outcomes are will be shown in decision tree, which gives the probability of consequences.

6.1 Economic optimization

Economic optimization is a method that can help finding out the most optimal design. This method can be applied to cases where failure probability level has to be decided for a system that is yet to be designed (Jonkman et al. [2017]). In this case, failure probability is equal to closure frequency. An economic optimization should take into account the costs of increasing the safety level and reducing the risks can be applied to derive an optimal closure frequency. The economic optimization was developed and applied by van Dantzig (1956), to derive the optimal dike height for South Holland after the 1953 storm surge disaster (Jonkman et al. [2017]).

In the economic optimization the total costs (C_{tot} [£]) are determined, consisting of the investments I [£] in a safer system and the present value of the risk R [£].

$$C_{\text{tot}} = I + R \quad (6.1)$$

For this study, risk is presented by the flood damage caused by wave overtopping when barrier is not closed. The annual risk cost, or expected economic damage is found by:

$$E(D) = P_f D \quad (6.2)$$

where:

$E(D)$ = expected value of the risk [£/yr].

P_f = failure probability of the system per year ([1/year]).

D = damage in case of failure [£].

The risk cost is expressed in terms of £per year, whereas the initial investments have the unit of £. There NPV (nett present value) is used to calculate risk reduction over 100 years design lifetime. The nett present value of cost values over a future range of years can be calculated with formula 6.3.

$$NPV = \sum_{t=1}^T \frac{C_t}{(1+r)^t} \quad (6.3)$$

where:

C_t = costs in year t [£].

T = reference period [years]

A method calculating present value of the risk for an infinite time horizon can be found as follows (Jonkman and Schweckendiek [2015]):

$$R = \frac{P_t D}{r} \quad (6.4)$$

To calculate the nett present value NPV[£], a discount rater r should be used. The discount rate represents a required return on an investment. Discount rate is assumed to be 2%¹.

Estimation of investments and damages are approximate results, in this way the cost-benefit analysis is of low-level of precision. Because necessary data does not exist, a rough determination of investments and damages are derived from academic research. A typical approach is carried out to estimate investments and damages. First, individual parameter of investments and damages will be listed, followed by developing databases based on academic research, then calculate and present values of investments and damages which will be used for cost-benefit analysis. Investments (I) is presented in Section 6.1.1, followed by flood damage (D) assessed in Section 6.1.2.

6.1.1 Investments

Investments include two major parts, construction cost and maintenance cost. The costs are a function of the height and shape of wave wall. Since the cross-section of plain vertical wave wall is fixed, costs are proportional to wall height. The height of wave wall depends on design return period. Recurved wave wall has composed of a vertical part and a bullnose, the cost is roughly donated as a sum of these two parts.

Although maintenance costs of wave wall depend on size of wave wall, in this study maintenance cost is assumed as a fix percent of construction costs. This fix percent is determined based on the fact that major part of maintenance is small repair and monitoring working status. Only severe damage can lead to high repair costs. However, the aim of regular maintenance is to avoid huge damage.

Individual parameters of investments that are considered in this study are listed in Table 6.1.

Table 6.1: Whole life cost estimate checklist for wave wall

Construction		
Enabling works	Site set-up, procurement of specialist materials.	one-off
Construction costs	Asset construction costs. Costs of replacing temporary defence.	one-off
Inspections		
Monitoring programme	Development and review of monitoring programme.	ongoing
Operational and public safety inspections	Cost of regular inspections including visual inspection at low tide, general, fixed aspect and aerial photography, profile surveys of structure and foreshore and inspection of voids.	ongoing
Maintenance		
Maintenance	Costs of maintenance and intermittent refurbishment works associated with new structures.	ongoing
Replacement costs	Costs of replacing temporary defence or erosion control	ngoing

To develop a database which is used as reference of estimate investments costs, many guidelines and references are reviewed. The most suitable reference is "Cost estimation for coastal protection – summary of evidence" provided by Environment Agency of the United Kingdom. This summary

¹2% is commonly used in lecture and is therefore adopted in this study.

of evidence provides indicative costs and guidance for coastal erosion and flood management activities. The unit cost of concrete wave retaining wall are extracted from this manual, see Table 6.2.

Table 6.2: Example costs from the Environment Agency Unit Cost Database associated with coastal walls.

Type	Description	Length (m)	Height (m)	Total cost (k)	Cost (/m)	Cost (/m ²)
Wave/retaining wall	Sea defences	1190	3.8	2456	2064	543
Wave/retaining wall	Reinforced concrete wave return wall	75	2.0	472	6,293	3,147
Wave/retaining	Wave return wall	822	1.8	1,237	1,505	836

For plain vertical wave wall, sea defences in table above is used as reference. Cost of plain wave wall per one-meter height per one-meter length is £543.15K. For recurved wave wall with bullnose, wave return wall is used as reference, unit cost is £836.11K.

Construction cost of wave wall per meter width is usually not proportional to wall height. The higher wall, the cheaper unit cost will be. In this study, this reduction factor caused by wave wall is roughly assumed, with a minimum of 0.6. Details can be found in Appendix C.

Maintenance costs are roughly estimated as 2% of construction costs, this number is selected based on empirical experience.

6.1.2 Risk

An often-used definition considers risk as expected value: risk is the probability of an undesired event multiplied by the consequences. The definition points out two parameters, failure probability of an event and the cost of consequence of this failure. To derive total risk, damages as consequence of each failure event, and their corresponding failure probability and consequences. To clearly present causal relationship among these three items, a tree diagram is developed. The diagram takes both overtopping hazard strategies that have been discussed in this study, wave wall and precaution, into consideration. In this section, damages of each failure event are discussed, followed by estimation of their probability and cost.

Damages

The term "flood damage" refers to all varieties of harm caused by flooding. It encompasses a wide range of harmful effects on humans, their health and their belongings, on public infrastructure, cultural heritage, ecological systems, industrial production and the competitive strength of the affected economy (Jonkman and Schweckendiek [2015]). The damage is divided into tangible and intangible damage, depending on whether or not the losses can be assessed in monetary values. Tangible damages and intangible damages are that could happen to Churchill Barrier during an overtopping event are summarised in Table 6.3

Table 6.3: Damages caused by overtopping at Churchill Barrier No.2

	Tangible	Intangible
Direct	Vehicles Infrastructure and other public facilities Evacuation and rescue operations	Fatalities Injuries
Indirect		Societal disruption

Each damage can be decided as:

- Vehicles: Damage to vehicles when being hit by overtopping splash water.

- Infrastructure and other public facilities: Damage to barrier slope surface, wave wall, road surface, road fence when being hit by overtopping splash water.
- Evacuation and rescue: Evacuation and rescue of injuries or fatalities when walking people, motorists or policemen are trapped or hurt by overtopping splash. Rescue of vehicles if they became swamped by water.
- Fatalities: Loss of life.
- Injuries: The costs associated with nonfatal injuries.
- Societal disruption: Including traffic disruption and delay of business due to waiting when barrier is closed.

Based on circumstances and consequences presented above, a tree diagram is developed, see Figure 6.1. Tree diagram summarises all circumstances that would happen to barrier. The diagram starts from left side, three overtopping situations are distinguished, intolerable overtopping with V_{max} larger than $2 \text{ m}^3/\text{m}$, tolerable overtopping with V_{max} between 0 and $2 \text{ m}^3/\text{m}$, and no overtopping. The threshold of tolerable wave overtopping is set to be $V_{max} = 2 \text{ m}^3/\text{m}$, in line with tolerable wave overtopping for vehicles given by Meer et al. [2016]. Situation without overtopping is excluded because no damage would happen when waves are calm. When overtopping happens, no matter its tolerable or intolerable, policeman will be sent to barrier to monitor overtopping splash water. Following the decisions made by policeman, two sub-circumstances, barrier open and barrier closed, are considered. Thus five consequences are formed (ω_1 to ω_5).

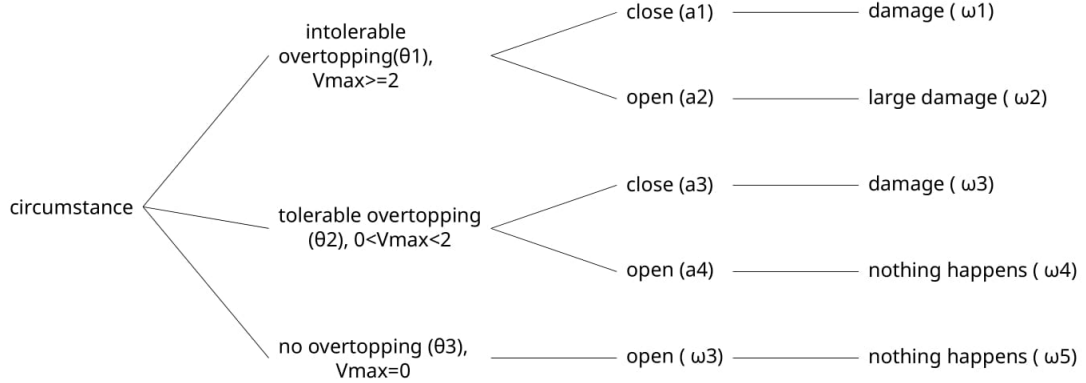


Figure 6.1: Tree diagram of circumstances and consequences that would happen to barrier. Unit of V_{max} is m^3/m .

Within the tree the diagram, following characteristics are defined:

- the set of all (natural) circumstances (θ) that influence the outcomes
- the set of all possible actions or decisions (a), from which the decision maker can choose
- the set of the set of all possible results (ω), which are functions of the actions and circumstances: $\omega=f(\theta)$.

Probability

Probability of circumstances θ are:

$$P_{\theta_1} + P_{\theta_2} + P_{\theta_3} = 1 \quad (6.5)$$

in which

$$\begin{aligned} P_{\theta 1} &= \frac{\text{number of intolerable overtopping waves}}{\text{total number of overtopping waves}} \\ P_{\theta 2} &= \frac{\text{number of tolerable overtopping waves}}{\text{total number of overtopping waves}} \\ P_{\theta 3} &= 0 \end{aligned} \quad (6.6)$$

Probability of circumstances a are:

$$\begin{aligned} P_{a1} + P_{a2} &= 1; \\ P_{a3} + P_{a4} &= 1; \end{aligned} \quad (6.7)$$

Number of intolerable overtopping wave ($N_{\text{int,ov}}$) per year is the same as design closure frequencies, which are 5, 2, 1, 0.5, 0.33, 0.25, 0.2. Closure frequency is reciprocal of design return period.

$$\begin{aligned} N_{\text{int,ov}}(rp = 0.2) &= 5; \\ N_{\text{int,ov}}(rp = 0.5) &= 2; \\ N_{\text{int,ov}}(rp = 1) &= 1; \\ N_{\text{int,ov}}(rp = 2) &= 0.5; \\ N_{\text{int,ov}}(rp = 3) &= 0.33; \\ N_{\text{int,ov}}(rp = 4) &= 0.25; \\ N_{\text{int,ov}}(rp = 5) &= 0.20; \end{aligned} \quad (6.8)$$

Probability of consequence ω are:

$$P_{\omega 1} + P_{\omega 2} + P_{\omega 3} + P_{\omega 4} = 1; \quad (6.9)$$

in which

$$\begin{aligned} P_{\omega 1} &= P_{\theta 1} * P_{a1}; \\ P_{\omega 2} &= P_{\theta 1} * P_{a2}; \\ P_{\omega 3} &= P_{\theta 2} * P_{a3}; \\ P_{\omega 4} &= P_{\theta 2} * P_{a4}; \\ P_{\omega 5} &= 0; \end{aligned} \quad (6.10)$$

Number of overtopping waves per year varies with wall height. The higher wall, the less waves will overtop. Since wave wall height is determined by design closure frequency, in other words, design return period, the number of overtopping waves ($N_{\text{t,ov}}$) per year will be a function of return period. Design return periods (rp) are 0.2, 0.5, 1, 2, 3, 4, 5 years. The larger rp, the less waves will overtop.

Theoretically, in order to derive probability of ω_1 , ω_2 , and ω_3 , probability of θ_1 and θ_2 , as well as a_1 to a_4 need to be assumed. However, none of these probability can be validated. Therefore these probabilities will be assumed based on author's personal experience accumulated from this study. In theory, probability of each circumstance of different rp should be different, however, in this study, it is assumed that probability of each circumstance is constant. Two limitations of assumption are, firstly, probabilities are not validated, secondly, probability of each circumstance does not vary with rp. Assumptions of probability of each circumstance are:

$$\begin{aligned} P_{\theta 1}(rp) &= 0.01; \\ P_{\theta 2}(rp) &= 0.99; \\ P_{a1}(rp) &= 0.85; \\ P_{a2}(rp) &= 0.15; \\ P_{a3}(rp) &= 0.20; \\ P_{a4}(rp) &= 0.80; \end{aligned} \quad (6.11)$$

Probability of each consequence will be:

$$\begin{aligned} P_{\omega_1}(rp) &= 0.0085; \\ P_{\omega_2}(rp) &= 0.0015; \\ P_{\omega_3}(rp) &= 0.1980; \\ P_{\omega_3}(rp) &= 0.7920; \end{aligned} \tag{6.12}$$

Number of overtopping waves per year (N_t) will be calculated as $N_t = N_{\text{int,ov}}/P_{\theta 1}$:

$$\begin{aligned} N_{\text{ov}}(rp = 0.2) &= 500; \\ N_{\text{ov}}(rp = 0.5) &= 200; \\ N_{\text{ov}}(rp = 1) &= 100; \\ N_{\text{ov}}(rp = 2) &= 50; \\ N_{\text{ov}}(rp = 3) &= 33; \\ N_{\text{ov}}(rp = 4) &= 25; \\ N_{\text{ov}}(rp = 5) &= 20; \end{aligned} \tag{6.13}$$

Cost Expected cost of flood damage **per wave** follows Equation 6.14 :

$$E_{D,\text{perwave}}(rp) = P_{\omega_1}(rp)D_{\omega_1} + P_{\omega_2}(rp)D_{\omega_2} + P_{\omega_3}(rp)D_{\omega_3} \tag{6.14}$$

Expected cost of flood damage **per year** follows Equation 6.15 :

$$E_{D,\text{peryr}}(rp) = (P_{\omega_1}(rp)D_{\omega_1} + P_{\omega_2}(rp)D_{\omega_2} + P_{\omega_3}(rp)D_{\omega_3}) * N_t \tag{6.15}$$

in which, N_t is number of overtopping waves per year.

In all consequences, undesired consequences are ω_1 , ω_2 , and ω_3 . Cost of each undesired consequence is different. In the following, components of each undesired consequence are described.

Consequence (ω_1) - when barrier is closed during intolerable overtopping event , risk costs are:

- Costs of social disruption, including cost of waiting time, associated cost of business delayed by passers, and costs of travel time unreliability in drivers transportation.
- Costs of damage on infrastructures and other public facilities.

Consequence (ω_2) - when barrier is open during intolerable overtopping event, severe consequence will happen. Risk costs are:

- Cost of damage to vehicles.
- Cost of fatalities.
- Cost of nonfatal injuries.
- Cost of evacuation and recuse operations.
- Costs of damage on infrastructures and other public facilities.

Consequence (ω_3) - when barrier is closed during tolerable overtopping event, risk costs are:

- Costs of social disruption, including cost of waiting time, associated cost of business delayed by passers, and costs of travel time unreliability in drivers transportation.

The cost of every consequence is calculated as cost per happening. By comparing the severity of each consequence, consequence (ω_2) is worst because lose of life is most undesired accident. Also cost per happening of Consequence (ω_2) is the highest. However, to determine which consequence is dominant, cost of each consequence should be calculated, as cost per happening times probability of happening.

The assumption is roughly approximate estimation based on experience of author. For a low-level precise study, these assumptions are sufficient enough. However, for further studies, costs should be estimated by experts. This investigating can be seen as another whole topic requiring information are not currently available, therefore it is not undertaken in this study.

Cost of consequence ω_1 consists multiple elements. Costs of travel time delay imposes to passers is calculated by assuming, one car passes every two minutes with two passengers, who makes £25 per hour. Average waiting time as donated as one hour because average storm is two hours. By assuming flow of traffic is evenly distributed as 30 vehicles/hr, waiting time is half of overtopping storm duration. Cost of waiting time is then £3000, the cost of damage is roughly assumed as £5,000 per closure. In conclusion, cost of consequence ω_1 is roughly assumed as £8,000 per storm. Cost of consequence ω_2 is roughly assumed as £50,000 per storm.

Cost of consequence ω_3 is roughly assumed as £5,000 per storm.

6.2 Cost-benefit analysis for plain vertical wall

For each return period, investment and present value of risk are calculated following the equations given in last section. The full calculation is performed in Matlab, script can be found in Appendix C.

Table 6.4: Total cost, investments, and risk cost of plain vertical wave wall, as a function of return period.

RP (yr/yrs)	Investment (M£)	Risk (M£)	Total cost (M£)
0.2 (present)	0.00	24.42	24.42
0.5	2.73	9.77	12.49
1	4.25	4.88	9.14
2	5.65	2.44	8.09
3	6.65	1.63	8.28
4	7.25	1.22	8.47
5	7.84	0.98	8.82

Note that for 0.2 year return period case, I is actually zero because present wave wall is one-meter vertical wall. However, even if $I_{RP=0.2} = 0$, the total cost is still much higher than the rest cases because its risk is too big. To keep the continuity of arrays, $I_{RP=0.2}$ will use the assumed value.

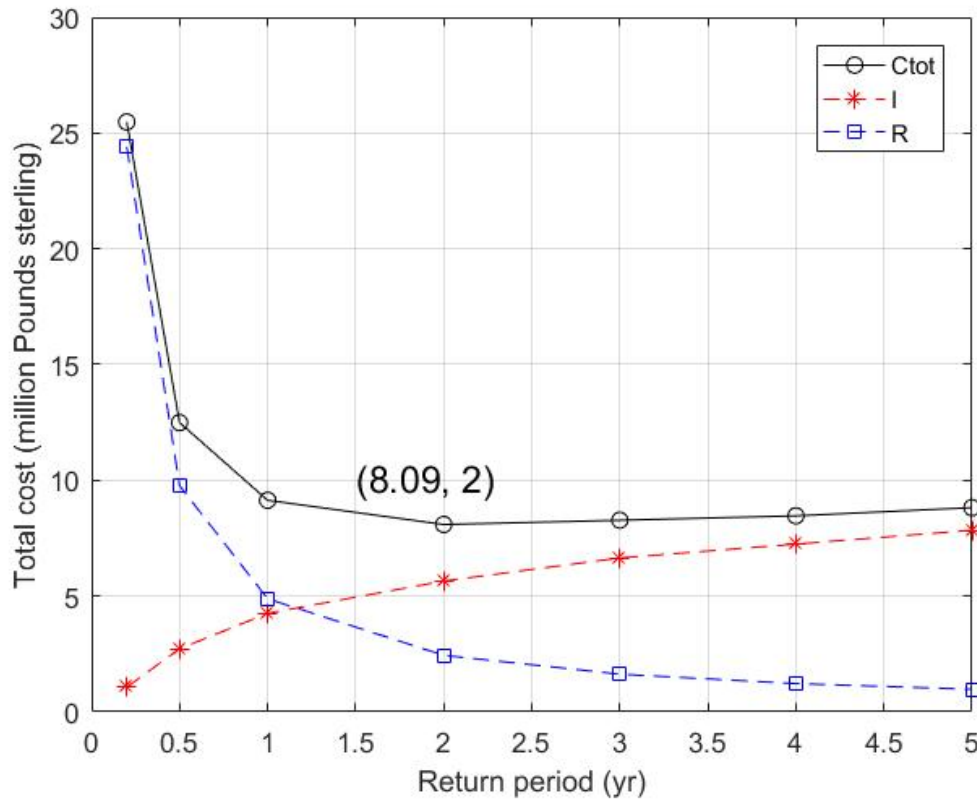


Figure 6.2: Total cost, investments, and risk cost of plain vertical wave wall, as a function of return period.

Figure 6.2 gives visualization of results of I , R and C_{tot} in Table 6.4. The higher C_{tot} value, the less economical this wave wall design will be. The best design for plain vertical wave wall is therefore two years return period, with $C_{tot} = \text{M£}8.09$ per year.

6.3 Cost-benefit analysis for recurved wall

Calculation method same as plain wave wall is applied to recurved wave wall. The full calculation is performed in Matlab, script can be found in Appendix C.

Table 6.5: Total cost, investments, and risk cost of recurved wave wall with bullnose, as a function of return period.

RP (yr/yrs)	Investment (M£)	Risk (M£)	Total cost (M£)
0.2 (present)	2.05	24.42	26.46
0.5	2.05	9.77	11.81
1	2.05	4.88	6.93
2	2.87	2.44	5.31
3	3.48	1.63	5.11
4	3.89	1.22	5.11
5	4.30	0.98	5.27

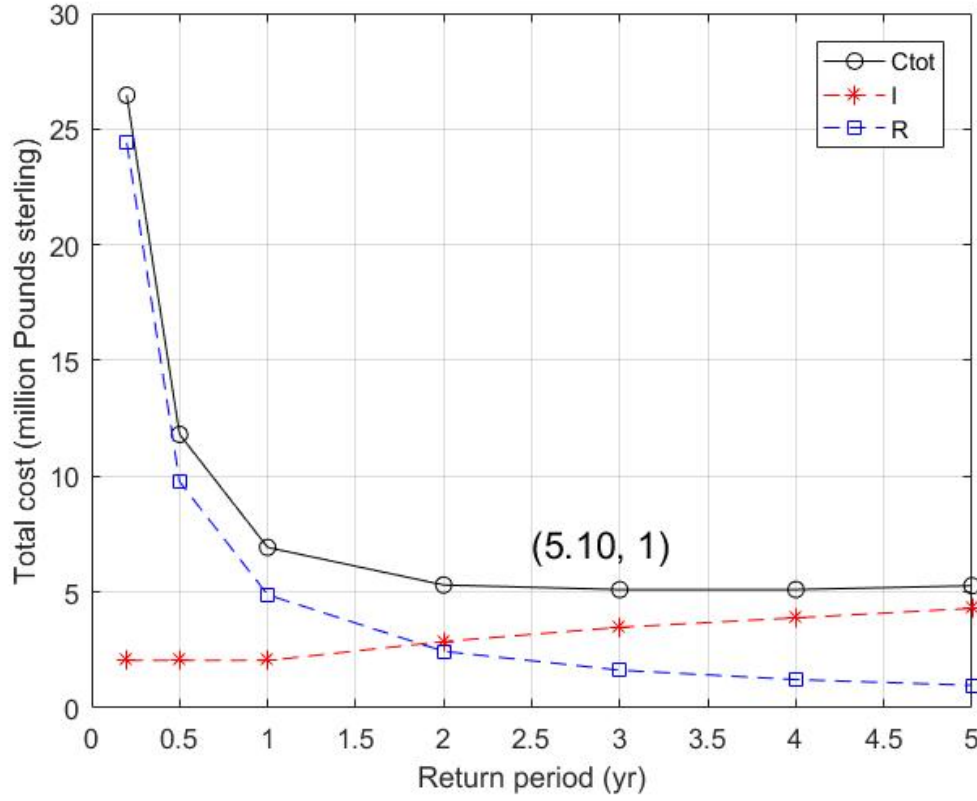


Figure 6.3: Total cost, investments, and risk cost of recurved wave wall with bullnose, as a function of return period.

The best design for recurved wave wall is three years return period, of which $C_{tot} = \text{M}\pounds 5.10$ per year.

6.4 Conclusion

Overall, recurved wall is more effective in reducing wave overtopping volumes at the same wall height. For each design return period, recurved wave wall is more economical than plain vertical wave wall. By comparing C_{tot} of optimal design of plain and recurved wave wall, the most optimal one is recurved wave wall of three years return period. The C_{tot} is approximately $\text{M}\pounds 5.10$ per year.

Chapter 7

Conclusions and Recommendations

Churchill barriers, a series of structures which are constructed as several permanent barriers to prevent attack from enemies during World War II, now serve as road links. These road links have to be closed more and more frequently due to dangerous overtopping flood. Although this research focuses on overtopping reduction strategy for Barrier No.2, the approach has been developed in such a way that the conclusions can also be applied to the other three barriers, which are experiencing similar issues of overtopping flood and traffic problem it caused.

7.1 Conclusions

To conclude this research, it is the best to start with the research questions. The research aims to provide insight in the optimal design of plain vertical wave wall and recurved wave wall with bullnose, then analysis policeman's estimation on when barrier should be closed during a storm. Before giving conclusion, some background should briefly introduced on the closures are operated. Barrier is currently closed 5 times per year on average, which corresponds to return period of hydraulic boundary condition being 0.2. The boundary conditions at barrier toe of 0.2 year return is obtained in this study, they are $H_s=3.32\text{m}$, $T_m=6.4\text{s}$, $w_l=3.6\text{ mCD}$. Present barrier with one-meter wave wall on crest gives $V_{\text{max}}^{\text{present}} = 1.48\text{ m}^3/\text{m}$. By comparing $V_{\text{max}}^{\text{present}}$ with $V_{\text{max}}^{\text{limit}} = 2\text{ m}^3/\text{m}$, policemen do a good job in keeping causeway safe. Duo to dynamic and irregular process of overtopping waves, it is difficult to give precise conclusion about policeman's estimation on when barrier should be closed.

A key parameter in wave wall design is design return period. Return period and number of closures per year (closure frequency) are reciprocals. Design return periods are set to be: 0.2, 0.5, 1, 2, 3, 4, 5 years. These return periods are much smaller than usual because barrier locates in relatively uninhabited area. smaller return periods can lead to lower wave wall and therefore largely reduce construction cost. Conclusions of wave wall design are given below.

Plain vertical wave wall

Vertical wave wall height of each design return period is simulated with empirical equation. The wave walls are evaluated with cost-benefit analysis. Total cost (C_{tot}), which is sum of investment and risk, of each wall forms a curve with a minimum value at two-year return period. The optimal design of plain vertical wave wall is 4.25m, associated C_{tot} is 8.09M£per year, associated barrier closure frequency is 0.5 time/yr.

Recurved wave wall with bullnose

Recurved wave wall with bullnose design is more complicated than plain vertical wall. This is because structural parameters of bullnose should be considered, they are bullnose angle, bullnose height and wave wall height. Sensitivity analysis against bullnose angles (0° to 90°) was undertaken under various of wave wall height (1, 1.5, 2, 1.5, 3, 3.5m), proving that V_{max} is influenced by bullnose angles. In general, V_{max} decrease with the increase of bullnose angle, within the range where empirical equation is valid. Bullnose height barely have effect on V_{max} and is set to be 0.5m.

Sensitivity analysis against wall height (1m to 5m) was undertaken under various of wave wall height (45, 50, 55, 60, 65, 70, 75 degree), proving that V_{\max} is influenced by wall height. In general, V_{\max} decrease with the increase of bullnose angle, within the range where empirical equation is valid. Optimal design is lowest wave wall that gives tolerable wave overtopping. Recurved wall design results shows that 70degree is optimal angle since it gives smallest Vmax under all wall height conditions. According to cost-benefit analysis on all recurved wall design, optimal recurved wall is 1.7m high, with bullnose angle = 70° , $C_{\text{tot}} = 5.10\text{M}\pounds$ and $\text{rp} = 3\text{yrs}$.

Optimal design

Table 7.1: Parameters of optimal wall design.

Wall shape	Recurved wall
RP(yr)	3
Closure frequency (times/yr)	0.33
Ctot(M \pounds /yr)	5.1
Wall height (m)	1.7
Bullnose angle ($^\circ$)	70
Bullnose height (m)	0.5

7.2 Limitations

No approach is perfect, and no design is ideal. The approach in this research has shortcoming and conclusion has limitations. The disadvantages were tried to be minimized with the best effort of author, but still some consequences have occurred. In the following, imitation will be discussed following the order of approach.

The first limitation occur to wave overtopping calculation and wall design due to lack of crucial data, wave conditions at barrier toe. The wave conditions at toe used in this study is generated based on limited offshore wave conditions. The accuracy of 0.2, 0.5, 2, 3, 4 years return periods' wave height and wave period are not enough for structure design in practice. The noise may caused by variation of bathymetry with seasons and wind. Besides, wave direction is assumed to be perpendicular to barrier, which may not be reality. Oblique wave attack will be weaker than normal wave attack, thus decrease wall height and investment cost.

The second limitation happens to evaluation of policeman's estimation. This evaluation is not validated. Policeman usually work on shift, a general evaluation can not give advise to each of them. Because observation and decisions are taken to be very personal. Although some injured have been reported by press, and general evaluation show closure frequency is not safe, but it is too early to say all policemen should be more strict on their estimation. It is possible that a strict policeman contribute to a high number of closure per year, and another policeman let a car across under danger. In that way, injured will still happen even if closure frequency is already very high.

7.3 Recommendations

Recommendations are given in this section, for further studies that contribute to a safe traffic at barrier.

First recommendation is given to data collection process of overtopping simulation. The raw data collected by wave buoy is necessary for generating extreme wave condition. To measure accurate and up-to date wave condition at toe with time series, it is advised to place wave buoy at 5m to 15m to the east of barrier, for at least six month duration, from October to March. Because closures happened at winter season, so in-situ measure in summer time is not necessary. Wave buoy at barrier to can also give accurate data on water levels.

Second recommendation is given to policeman on site. When policeman are sent to barrier, they can bring a camera and set it up at the end of barrier where both overtopping splash and

passing vehicles can be captured. By filming overtopping splash, we can get visualized overtopping impressions and get to know when barrier are closed. By studying images of splashes during closed time, and computing their the overtopping volumes (use data collected by first recommendation), engineers can build up a relation between image and volume. This will be very helpful for training policeman to improve their accuracy in estimation. Furthermore, with accumulation of experience over years, engineer can study which wave condition at toe will lead to closure. Then wave buoy can provide information on when barrier should be closed. This information can be linked to a automatic road gate, controlled by a computer program. Thus human labor will not be necessary anymore.

Appendix A

Water level and wave condition

Hydraulic boundary conditions, including wave height, wave period, and water level, are essential for wave overtopping simulation. In this study, only offshore hydraulic boundary condition is available. Usually extreme conditions should be computed by using raw data with time series measured by buoy or sensors. However, according to data collection, available conditions are joint probability extreme boundary conditions provided by JBA, instead of raw data with time series. Thus, main challenge is that return period of available offshore extreme conditions are different from design return period of this study. Therefore, aim of this Appendix A is to predict extreme conditions of design return period based on available extreme conditions.

To explore method of predicting extreme conditions of design return period, first available extreme conditions should be analysed which is the only input information. Available offshore joint probability extreme conditions are presented in Table A.1

Table A.1: Joint probability offshore extreme conditions (Bassett et al. [2015]).

Return Period (years)	H_s (m)	T_m (s)	WL (mCD)	WL + Climate Change (m)
1	4.19	9.37	3.82	4.54
5	5.43	11.92	4.27	4.99
10	5.68	12.22	4.44	5.16
20	5.91	12.49	4.52	5.24
50	6.18	12.82	4.63	5.35
100	6.37	13.04	4.7	5.42
200	6.53	13.24	4.78	5.5

In following sections, firstly, method of computing hydraulic boundary conditions of design return periods is developed. The method is a curve fitting, in the form of a mathematical function, that gives the best predict of boundary conditions of return period between 1 and 5 years. This is because target return periods are smaller than 5 years. Developing method is a journey of exploration, many trials on various mathematical function haven been tested and evaluated. Afterwards, evaluation is undertaken by comparing sum of squared deviation of value of 1 and 5 years' return period. Values are wave height, wave period, and water level. These values will be predicted and evaluated separately, in sections A.2 to A.4.

A.1 Method of computing hydraulic boundary conditions of design return periods

In this section, mathematical functions that have been tested to find out method are presented. Those trials on mathematical function are tested one after one. If results of last trial is not good enough, a new trial will be tested. In the following, development of method will be summarised.

Results of each trial will be presented in A.3 to A.5.

Development of method starts from most commonly used mathematical function for curve fitting, logarithm. Axis X is return period. Axis Y is wave height, wave period or water level. Trials are listed below.

Four combinations of logarithm curve fitting are:

- Type -> xscale, yscale
 - loglog -> log, log
 - logy -> linear, log
 - logx -> log, linear
 - linear -> linear, linear

Two combinations of polynomial curve fitting are:

- Type -> xscale, yscale
 - ploy2 -> Quadratic, linear
 - ploy3 -> Cubic, linear

Firstly, hydraulic boundary conditions of return period between 1 to 200 years are tested. Unfortunately the curves do not fit conditions of 1 and 5 years very well.

Secondly, same mathematical function are tested to fit boundary conditions between 1 to 50 years. The purpose of this step is to test whether fitting curve can fit 1 and 5 years boundary condition. Unfortunately predicted boundary condition of 1 and 5 years is far from original data. This means that original data is not a typical mathematical function.

In the end, to precisely fit boundary condition of 1 and 5 years, same mathematical function are tested to fit boundary conditions between 1 to 5 years. This means original data that correspond to return period larger than 5 years will be neglected. However, in approximate estimation, neglecting data that correspond to return period larger than 5 years is acceptable. Because extreme boundary conditions of return period between 1 and 5 years will always be between original boundary condition of 1 and 5 years. For future studies, generating boundary conditions from raw data with time series measured by wave buoy is recommended.

A.2 Water height

First, trials of logarithm and polynomial curve fitting to available offshore extreme wave height, as a function of return period between 1 to 200 years are tested. None of the curves fit 1 to 5 years' original data very well.

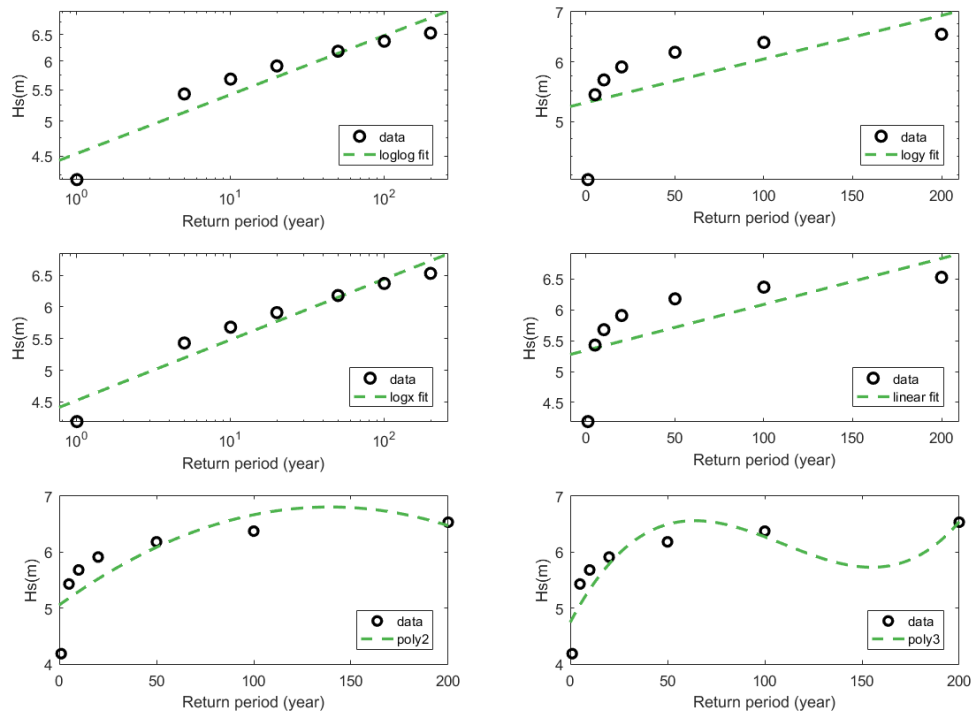


Figure A.1: Visualized results of trials of logarithm and polynomial curve fitting to available offshore extreme wave height, as a function of return period between 1 to 200 years.

Second, trials of logarithm and polynomial curve fitting to available offshore extreme wave height, as a function of return period between 1 to 50 years are tested. Curves fit 1 to 5 years' original data better than first trial, but still not good enough.

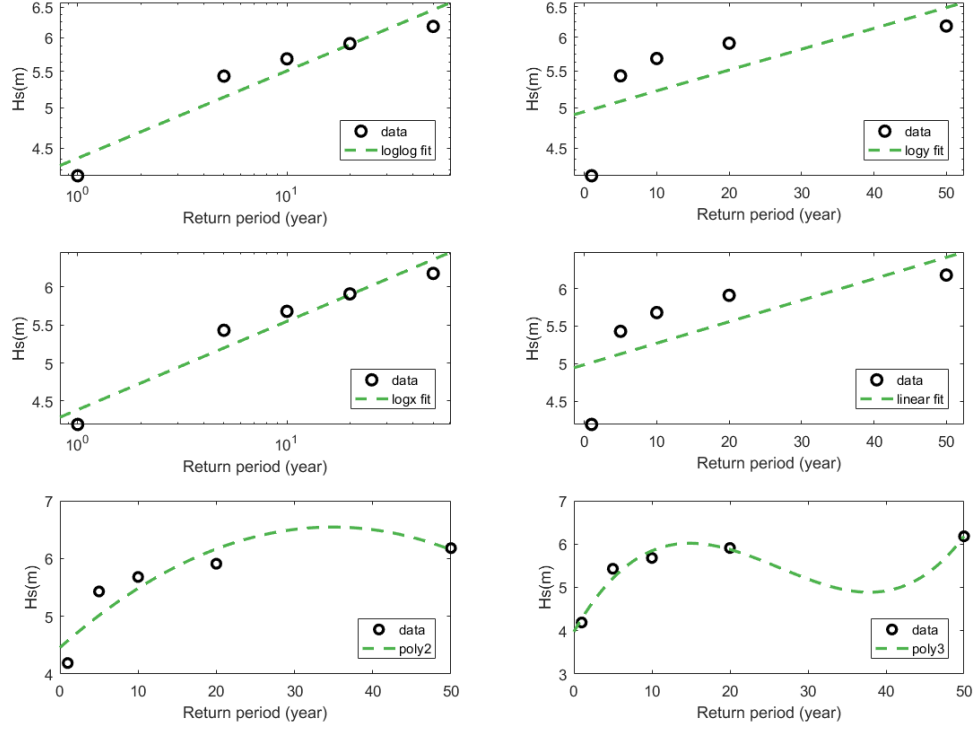


Figure A.2: Visualized results of trials of logarithm and polynomial curve fitting to available offshore extreme wave height, as a function of return period between 1 to 50 years.

At last, trials of logarithm and polynomial curve fitting to available offshore extreme wave height, as a function of return period between 1 to 5 years are tested. Curves pass 1 to 5 years' original data and approximately estimation wave heights of design return period.

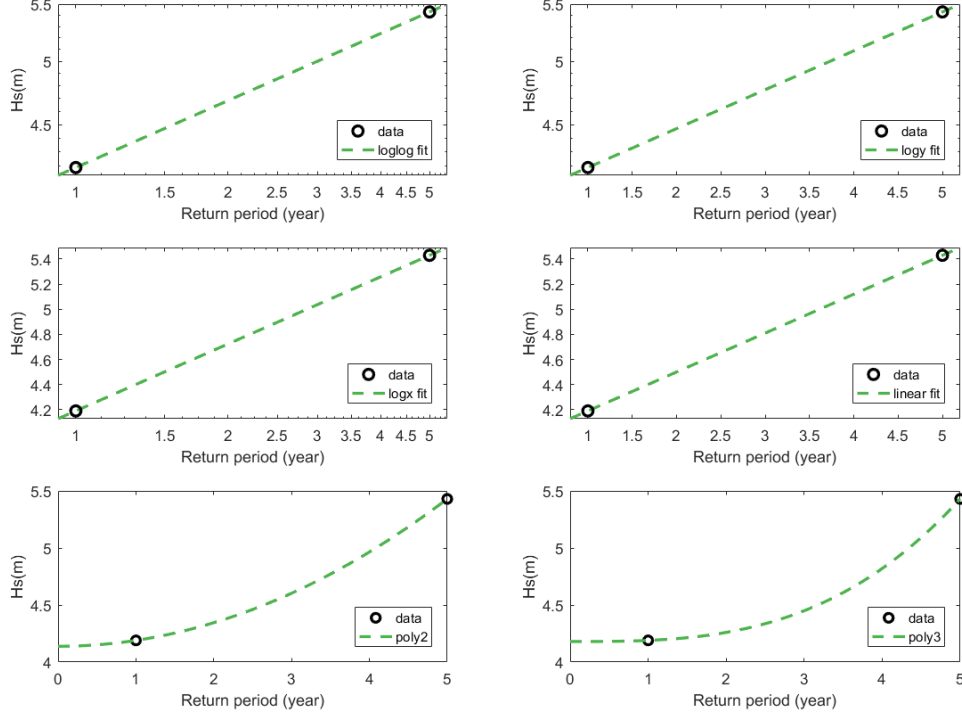


Figure A.3: Visualized results of trials of logarithm and polynomial curve fitting to available offshore extreme wave height, as a function of return period between 1 to 5 years.

In conclusion, type 'logx -> log, linear' is the best fit for two reasons. Not only because 'logx, lineary' is the most commonly used fitting curve, but also because it fit wave height of 1 to 200 years return period for the best among six mathematical functions.

Table A.2: Extreme offshore wave height of design return period

Return period (years)	Wave height (m)
0.2	2.95
0.5	3.66
1	4.19
2	4.72
3	5.04
4	5.26
5	5.43

A.3 Wave period

Same procedure of wave height is repeated to find out best fitting curve for wave period.

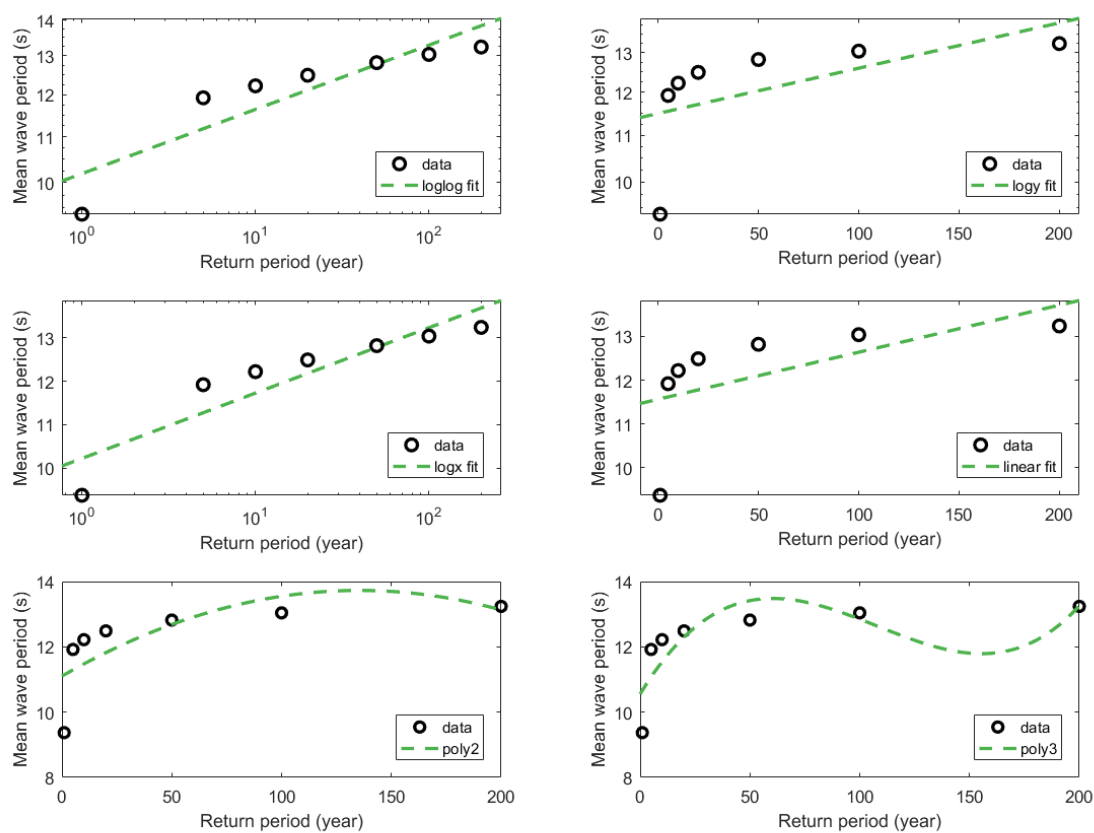


Figure A.4: Visualized results of trials of logarithm and polynomial curve fitting to available offshore extreme mean wave period, as a function of return period between 1 to 200 years.

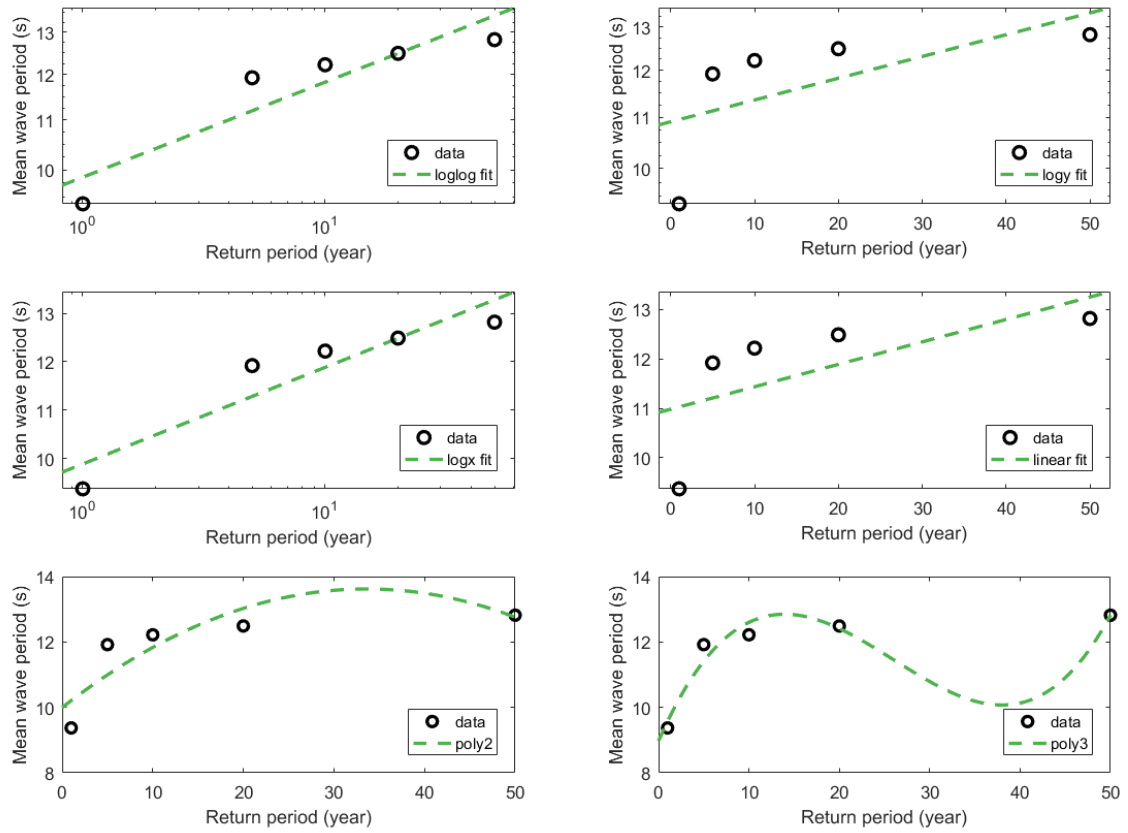


Figure A.5: Visualized results of trials of logarithm and polynomial curve fitting to available offshore extreme mean wave period, as a function of return period between 1 to 50 years.

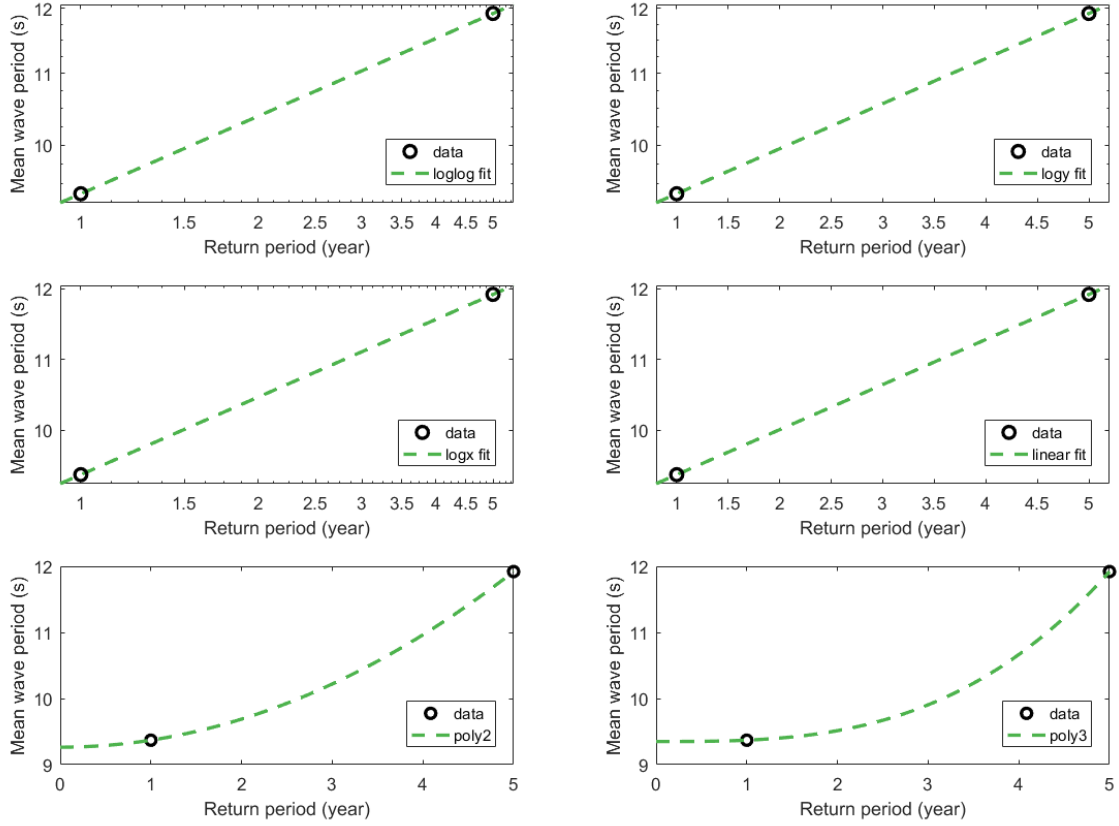


Figure A.6: Visualized results of trials of logarithm and polynomial curve fitting to available offshore extreme mean wave period, as a function of return period between 1 to 5 years.

In conclusion, type 'logx -> log, linear' is the best fit for two reasons. Not only because 'logx, lineary' is the most commonly used fitting curve, but also because it fit wave height of 1 to 200 years return period for the best among six mathematical functions.

Table A.3: Extreme offshore mean wave period of design return period

Return period (years)	Mean wave period (s)
0.2	6.82
0.5	8.27
1	9.37
2	10.46
3	11.11
4	11.56
5	11.92

A.4 Water level

Same procedure of wave height is repeated to find out best fitting curve for water level.

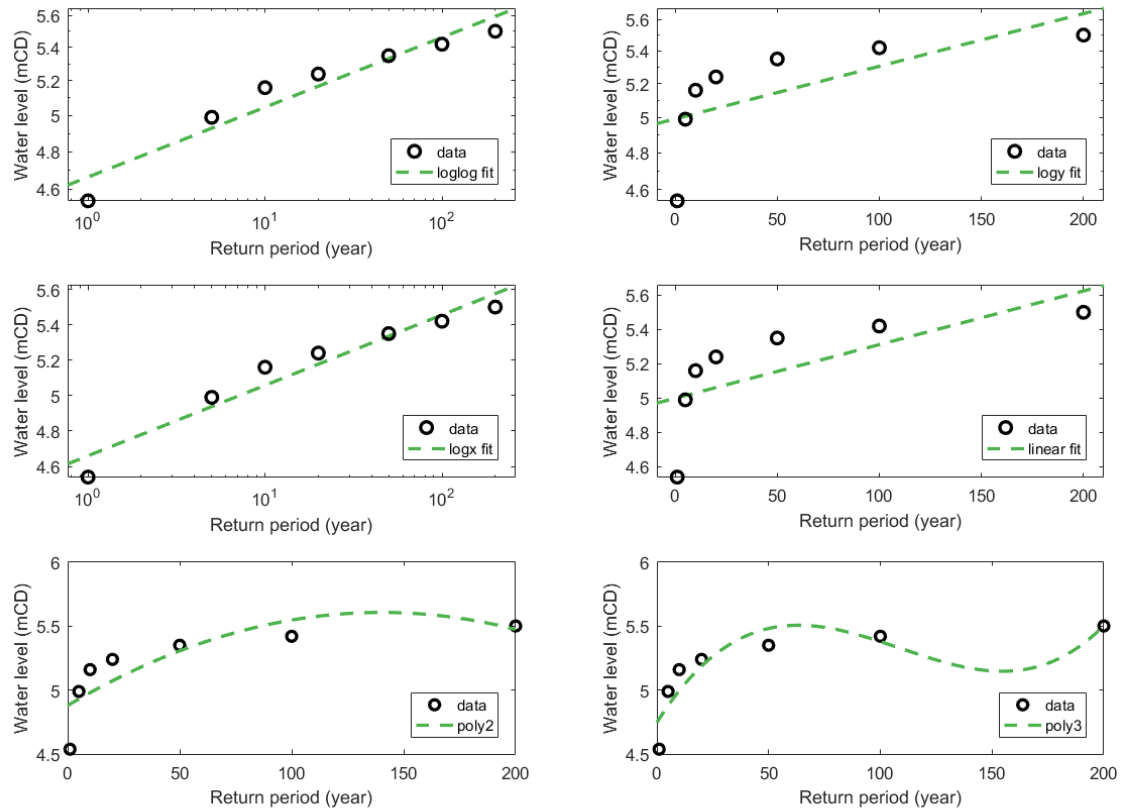


Figure A.7: Visualized results of trials of logarithm and polynomial curve fitting to available offshore extreme water levels, as a function of return period between 1 to 200 years.

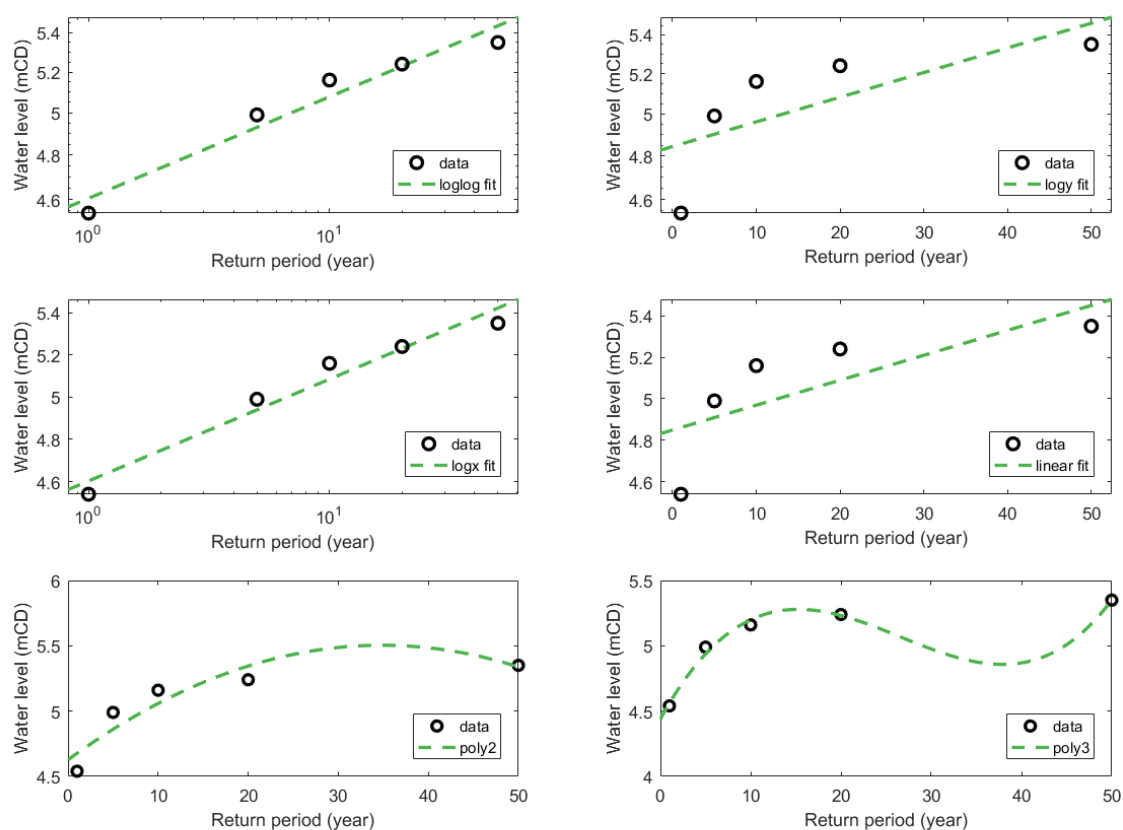


Figure A.8: Visualized results of trials of logarithm and polynomial curve fitting to available offshore extreme water levels, as a function of return period between 1 to 50 years.

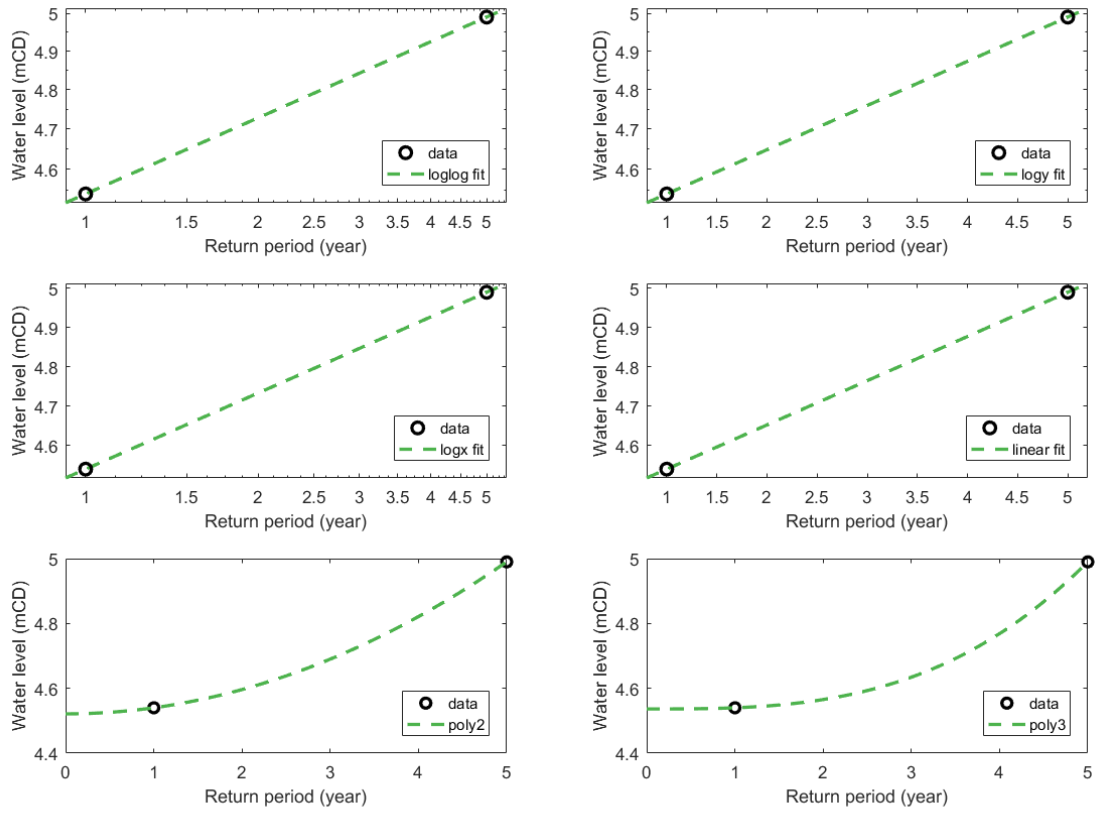


Figure A.9: Visualized results of trials of logarithm and polynomial curve fitting to available offshore extreme water levels, as a function of return period between 1 to 5 years.

In conclusion, type 'logx -> log, linear' is the best fit for two reasons. Not only because 'logx, lineary' is the most commonly used fitting curve, but also because it fit wave height of 1 to 200 years return period for the best among six mathematical functions.

Table A.4: Extreme offshore water level of design return period

Return period (years)	Water level (mCD)
0.2	4.09
0.5	4.34
1	4.54
2	4.73
3	4.84
4	4.92
5	4.99

Appendix B

Numerical modelling of wave transformation

B.1 SWASH script of wave transformation simulation for 1 and 5 years return periods

```

$*****HEADING*****
$
PROJ 'RP11' '01'
$
$*****MODEL INPUT*****
$
MODE NONST ONED
SET LEVEL 4.54
SET SEED 111111
$
CGRID 0.0 0.0 0.0 320.0 0.0 640 0 VERT 1
$
INPGRID BOTTOM 0.0 0.0 0.0 640 1 0.5 0
READINP BOTTOM -1. 'RP11.bot' 1 0 FREE
$
INIT zero
$
BOU SHAP JON 3.3
BOU SIDE W BTYPE WEAK HYPER ADDBoundwave CON SPECT 4.19 9.37
BOU SIDE E CCW BTYPE RADIATION
SPON RI 15.0
Wind 17.3 0
$
FRIC MANN 0.24
Break
$ VISC Horizontal CON
$
NONHYDROSTATIC
DISCRET UPW MOM
TIMEI
$
$***** OUTPUT *****

```

```

$
POINTS 'GAUGE' FILE 'RP11.wvg'
TABLE 'GAUGE' NOHEAD 'RP11.tbl' TSEC DIST BOTL WATL OUTPUT 000000.000 0.20
SEC
POINTS 'LAYER' FILE 'RP11.lay'
TABLE 'LAYER' NOHEAD 'RP11.ltn' TSEC DIST BOTL WATL OUTPUT 000000.000 0.20
SEC
TABLE 'LAYER' NOHEAD 'RP11.lsp' TSEC DIST BOTL VEL OUTPUT 000000.000 0.20 SEC
BLOCK 'COMPGRID' NOHEAD 'RP11.mat' HSIG SETUP
QUANT HSIG dur 100 min
QUANT SETUP dur 100 min
$
TEST 1 0
COMPUTE 000000.000 0.100 SEC 015010.000
STOP
$

```

B.1.1 Limitation of wave transformation model

Friction factor

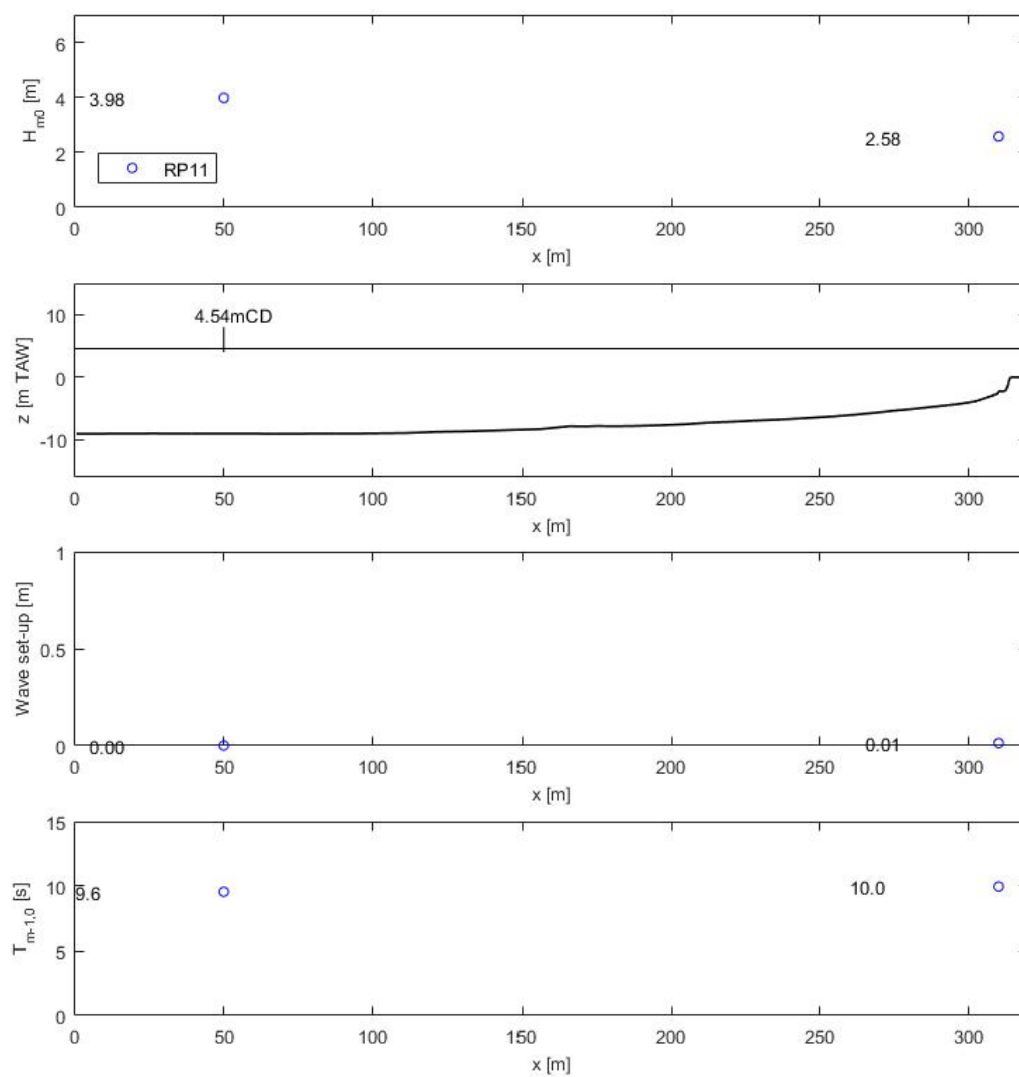
Friction factor is given by Bassett et al. [2015]. However, due to accumulation of sediments at barrier toe, grain size of seabed grains will change with time.

Sponge layer

Multiple sponge layer lengths have been tested, which range from 10 to 200 meters. The test aims to find the minimum length of sponge layer that can absorb all wave energy, and make sure waves will not be reflected.

1-D model

This SWASH model is a 1-D model, only waves that are perpendicular to the barrier are considered. However, in harbour, wave propagation is a very dynamic process. Interaction of waves from different directions can not be modeled by a 1-D model.

Figure B.1: Wave transformation simulation of one year return period: wave set-up, H_{m0} , $T_{m-1,0}$

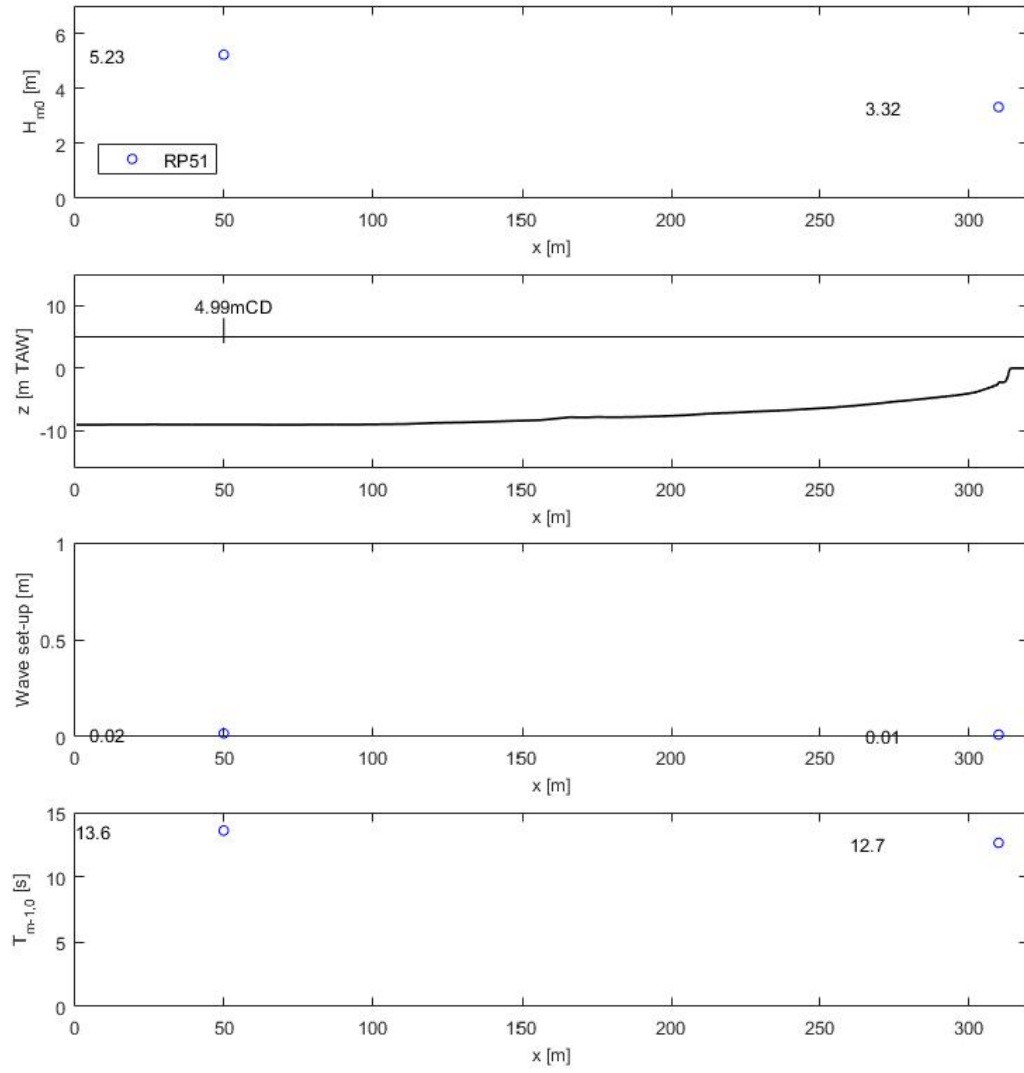


Figure B.2: Wave transformation simulation of five years return period: wave set-up, H_{m0} , $T_{m-1,0}$

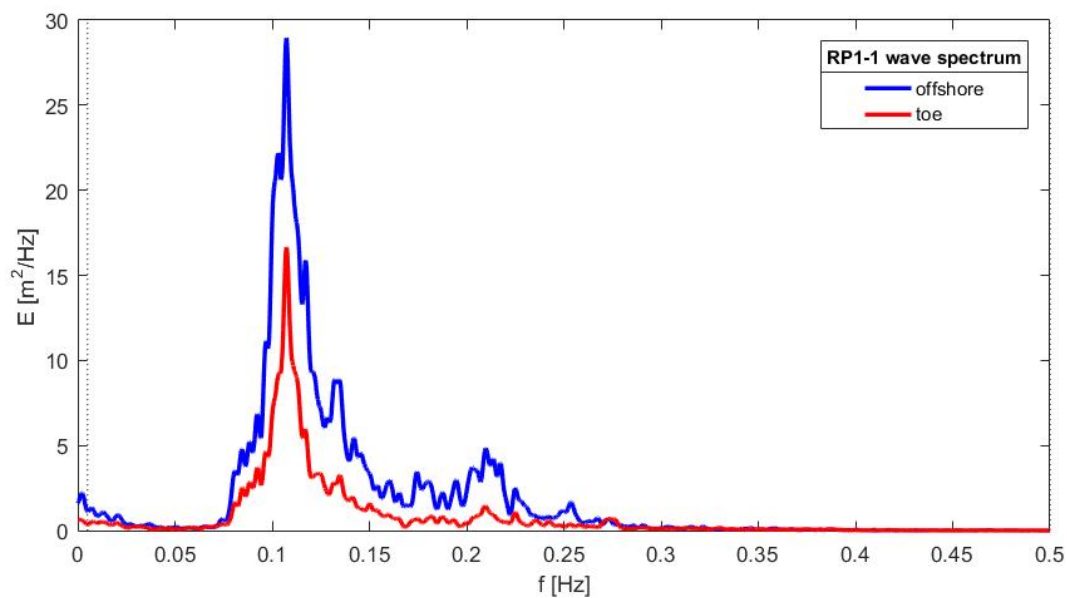


Figure B.3: Wave transformation simulation one year return period: wave spectrum

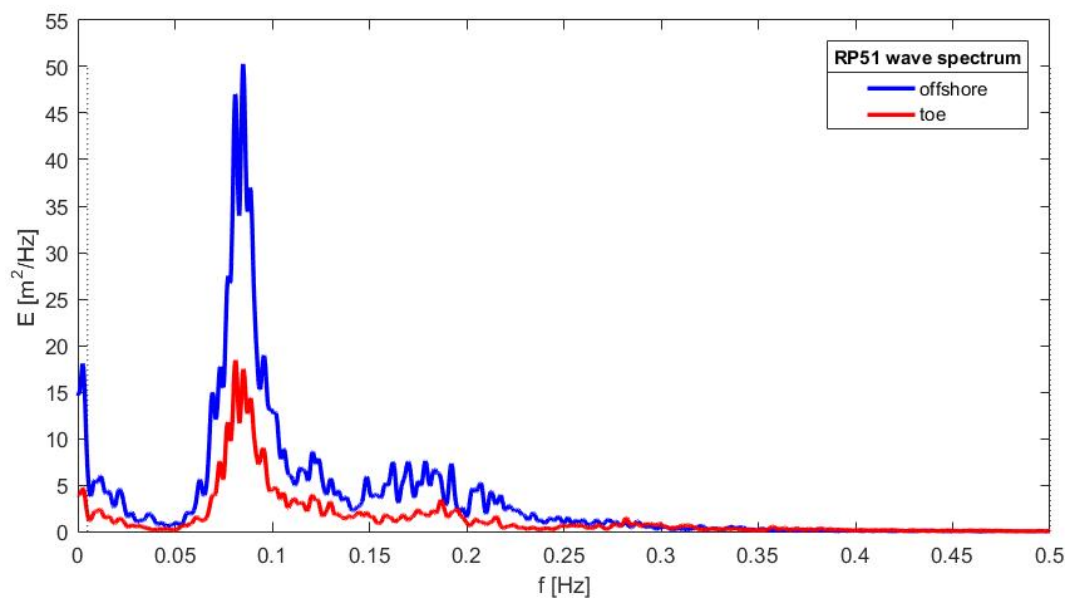


Figure B.4: Wave transformation simulation of five years return period: wave spectrum

Appendix C

Cost-benefit analysis

Matlab script of economic optimization calculation for plain vertical wave wall

```
%straight wall is sea defence
cost_m_h= 543.15;%cost per width per height
h=0:0.05:6;
costplain = cost_m_h*h;%cost of plain vertical wall per meter length
figure;plot(h,costplain);
grid on
xlabel('Height of plain vertical wave wall (m)')
ylabel('Cost of plain vertical wave wall per length (Pound sterling)')
%calculate I
rp=[0.2 0.5 1 2 3 4 5];
h=[0.80 2.05 3.20 4.25 5.00 5.45 5.90];
re= [0.84 0.80 0.70 0.60 0.60 0.60 0.60];

I = h*120*cost_m_h.*re*1.02/1000;%k pounds

ED= (1./rp*100)*(53000*0.0085+500000*0.0015+0.198*50000)/1000000;
ED=ED';
for p=1:7
    syms k
    f = ED(p,:)/((1+0.02)^k);
    V = subs(f, k, 1:100)
    S_sum = sum(V)
    R(p,:)=double(S_sum)%K POUNDS
end

I=I'
Ctot=R+I;

c = min(Ctot)

result = [I,R,Ctot];
rp=rp';
figure;
h=plot(rp,Ctot,'k-o');
t=text(rp(4)-0.5, 205, '(193, 2)', 'FontSize',14);
t.Color = 'black';

hold on
plot(rp,I, 'r--*');
hold on
plot(rp,R, 'b--s');
grid on
legend('Ctot','I','R')
xlabel('Return period (yr)')
ylabel('Total cost (million Pounds sterling)')
```

Matlab script of economic optimization calculation for recurved wave wall with bullnose

```

%straight wall is sea defence
cost_m_h= 836.11;
h=0:0.05:2.5;
costcurve = cost_m_h*h;%cost of plain vertical wall per meter length
figure;plot(h,costcurve);
grid on
xlabel('Height of recurved wave wall (m)')
ylabel('Cost of recurved wave wall per length (Pound sterling)')
%calculate I
rp=[0.2 0.5 1 2 3 4 5];
h=[1.0 1.0 1.0 1.4 1.7 1.9 2.1];
re= [0.84 0.84 0.84 0.78 0.73 0.67 0.65];
I = h*120*cost_m_h*1.02/1000;%k pounds

ED= (1./rp*100)*(53000*0.0085+1000000*0.0015+0.198*50000)/1000000;
ED=ED';
for p=1:7
    syms k
    f = ED(p,:)/((1+0.02)^k);
    V = subs(f, k, 1:100)
    S_sum = sum(V)
    R(p,:)=double(S_sum)%K POUNDS
end

I=I'
Ctot=R+I
c = min(Ctot)
result = [I,R,Ctot];

figure;
plot(rp,Ctot,'k-o');
t=text(0.7, 180, '(153.4, 1)', 'FontSize',14);
t.Color = 'black';
hold on
plot(rp,I,'r--*');
hold on
plot(rp,R,'b-s');
grid on
legend('Ctot','I','R')
xlabel('Return period (yr)')
ylabel('Total cost (million Pounds sterling)')

```


Bibliography

- W. Allsop, T. Bruce, J. Pearson, and P. Besley. Wave overtopping at vertical and steep seawalls. *Proceedings of the Institution of Civil Engineers - Maritime Engineering*, 158(3):103–114, 9 2005. doi: 10.1680/maen.2005.158.3.103. 15
- D. Bassett, G. Kenn, and N. Bucklry. Churchill Barrier No.2 wave overtopping and tidal energy assessment. Technical Report 2, 2015. ix, ix, 1, 5, 14, 21, 22, 23, 24, 25, 26, 28, 65, 77
- T. Bruce, J. Pearson, and W. Allsop. Hazards at coast and harbour seawalls-velocities and trajectories of violent overtopping jets. In *Coastal Engineering Conference*, 2002. ISBN 9812382380. doi: 10.1142/9789812791306{_}0186. 6
- T. Bruce, J. W. Van Der Meer, L. Franco, and J. M. Pearson. Overtopping performance of different armour units for rubble mound breakwaters. *Coastal Engineering*, 56:166–179, 2008. doi: 10.1016/j.coastaleng.2008.03.015. 8, 10, 29, 30
- A. R. Carrasco, M. T. Reis, M. G. Neves, Ferreira, A. Matias, and S. Almeida. Overtopping hazard on a rubble mound breakwater. *Journal of Coastal Research*, pages 247–252, 2014. doi: 10.2112/SI70-042.1. 8
- E. Coeveld, M. Busnelli, M. van Gent, and G. Wolters. Wave overtopping of rubble mound breakwaters with crest elements. In *Coastal Engineering 2006*, pages 4592–4604. World Scientific Publishing Company, 4 2007. ISBN 978-981-270-636-2. doi: 10.1142/9789812709554{_}0385. 15
- S. Formentin, B. Zanuttigh, J. van der Meer, and J. Lara. Overtopping flow characteristics at emerged and over-washed dikes, 2014. 15
- S. Hughes and N. Nadal. Laboratory study of combined wave overtopping and storm surge overflow of a levee. *Coastal Engineering*, 56(3):244–259, 3 2009. ISSN 03783839. doi: 10.1016/j.coastaleng.2008.09.005. 15
- S. Jonkman and T. Schweckendiek. *Flood Defences*. TU Delft, april, 201 edition, 2015. 52, 53
- S. Jonkman, R. Steenbergen, O. Morales-Nápoles, J.K.Vrijling, and A. Vrouwenvelder. PROBABILISTIC DESIGN:RISK AND RELIABILITY ANALYSIS IN CIVIL ENGINEERING. 318 (8):2010–2011, 2017. 51
- J. v. d. Meer, N. Allsop, T. Bruce, J. D. Rouck, A. Kortenhuis, T. Pullen, P. Troch, and B. Zanuttigh. *Manual on wave overtopping of sea defences and related structures An overtopping manual largely based on European research, but for worldwide application*. 2016. vii, vii, vii, viii, 8, 11, 13, 14, 28, 29, 30, 34, 40, 41, 42, 46, 54
- Sara Bailey. Finding the words - Hoxa Tapestry Gallery, 2015. 4
- J. van der Meer and T. Bruce. New physical insights and design formulas on wave overtopping at sloping and vertical structures. *Journal of Waterway, Port, Coastal, and Ocean Engineering*, 140(6):04014025, 11 2014. doi: 10.1061/(ASCE)WW.1943-5460.0000221. 12, 13, 14, 34, 43

- J. W. Van Der Meer, J. P. F. M. Janssen, J. W. Van Der Meer, and J. P. F. M. Janssen. Wave run-up and wave overtopping at dikes and revetments. (485), 1994. 15, 30
- J. W. Van der Meer, W. Allsop, T. Bruce, J. De Rouck, T. Pullen, H. Schuttrumpf, P. Troch, and B. Zanuttigh. Update of the eurotop manual: new insights on wave overtopping. *Coastal Engineering Proceedings*, 1(35):40, 6 2017. ISSN 2156-1028. doi: 10.9753/icce.v35.structures.40. 10
- L. Victor. *Optimization of the hydrodynamic performance of overtopping wave energy converters: experimental study of optimal geometry and probability distribution of overtopping volumes*. Phd manuscript, Ghent university. 2012. ISBN 9789085784784. 10, 11, 30
- L. Victor, J. van der Meer, and P. Troch. Probability distribution of individual wave overtopping volumes for smooth impermeable steep slopes with low crest freeboards. *Coastal Engineering*, 64:87–101, 6 2012. ISSN 0378-3839. doi: 10.1016/J.COASTALENG.2012.01.003. 15, 31